2018

HIGH ACCURACY METHODS AND REGULARIZATION TECHNIQUES FOR FLUID FLOWS AND FLUID-FLUID INTERACTION

Mustafa Aggul
Michigan Technological University, maggul@mtu.edu

HIGH ACCURACY METHODS AND REGULARIZATION TECHNIQUES FOR FLUID FLOWS AND FLUID-FLUID INTERACTION

By

Mustafa Aggul

A DISSERTATION

Submitted in partial fulfillment of the requirements for the degree of

DOCTOR OF PHILOSOPHY

In Mathematical Sciences

MICHIGAN TECHNOLOGICAL UNIVERSITY

2018

This dissertation has been approved in partial fulfillment of the requirements for the Degree of DOCTOR OF PHILOSOPHY in Mathematical Sciences.

Department of Mathematical Sciences

Dissertation Advisor:	*Dr. Alexander E. Labovsky*
Committee Member:	*Dr. Allan A. Struthers*
Committee Member:	*Dr. Jiguang Sun*
Committee Member:	*Dr. Aleksandr V. Sergeyev*
Department Chair:	*Dr. Mark S. Gockenbach*

Dedication

Dedicated to three outstanding women.

Love of my life Deniz

Joy of my life Almila

&

Source of my life Guldane!

Contents

List of Figures

List of Tables

Author Contribution Statement

Some of the materials present in this dissertation are product of collaboration with various researchers, and are also published or to be published in various research journals.

In the first and second chapter, author has collaborated with Alexander E. Labovsky[1], and published a research article in Numerical Methods for Partial Differential Equations (NMPDEs) with the material in chapter 1, and submitted another research article to Computers & Mathematics with Applications (CAMWA) with those in chapter 2.

In the third chapter, author has collaborated with Jeffrey M. Connors[2], Dilek Erkmen[1] [3], Alexander E. Labovsky [1], and submitted a research article to SIAM Journal on Numerical Analysis (SINUM), undergoing second rounds of reviews.

In the fourth chapter, author has worked alone, and submitted a research article to Journal of Computational and Applied Mathematics (JCAM), undergoing the first round of reviews.

[1]Department of Mathematical Sciences, Michigan Technological University, Houghton, MI, 49931.
[2]Department of Mathematics, University of Connecticut, Storrs, CT 06269.
[3]Department of Mathematical Sciences, Agri Ibrahim Cecen University, 04100, Agri, TURKEY.

Acknowledgments

Firstly, I would like to express my sincere gratitude to my advisor Dr. Alexander E. Labovsky for the continuous support of my Ph.D study and related research, for his patience, motivation, and immense knowledge. His endless guidance helped me in all the time of research and writing of this thesis. I could not have imagined having a better advisor and mentor for my Ph.D study.

Besides my advisor, I would like to thank the rest of my thesis committee: Dr. Allan A. Struthers, Dr. Jiguang Sun, and Dr. Aleksandr V. Sergeyev, for their insightful comments which widen my research from various perspectives.

Last but not the least, I would like to thank my family: my mom, my spouse and her family and to my brothers and sister for supporting me spiritually throughout writing this thesis and my life in general.

Abstract

This dissertation contains several approaches to resolve irregularity issues of CFD problems, including a decoupling of non-linearly coupled fluid-fluid interaction, due to high Reynolds number. New models present not only regularize the linear systems but also produce high accurate solutions both in space and time. To achieve this goal, methods solve a computationally attractive artificial viscosity approximation of the target problem, and then utilize a correction approach to make it high order accurate. This way, they all allow the usage of legacy code — a frequent requirement in the simulation of fluid flows in complex geometries. In addition, they all pave the way for parallelization of the correction step, which roughly halves the computational time for each method, i.e. solves at about the same time that is required for DNS with artificial viscosity. Also, methods present do not requires all over function evaluations as one can store them, and reuse for the correction steps. All of the chapters in this dissertation are self-contained, and introduce model first, and then present both theoretical and computational findings of the corresponding method.

Chapter 1

A High Accuracy Minimally Invasive Regularization Technique for Navier-Stokes Equations at High Reynolds Number

1.1 Introduction

The motion of incompressible fluid flow in the flow domain $\Omega = (0, L)^d$ is governed by the Navier-Stokes equations: find the velocity-pressure pair $u : \Omega \times (0, T] \to R^d, (d =$

2, 3) and $p : \Omega \times (0, T] \to R$ satisfying

$$
\begin{aligned}
& u_t + u \cdot \nabla u - \nu \Delta u + \nabla p = f, \text{ for } x \in \Omega, 0 < t \leq T \qquad (1.1.1) \\
& \nabla \cdot u = 0, \ x \in \Omega, \text{ for } 0 \leq t \leq T, \\
& u(x, 0) = u_0(x), \text{ for } x \in \Omega,
\end{aligned}
$$

with the normalization condition $\int_\Omega p(x,t)\ dx = 0$ for $0 < t \leq T$, and viscosity coefficient ν. Throughout this chapter, we consider the case of homogeneous Dirichlet boundary conditions to simplify the proofs; non-homogeneous Dirichlet boundary conditions can be treated in exactly the same manner and the same results hold.

According to the Kolmogorov theory [66], there exists a continuum of scales in turbulent fluid flow, with the smallest scales (in the case of a $3-D$ flow) being of the order $O(Re^{-3/4})$, where the Reynolds number Re is inverse proportional to ν. Thus, capturing all the small structures in a turbulent flow requires the number of mesh points in space for each time step to be $O(Re^{9/4})$ for three-dimensional problems. It is not uncommon to have $Re \sim O(10^8)$ in real-life applications.

Hence, the direct numerical simulation (DNS) of a $3-D$ turbulent flow is often not computationally economical or even feasible. Sometimes it is desirable (especially for

turbulent flows in complex geometries) to be able to use pre-existing codes. Thus, we are aiming at constructing a method that would approximate a flow at high Reynolds number, while being computationally attractive, stable and of high accuracy in both space and time.

To that end, we consider a defect correction approach from [25]. Defect correction strategies have been successfully applied to stiff systems [50, 53, 58, 62, 64], and in particular to evolutionary Navier Stokes Equation (NSE) - see, e.g., [25] and references therein.

The general idea of any Defect Correction Method (DCM) can be formulated as follows (see, e.g., [48, 68]):

Find a unique solution of $Fx = 0$ by

DCM: Use an approximation $\tilde{F}$ to build an iterative procedure:

$$\tilde{F}x_1 = 0,$$

$$x_{i+1} = (I - \tilde{F}^{-1}F)x_i, i \geq 1.$$

The choice of a particular approximation $\tilde{F}$ determines the defect correction method in use. As a result of using the artificial viscosity approximation-based defect correction

method of [25], we have an approach that allows for the usage of legacy codes and gives a second order accurate in space approximation of a flow at high Reynolds number. This is obtained by computing two consecutive approximations u_1 and u_2 with Backward Euler method and with exactly the same matrix (the correction step only modifies the right hand side of the system for u_2 by a function of the previously computed u_1). These approximations, however, are first order accurate in time. The question is: can we increase the time accuracy without increasing the computational cost? The answer lies in the temporal counterpart of the defect correction idea, known as deferred correction.

The main advantage of the deferred correction approach is that a simple low-order method can be employed, and the recovered solution is of high-order accuracy, due to a sequence of deferred correction equations. The classical deferred correction approach could be seen, e.g., in [69]. However, in 2000 a modification of the classical deferred correction approach was introduced by Dutt, Greengard and Rokhlin [39]. This allowed the construction of stable and high-order accurate *spectral deferred correction* methods. In [34], M.L. Minion discusses these spectral deferred correction (SDC) methods in application to an initial value ODE

$$\begin{aligned} \phi'(t) &= F(t, \phi(t)),\ t \in [a, b] \\ \phi(a) &= \phi_a. \end{aligned} \tag{1.1.2}$$

The solution is written in terms of the Picard integral equation; a polynomial is used to interpolate the subintegrand function and the obtained integral term is replaced by its quadrature approximation. The deferred correction approach was used to improve the temporal accuracy of a turbulence model in [71].

When both the defect and deferred correction are combined into one method, we seek two approximations $u_1^{h,i}$ and $u_2^{h,i}$ to the true solution $u(t_i)$. Both are computed with the same matrix of the system, but with different right hand sides. The computational attractiveness is due to two important factors. First, the cost of computing each approximation is the cost of solving a Backward Euler method for the NSE with increased viscosity coefficient - a method which is hard to beat in terms of computational cost. Secondly, the defect-deferred correction methods are readily parallelizable, as the solutions $u_1^{h,i+k}$, $u_2^{h,i+k-1}$,...,$u_{k+1}^{h,i}$ can be computed simultaneously on $k+1$ cores to produce a potentially $(k+1)$-order accurate approximation.

We propose the following two-step method that produces a sequence of approximations $(u_1^h, p_1^h), (u_2^h, p_2^h)$ of the true solution (u, p).

$$\begin{aligned}(\frac{u_1^{h,n+1}-u_1^{h,n}}{k}, v^h) + (h+\nu)(\nabla u_1^{h,n+1}, \nabla v^h) + b^*(u_1^{h,n+1}, u_1^{h,n+1}, v^h) \\ -(p_1^{h,n+1}, \nabla \cdot v^h) = (f(t_{n+1}), v^h),\end{aligned} \tag{1.1.3}$$

$$
\begin{aligned}
&(\frac{u_2^{h,n+1}-u_2^{h,n}}{k},v^h)+(h+\nu)(\nabla u_2^{h,n+1},\nabla v^h)+b^*(u_2^{h,n+1},u_2^{h,n+1},v^h)\\
&-(p_2^{h,n+1},\nabla\cdot v^h)=(\frac{f(t_{n+1})+f(t_n)}{2},v^h)+\frac{\nu}{2}k(\nabla(\frac{u_1^{h,n+1}-u_1^{h,n}}{k}),v^h)\\
&+\frac{1}{2}b^*(u_1^{h,n+1},u_1^{h,n+1},v^h)-\frac{1}{2}b^*(u_1^{h,n},u_1^{h,n},v^h)+h(\nabla u_1^{h,n+1},\nabla v^h),
\end{aligned}
\tag{1.1.4}
$$

where $b^*(\cdot,\cdot,\cdot)$ is the explicitly skew-symmetrized trilinear form, defined later.

The remainder of this chapter is organized as follows. Section 1.2 introduces the necessary notation and preliminaries; Section 1.3 then follows on the accuracy and stability of the defect step approximation. These results come mostly from [25], as the equation for the defect step of the defect-deferred approach is exactly the defect step of the approach in [25]. The novelty of the proposed method appears in Section 1.7, where stability and increased accuracy (both time and space) of the correction step is studied. The quantitative and qualitative computational tests are presented in Section 1.10.

1.2 Mathematical Preliminaries and Notations

Throughout this chapter, the norm $||.||$ denotes the usual $L^2(\Omega)$ norm of scalars, vectors and tensors, induced by the usual L^2 inner-product, denoted by $(\cdot,\cdot)$. The space in which velocity sought(at time t) is

$$X = H_0^1(\Omega)^d = \{v \in L^2(\Omega)^d : \nabla v \in L^2(\Omega)^{dxd} \text{ and } v = 0 \text{ on } \partial\Omega\}.$$

with the norm $||v||_X = ||\nabla v||$. The space dual to X is equipped with the norm

$$||f||_{-1} = \sup_{v \in X} \frac{(f, v)}{||\nabla v||}.$$

The space that velocity (at time t) belongs to is

$$Q = L_0^2(\Omega) = \{q \in L^2(\Omega) : \int_\Omega q(x)dx = 0\}.$$

Introduce the space of weakly divergence-free functions

$$X \supset V = \{v \in X : (\nabla \cdot v, q) = 0, \forall q \in Q\}.$$

For measurable $v : [0, T] \to X$, we define

$$||v||_{L^p(0,T;X)} = \Big(\int_0^T ||v||_X^P dt \Big)^{\frac{1}{p}}, 1 \leq p < \infty,$$

and

$$||v||_{L^\infty(0,T;X)} = ess \sup_{0 \leq t \leq T} ||v(t)||_X.$$

Define the trilinear form on $X \times X \times X$

$$b(u, v, w) = \int_{\Omega} u \cdot \nabla v \cdot w dx.$$

The following lemma is also necessary for the analysis.

Lemma 1 *There exist finite constant $M = M(d)$ and $N = N(d)$ s.t. $M \geq N$ and*

$$M = \sup_{u,v,w \in X} \frac{b(u, v, w)}{||u||||v||||w||} < \infty, N = \sup_{u,v,w \in V} \frac{b(u, v, w)}{||u||||v||||w||} < \infty.$$

The proof can be found in [32]. The corresponding constants M^h and N^h are defined by replacing X by the finite element space $X^h \subset X$ and V by $V^h \subset X$. Note that $M \geq \max(M^h, N, N^h)$ and that as $h \to 0$, $N^h \to N$ and $M^h \to M$ (see [32]).

Throughout the chapter, assume that the velocity-pressure finite element spaces $X^h \subset X$ and $Q^h \subset Q$ are conforming, have typical approximation properties of finite element spaces commonly in use, and satisfy the discrete inf-sup, or LBB^h, condition

$$\inf_{q^h \in Q^h} \sup_{v^h \in X^h} \frac{(q^h, \nabla \cdot v^h)}{\|\nabla v^h\| \|q^h\|} \geq \beta^h > 0, \tag{1.2.1}$$

where β^h is bounded away from zero uniformly in h. Examples of such spaces can be found in [32]. Consider $X^h \subset X$, $Q^h \subset Q$ to be spaces of continuous piecewise polynomials of degree m and $m-1$, respectively, with $m \geq 2$. The case of $m = 1$ is not considered, because the optimal error estimate (of the order h) is obtained after the first step of the method, and therefore the DCM in this case is reduced to the artificial viscosity approach.

The space of discretely divergence-free functions is defined as follows

$$V^h = \{v^h \in X^h : (q^h, \nabla \cdot v^h) = 0, \forall q^h \in Q^h\}.$$

In the analysis, the properties of the following Modified Stokes Projection are used.

Definition 1 (Modified Stokes Projection) *Define the Stokes projection operator* P_S*:* $(X, Q) \to (X^h, Q^h)$*,* $P_S(u, p) = (\tilde{u}, \tilde{p})$*, satisfying*

$$\begin{aligned} (h+\nu)(\nabla(u-\tilde{u}), \nabla v^h) - (p - \tilde{p}, \nabla \cdot v^h) &= 0, \\ (\nabla \cdot (u - \tilde{u}), q^h) &= 0, \end{aligned} \tag{1.2.2}$$

for any $v^h \in V^h, q^h \in Q^h$.

In (V^h, Q^h) this formulation reads: given $(u, p) \in (X, Q)$, find $\tilde{u} \in V^h$ satisfying

$$(h + \nu)(\nabla(u - \tilde{u}), \nabla v^h) - (p - q^h, \nabla \cdot v^h) = 0, \tag{1.2.3}$$

for any $v^h \in V^h, q^h \in Q^h$.

Define the explicitly skew-symmetrized trilinear form

$$b^*(u, v, w) := \frac{1}{2}(u \cdot \nabla v, w) - \frac{1}{2}(u \cdot \nabla w, v).$$

The following estimate is easy to prove (see, e.g., [32]): there exists a constant $C = C(\Omega)$ such that

$$|b^*(u, v, w)| \leq C(\Omega)\|\nabla u\|\|\nabla v\|\|\nabla w\|. \tag{1.2.4}$$

The proofs will require the sharper bound on the nonlinearity. This upper bound is improvable in R^2.

Lemma 2 (The sharper bound on the nonlinear term) *Let $\Omega \subset R^d$, $d = 2, 3$. For all $u, v, w \in X$*

$$|b^*(u, v, w)| \leq C(\Omega)\sqrt{\|u\|\|\nabla u\|}\|\nabla v\|\|\nabla w\|.$$

Proof 1 *See [32].*

Also the following inequalities are needed: for any $u \in V$

$$\inf_{v \in V^h} \|\nabla(u - v)\| \leq C(\Omega) \inf_{v \in X^h} \|\nabla(u - v)\|, \tag{1.2.5}$$

$$\inf_{v \in V^h} \|u - v\| \leq C(\Omega) \inf_{v \in X^h} \|\nabla(u - v)\|, \tag{1.2.6}$$

The proof of (1.2.5) can be found, e.g., in [32], and (1.2.6) follows from the Poincare-Friedrich's inequality and (1.2.5).

Assume that the inverse inequality holds: there exists a constant C independent of

h, such that

$$||\nabla v|| \leq Ch^{-1}||v||, \ \forall v \in X^h. \tag{1.2.7}$$

Define also the number of time steps $N := \frac{T}{k}$.

The following error decomposition will be used.

$$\begin{gathered} e_\ell^i = u^i - u_\ell^{h,i} = u^i - \tilde{u}^i + \tilde{u}^i - u_\ell^{h,i} = \eta_\ell^i - \phi_\ell^{h,i}, \\ \text{where } \tilde{u}^i \in V^h \text{ is some projection of } u^i \text{ onto } V^h, \\ \text{and } \eta_\ell^i = u^i - \tilde{u}^i, \phi_\ell^{h,i} = u_\ell^{h,i} - \tilde{u}^i, \phi_\ell^{h,i} \in V^h, \forall i, \forall \ell = 1, 2. \end{gathered} \tag{1.2.8}$$

Conclude the preliminaries by formulating the discrete Gronwall's lemma, see, e.g. [70]

Lemma 3 *Let $k, B,$ and $a_\mu, b_\mu, c_\mu, \gamma_\mu,$ for integers $\mu \geq 0,$ be nonnegative numbers such that:*

$$a_n + k\sum_{\mu=0}^{n} b_\mu \leq k\sum_{\mu=0}^{n} \gamma_\mu a_\mu + k\sum_{\mu=0}^{n} c_\mu + B \text{ for } n \geq 0.$$

Suppose that $k\gamma_\mu < 1$ for all μ, and set $\sigma_\mu = (1 - k\gamma_\mu)^{-1}$. Then

$$a_n + k\sum_{\mu=0}^{n} b_\mu \leq e^{k\sum_{\mu=0}^{n} \sigma_\mu \gamma_\mu} \cdot [k\sum_{\mu=0}^{n} c_\mu + B].$$

Upon giving the relationship between Reynolds Number and the kinetic viscosity (ν) below, we will use ν instead of Re^{-1}.

$$Re = \frac{\rho v L}{\mu} = \frac{vL}{\nu},$$

where v is the maximum velocity of the object relative to the fluid, L is a characteristic linear dimension, μ is the dynamic viscosity of the fluid and ρ is the density of the fluid.

1.3 AV Approximation

In this section we prove the unconditional stability and error estimate of the discrete artificial viscosity approximation u_1^h and use this result to prove an error estimate of its time derivative $\frac{de_1}{dt}$. Over $0 \leq t \leq T < \infty$ the approximations u_1^h is bounded uniformly in ν.

Hence, the formulation (1.1.3) gives $O(h + k)$ accurate, unconditionally stable extension of the artificial viscosity approximation to the time-dependent Navier-Stokes equations.

We start by giving stability and error estimate of the modified Stokes Projection, that we use as the approximation $\tilde{u}^0$ to the initial velocity u_0.

1.4 Stokes Projection

Proposition 4 (Stability of the Stokes projection) *Let u, $\tilde{u}$ satisfy (1.2.3). The following bound holds*

$$(h+\nu)\|\nabla\tilde{u}\|^2 \leq 2(h+\nu)\|\nabla u\|^2 \tag{1.4.1}$$
$$+2d(h+\nu)^{-1}\inf_{q^h\in Q^h}\|p-q^h\|^2,$$

where d is the dimension, $d=2,3$.

Proposition 5 *(Error estimate for Stokes Projection). Suppose the discrete inf-sup condition (4.2.1) holds. Then the error in Stokes Projection satisfies*

$$(h+\nu)||\nabla(u-\tilde{u})||^2 \leq C[(h+\nu)\inf_{v^h\in V^h}||\nabla(u-v^h)||^2$$
$$+(h+\nu)^{-1}\inf_{q^h\in Q^h}||p-q^h||^2], \tag{1.4.2}$$

where C is a constant independent of h and Re.

Proof 2 *Proofs can be found in [25]*

1.5 Stability of the AV approximation

Lemma 6 *Let u_1^h satisfy the equation (1.1.3). Let $f \in L^2(0,T;H^{-1}(\Omega))$. Then for $n = 0, ..., N-1$*

$$\|u_1^{h,n+1}\|^2 + k\Sigma_{i=1}^{n+1}(h+\nu)\|\nabla u_1^{h,i}\|^2 \leq \|u_0^s\|^2$$

$$+\frac{1}{h+\nu}k\Sigma_{i=1}^{n+1}\|f(t_i)\|_{-1}^2.$$

Also, if $f \in L^2(0,T;L^2(\Omega))$ and the time constraint T is finite, then there exists a constant $C = C(T)$ such that

$$\begin{aligned}&\|u_1^{h,n+1}\|^2 + k\Sigma_{i=1}^{n+1}(h+\nu)\|\nabla u_1^{h,i}\|^2 \\ &\quad\leq C(\|u_0^s\|^2 + k\Sigma_{i=1}^{n+1}\|f(t_i)\|^2).\end{aligned} \tag{1.5.1}$$

Proof 3 *Can be found in [25].*

1.6 Error Estimates of AV Approximation

Definition 2 *Let*

$$C_u := ||u(x,t)||_{L^\infty(0,T;L^\infty(\Omega))},$$

$$C_{\nabla u} := ||\nabla u(x,t)||_{L^\infty(0,T;L^\infty(\Omega))},$$

$$\tilde{C}_u := ||u(x,t)||_{L^\infty(0,T;L^2(\Omega))},$$

$$\tilde{C}_{\nabla u} := ||\nabla u(x,t)||_{L^\infty(0,T;L^2(\Omega))},$$

and introduce $\tilde{C}$*, satisfying*

$$\inf_{v\in V^h} ||\nabla(u-v)|| \le C_1 \inf_{v\in X^h} ||\nabla(u-v)|| \le C_2 h^m ||u||_{H^{m+1}} \le \tilde{C} h^m \tag{1.6.1}$$

Also, using the constant $C(\Omega)$ *from Lemma 2.3, we define* $\bar{C} := 1728 C^4(\Omega)$*.*

Theorem 7 *Let* $f \in L^2(0,T;H^{-1})$*, let* u_1^h, u_2^h *satisfy (1.1.3) and (1.1.4), respectively,*

$$k \le \frac{h+\nu}{4C_u^2 + 2(h+\nu)C_{\nabla u} + 2\bar{C}\tilde{C}^4(h+\nu)^{-2}h^{4m}},$$

$$u \in L^2(0,T;H^{m+1}(\Omega)) \cap L^\infty(0,T;L^\infty(\Omega)), \nabla u \in L^\infty(0,T,L^\infty(\Omega)),$$

$$u_t \in L^2(0,T;H^{m+1}(\Omega)), u_{tt} \in L^2(0,T;L^2(\Omega)), p \in L^2(0,T;H^m(\Omega)).$$

Then there exist a constant $C = C(\Omega, T, u, p, f, h+\nu)$*, such that*

$$\max_{1\le i\le N} ||u(t_i) - u_1^{h,i}|| + \Big(k\sum_{i=1}^{n+1}(h+\nu)||\nabla(u(t_i) - u_1^{h,i})||^2\Big)^{1/2} \le C(h^m + h + k)$$

Proof 4 *Can be found [25].*

We will need the following lemma in the proof of Theorem (9).

Lemma 8 *Let* $f \in L^2(0,T;H^{-1}(\Omega))$*. Suppose* ϕ^0 *and* ϕ^1 *to be the Stokes projections of the initial velocity and velocity at the first time level, respectively. Let* $m \ge 2$ *and*

$$k < \frac{4(h+\nu)}{13(4(h+\nu)C_{\nabla u} + 3C_u^2)}.$$

Then there exist a constant $C = C(\Omega, T, u, p, f, h+\nu)$*, such that*

$$||\frac{\phi^1 - \phi^0}{k}||^2 + \frac{13}{2}(h+\nu)k||\nabla\frac{\phi^1 - \phi^0}{k}||^2 \le C(kh^{2m} + h^2 + k^2 + k^2h^{2m-3}) \qquad (1.6.2)$$

Proof 5 *From the Stokes Projection(1) and error decomposition(1.2.8), we have*

$$(h+\nu)(\nabla\phi^0,\nabla v)-(h+\nu)(\nabla\eta^0,\nabla v)-(p^0-q,\nabla.v)=0 \tag{1.6.3}$$

On the other hand the solution at the first time level satisfies the following

$$\begin{aligned}
||\frac{\phi^1-\phi^0}{k}||^2+(h+\nu)(\nabla\phi^1,\nabla\frac{\phi^1-\phi^0}{k})+b^*(u^1,u^1,\frac{\phi^1-\phi^0}{k})\\
-b^*(u_1^1,u_1^1,\frac{\phi^1-\phi^0}{k})+(p^1,\nabla.\frac{\phi^1-\phi^0}{k})\\
=h(\nabla u^1,\nabla\frac{\phi^1-\phi^0}{k})+k(\rho^1,\frac{\phi^1-\phi^0}{k})\\
+(\frac{\eta^1-\eta^0}{k},\frac{\phi^1-\phi^0}{k})+(h+\nu)(\nabla\eta^1,\frac{\phi^1-\phi^0}{k}),\\
\text{where } k\rho^1=\frac{u^1-u^0}{k}-u_t^1=ku_{tt}^\theta, \text{ for some } \theta\in(0,k).
\end{aligned} \tag{1.6.4}$$

Subtracting equation 1.6.3 from equation 1.6.4 for $v=\frac{\phi^1-\phi^0}{k}$*, we have*

$$\begin{aligned}
||\frac{\phi^1-\phi^0}{k}||^2+k(h+\nu)||\nabla\frac{\phi^1-\phi^0}{k}||^2\\
+b^*(u^1,u^1,\frac{\phi^1-\phi^0}{k})-b^*(u_1^1,u_1^1,\frac{\phi^1-\phi^0}{k})\\
-k(\frac{p^1-p^0}{k}-q,\nabla.\frac{\phi^1-\phi^0}{k})\\
=h(\nabla u^1,\nabla\frac{\phi^1-\phi^0}{k})+(\rho^1,\frac{\phi^1-\phi^0}{k})+(\frac{\eta^1-\eta^0}{k},\frac{\phi^1-\phi^0}{k})\\
+k(h+\nu)(\nabla\frac{\eta^1-\eta^0}{k},\nabla\frac{\phi^1-\phi^0}{k})
\end{aligned} \tag{1.6.5}$$

Adding and subtracting $b^*(u_1^1, u^1, \frac{\phi^1-\phi^0}{k})$ *to the nonlinear terms in equation (1.6.5) together with error decomposition (1.2.8) gives*

$$\begin{aligned} b^*(u^1, u^1, \frac{\phi^1-\phi^0}{k}) - b^*(u_1^1, u_1^1, \frac{\phi^1-\phi^0}{k}) \\ &= b^*(e_1^1, u^1, \frac{\phi^1-\phi^0}{k}) + b^*(u_1^1, e_1^1, \frac{\phi^1-\phi^0}{k}) \\ &= b^*(\phi^1, u^1, \frac{\phi^1-\phi^0}{k}) - b^*(\eta^1, u^1, \frac{\phi^1-\phi^0}{k}) \\ &\quad + b^*(u_1^1, \phi^1, \frac{\phi^1-\phi^0}{k}) - b^*(u_1^1, \eta^1, \frac{\phi^1-\phi^0}{k}) \end{aligned} \tag{1.6.6}$$

Adding and subtracting ϕ^0 *to the first component of the first nonlinear term in the equation (1.6.6) gives*

$$b^*(\phi^1, u^1, \frac{\phi^1-\phi^0}{k}) = kb^*(\frac{\phi^1-\phi^0}{k}, u^1, \frac{\phi^1-\phi^0}{k}) + b^*(\phi^0, u^1, \frac{\phi^1-\phi^0}{k}) \tag{1.6.7}$$

In the first nonlinear term of (1.6.7), applying Cauchy-Schwarz and Young's inequalities together with the regularity assumption of u *and bound 1.2.4 gives*

$$k|b^*(\frac{\phi^1-\phi^0}{k},u^1,\frac{\phi^1-\phi^0}{k})| \leq kC_{\nabla u}||\frac{\phi^1-\phi^0}{k}||^2$$
$$+k\mu^*(h+\nu)||\nabla\frac{\phi^1-\phi^0}{k}||^2+k\frac{C_u^2}{16(h+\nu)\mu^*}||\frac{\phi^1-\phi^0}{k}||^2 \tag{1.6.8}$$

In the second nonlinear term of (1.6.7), applying Cauchy Schwarz and Young's inequalities together with bound 1.2.4 and inverse inequality (1.2.7) gives

$$|b^*(\phi^0,u^1,\frac{\phi^1-\phi^0}{k})| \leq \mu||\frac{\phi^1-\phi^0}{k}||^2+\frac{Ch^{-2}}{4\mu}||\nabla\phi^0||^2 \tag{1.6.9}$$

In the second nonlinear term of (1.6.6), applying Cauchy Schwarz and Young's inequalities together with bound 1.2.4 and inverse inequality (1.2.7) gives

$$|b^*(\eta^1,u^1,\frac{\phi^1-\phi^0}{k})| \leq \mu||\frac{\phi^1-\phi^0}{k}||^2+\frac{Ch^{-2}}{4\mu}||\nabla\eta^1||^2 \tag{1.6.10}$$

For the third nonlinear term of equation (1.6.6), applying error decomposition (1.2.8) gives

$$|b^*(u_1^1, \phi^1, \frac{\phi^1 - \phi^0}{k})| \leq |b^*(u^1, \phi^1, \frac{\phi^1 - \phi^0}{k})| + |b^*(\phi^1, \phi^1, \frac{\phi^1 - \phi^0}{k})| + |b^*(\eta^1, \phi^1, \frac{\phi^1 - \phi^0}{k})| \tag{1.6.11}$$

Since nonlinear form is skew-symmetric in the second and third entry, we can replace terms like the first nonlinear term in the inequality (1.6.11) with terms like $|b^*(u^1, \phi^0, \frac{\phi^1 - \phi^0}{k})|$. *Applying Cauchy-Schwarz and Young's inequalities together with the regularity assumption of u and inverse inequality gives*

$$|b^*(u^1, \phi^0, \frac{\phi^1 - \phi^0}{k})| \leq 2\mu||\frac{\phi^1 - \phi^0}{k}||^2 + \frac{C_u^2}{4\mu}(||\nabla\phi^0||^2 + h^{-2}||\phi^0||^2) \tag{1.6.12}$$

Applying Young's inequality together with the sharper bound (2) and inverse inequality (1.2.7) in the second nonlinear term of 1.6.11 gives

$$|b^*(\phi^1, \phi^1, \frac{\phi^1 - \phi^0}{k})| = |b^*(\phi^1, \phi^0, \frac{\phi^1 - \phi^0}{k})| \leq \mu||\frac{\phi^1 - \phi^0}{k}||^2 + \frac{Ch^{-3}}{4\mu}||\phi^1||^2||\nabla\phi^0||^2 \tag{1.6.13}$$

For the last nonlinear term in the inequality (1.6.11), we can apply 1.2.4 and inverse inequality followed by Young's inequality to have

$$
\begin{aligned}
|b^*(\eta^1, \phi^1, \frac{\phi^1 - \phi^0}{k})| &= |b^*(\eta^1, \phi^0, \frac{\phi^1 - \phi^0}{k})| \\
&\leq \mu ||\frac{\phi^1 - \phi^0}{k}||^2 + \frac{Ch^{-2}}{4\mu} ||\nabla \eta^1||^2 ||\nabla \phi^0||^2
\end{aligned}
\tag{1.6.14}
$$

For the forth nonlinear term of equation (1.6.6), applying error decomposition gives

$$
\begin{aligned}
|b^*(u_1^1, \eta^1, \frac{\phi^1 - \phi^0}{k})| \leq |b^*(u^1, \eta^1, \frac{\phi^1 - \phi^0}{k})| + |b^*(\phi^1, \eta^1, \frac{\phi^1 - \phi^0}{k})| \\
+ |b^*(\eta^1, \eta^1, \frac{\phi^1 - \phi^0}{k})|
\end{aligned}
\tag{1.6.15}
$$

For all the nonlinear terms in the inequality (1.6.15), we can apply bound 1.2.4 and inverse inequality followed by Young's inequality to have

$$
|b^*(u^1, \eta^1, \frac{\phi^1 - \phi^0}{k})| \leq \mu ||\frac{\phi^1 - \phi^0}{k}||^2 + \frac{Ch^{-2}}{4\mu} ||\nabla \eta^1||^2 \tag{1.6.16}
$$

$$
|b^*(\phi^1, \eta^1, \frac{\phi^1 - \phi^0}{k})| \leq \mu ||\frac{\phi^1 - \phi^0}{k}||^2 + Ch^{-4} ||\nabla \eta^1||^2 ||\phi^1||^2 \tag{1.6.17}
$$

$$|b^*(\eta^1,\eta^1,\frac{\phi^1-\phi^0}{k})| \leq \mu||\frac{\phi^1-\phi^0}{k})||^2 + Ch^{-2}||\nabla\eta^1||^4 \tag{1.6.18}$$

Apply Cauchy-Schwarz and Young's inequalities to (1.6.5).

Since $||\nabla.\frac{\phi^1-\phi^0}{k}|| \leq d||\nabla\frac{\phi^1-\phi^0}{k}||$,

$$\begin{aligned}
&(1-12\mu-(\frac{C_{\nabla u}}{2}+\frac{C_u^2}{16(h+\nu)\mu^*})k)||\frac{\phi^1-\phi^0}{k}||^2 \\
&+(1-3\mu^*)(h+\nu)k||\nabla\frac{\phi^1-\phi^0}{k}||^2 \\
\leq \frac{dk}{4\mu^*(h+\nu)}\inf_{q\in Q^h}||\frac{p^1-p^0}{k}-q||^2 &+ \frac{h^2}{4\mu}||\Delta u^1||^2 + \frac{k^2}{4\mu}||\rho^1||^2 + \frac{1}{4\mu}||\frac{\eta^1-\eta^0}{k}||^2 \\
&+\frac{k(h+\nu)}{4\mu^*}||\nabla\frac{\eta^1-\eta^0}{k}||^2 + \frac{Ch^{-2}}{4\mu}||\nabla\phi^0||^2 + \frac{C_u^2}{4\mu}||\nabla\phi^0||^2 + \frac{C_u^2h^{-2}}{4\mu}||\phi^0||^2 \\
&+\frac{Ch^{-3}}{4\mu}||\phi^1||^2||\nabla\phi^0||^2 + \frac{Ch^{-2}}{4\mu}||\nabla\eta^1||^2||\nabla\phi^0||^2 \\
&+\frac{Ch^{-2}}{2\mu}||\nabla\eta^1||^2 + Ch^{-4}||\phi^1||^2||\nabla\eta^1||^2 + Ch^{-2}||\nabla\eta^1||^4
\end{aligned} \tag{1.6.19}$$

Use the approximation properties of X^h, Q^h. *Since the mesh nodes do not depend upon the time level, it follows from (1.2.5), (1.2.6) that*

$$\begin{aligned}\inf_{q\in Q}||\frac{p^1+p^0}{k}-q||^2 &\leq Ch^{2m},\\ ||\frac{\eta_2^1-\eta_2^0}{k}||^2 &\leq Ch^{2m+2},\\ ||\eta_2^1||^2 &\leq Ch^{2m+2}.\end{aligned} \tag{1.6.20}$$

Taking $\mu = 1/13$ and $\mu^* = 1/6$ and using bounds (1.6.20) for each term, it follows from the regularity assumption of u that

$$\begin{aligned}(\frac{1}{13}-(\frac{C_{\nabla u}}{2}+\frac{3C_u^2}{8(h+\nu)})k)||\frac{\phi^1-\phi^0}{k}||^2+\frac{1}{2}(h+\nu)k||\nabla\frac{\phi^1-\phi^0}{k}||^2\\ \leq C(h^{2m-2}+h^2+k^2+k^2h^{2m-3})\end{aligned} \tag{1.6.21}$$

The last inequality implies the lemma statement.

Theorem 9 *Let the assumptions of Lemma (8) and Theorem (7) be satisfied.*

Let $k \leq \min\{\frac{h+\nu}{2CC_{\nabla u}(h+\nu)+2CC_u^2}, C(h+\nu)^{\frac{5}{3}}, C(h+\nu)^3\}$

Then

$$||\frac{e_1^{n+1}-e_1^n}{k}||^2+k\sum_{i=0}^{n}(h+\nu)||\nabla\frac{e_1^{i+1}-e_1^i}{k}||^2 \leq C[h^{2m}+h^2+k^2]$$

Proof 6 *Start with the proof of the bound for* $||\frac{\phi^{n+1}-\phi^n}{k}||$.

From the inequality (5.14) in [25], we have

$$\begin{aligned} ||s^{h,n+1}||^2 + k(h+\nu)\sum_{i=1}^{n}||\nabla s^{h,i+1}||^2 \\ \leq ||s^{h,1}||^2 + C[h^{2m}+h^2+k^2] \\ +Ck\sum_{i=1}^{n}(C_{\nabla u}+\frac{C_u^2}{h+\nu}+\frac{1}{(h+\nu)^3}||\nabla e_1^i||^4)||s^{h,i+1}||^2, \\ where\ s^{h,n+1}=\frac{\phi^{n+1}-\phi^n}{k} \end{aligned} \tag{1.6.22}$$

In order to apply Gronwall's Lemma 3 in the inequality 1.6.22, we have to verify that

$$Ck(C_{\nabla u}+\frac{C_u^2}{h+\nu}+\frac{1}{(h+\nu)^3}||\nabla e_1^i||^4)<1.$$

To this end, we can first assume

$$Ck(C_{\nabla u}+\frac{C_u^2}{h+\nu})<\frac{1}{2}\ and\ \frac{Ck}{(h+\nu)^3}||\nabla e_1^i||^4<\frac{1}{2}.$$

Due to the first inequality, we have a bound on k in the form

$$k < \frac{h+\nu}{CC_{\nabla u}(h+\nu) + CC_u^2}.$$

For the second inequality we investigate case by case.

For $k \leq h$, it follows from the inverse inequality and theorem (7) that

$$\begin{aligned}\frac{Ck}{(h+\nu)^3}||\nabla e_1^i||^4 \leq \frac{Ckh^{-4}}{(h+\nu)^3}||e_1^i||^4 \leq \frac{Ck}{(h+\nu)^3}(1+\frac{k}{h})^4 \\ \leq \frac{Ck}{(h+\nu)^3} < \frac{1}{2}.\end{aligned}$$

Thus, we have a bound on k in the form $k < C(h+\nu)^3$.

For $h \leq k$, it follows from the theorem (7) that

$$\frac{Ck}{(h+\nu)^3}||\nabla e_1^i||^4 \leq \frac{Ck^{-1}}{(h+\nu)^5}(h^4+k^4) \leq \frac{2Ck^3}{(h+\nu)^5} < \frac{1}{2}.$$

It follows from the above calculations and theorem statement that

$$(C_{\nabla u} + \frac{C_u^2}{h+\nu} + \frac{1}{(h+\nu)^3}||\nabla e_1^i||^4)k < 1.$$

Now, we can apply discrete Gronwall's Lemma in the inequality (1.6.22) to have following bound

$$||\frac{\phi^{n+1}-\phi^n}{k}||^2 + (h+\nu)k\sum_{i=1}^{n}||\nabla\frac{\phi^{i+1}-\phi^i}{k}||^2 \leq C[h^{2m}+h^2+k^2] \tag{1.6.23}$$

Using the triangle inequality in the error decomposition (1.2.8), we obtain

$$||\frac{e_1^{n+1}-e_1^n}{k}||^2 + k\sum_{i=0}^{n}(h+\nu)||\nabla\frac{e_1^{n+1}-e_1^n}{k}||^2 \leq C[h^{2m}+h^2+k^2] \tag{1.6.24}$$

This result proves the theorem.

1.7 Correction Step Approximation

In this section we prove the unconditional stability and error estimate of the correction step approximation u_2^h. Over $0 \leq t \leq T < \infty$ the approximations u_2^h is bounded uniformly in Re.

Hence, the formulation (1.1.4) gives $O(h^2+k^2)$ accurate, unconditionally stable extension of correction step approximation to the time-dependent Navier-Stokes equations.

We start by proving stability of correction step approximation.

1.8 Stability of the CS Approximation

Theorem 10 *Let $f \in L^2(0,T;H^{-1}(\Omega))$, let u_1^h, u_2^h satisfy (1.1.3) and (1.1.4), respectively. Then for n=0,...,N-1,*

$$||u_2^{h,n+1}||^2 + 5h^2(h+\nu)^{-2}||u_1^{h,n+1}||^2 + k\sum_{i=1}^{n+1}(h+\nu)||\nabla u_2^{h,i}||^2$$
$$\leq C[||u_0^s||^2 + (h+\nu)^{-1}k\sum_{i=1}^{n+1}||f(t_i)||_{-1}^2].$$

Proof 7 *Take $v^h = u_2^{h,n+1} \in V^h$ in the equation (1.1.4). This gives with Cauchy-Schwarz and Young's inequality that*

$$\begin{aligned}
&\frac{1}{2k}(||u_2^{h,n+1}||^2 - ||u_2^{h,n}||^2) + (h+\nu)||\nabla u_2^{h,n+1}||^2 \\
&\leq (\frac{f(t_{n+1}) + f(t_n)}{2}, u_2^{h,n+1}) + \frac{\nu}{2}k(\nabla(\frac{u_1^{n+1} - u_1^{n+1}}{k}, \nabla u_2^{h,n+1}) \qquad (1.8.1) \\
&+\frac{1}{2}b^*(u_1^{h,n+1}, u_1^{h,n+1}, u_2^{h,n+1}) - \frac{1}{2}b^*(u_1^{h,n}, u_1^{h,n}, u_2^{h,n+1}) + h(\nabla u_1^{h,n}, \nabla u_2^{h,n})
\end{aligned}$$

It follows from Cauchy-Schwarz, Young's and triangle inequalities with the error estimate $e_1^i = u(t_i) - u_1^i$ *that*

$$\begin{aligned}
&\frac{\nu}{2}k(\nabla(\frac{u_1^{n+1} - u_1^n}{k}, \nabla u_2^{h,n+1}) \leq \mu(h+\nu)||\nabla u_2^{h,n+1}||^2 \\
&+\frac{\nu^2 k^2}{8\mu(h+\nu)}||\nabla(\frac{u^{n+1} - u^n}{k})||^2 + \frac{\nu^2 k}{8\mu(h+\nu)}k||\nabla(\frac{e_1^{n+1} - e_1^n}{k})||^2. \qquad (1.8.2)
\end{aligned}$$

Adding and subtracting $\frac{1}{2}b^*(u_1^{h,n+1}, u_1^{h,n}, u_2^{h,n+1})$ *to the nonlinear terms and applying the bound (1.2.4) followed by Cauchy-Schwarz, Young's and triangle inequalities with regularity assumption of* u*, we have*

$$
\begin{aligned}
&\frac{1}{2}b^*(u_1^{h,n+1},u_1^{h,n+1},u_2^{h,n+1})-\frac{1}{2}b^*(u_1^{h,n},u_1^{h,n},u_2^{h,n+1})\\
&\leq\frac{1}{2}[kb^*(u_1^{h,n+1},\frac{u_1^{h,n+1}-u_1^{h,n}}{k},u_2^{h,n+1})+kb^*(\frac{u_1^{h,n+1}-u_1^{h,n}}{k},u_1^{h,n},u_2^{h,n+1})]\\
&\leq 2\mu(h+\nu)||\nabla u_2^{h,n+1}||^2\\
&+\frac{1}{16\mu(h+\nu)^3}(h+\nu)k||\nabla(\frac{u_1^{h,n+1}-u_1^{h,n}}{k})||^2[(h+\nu)k||\nabla u_1^{h,n+1}||^2\\
&+(h+\nu)k||\nabla u_1^{h,n}||^2]\\
&\leq 2\mu(h+\nu)||\nabla u_2^{h,n+1}||^2\\
&+\frac{1}{8\mu(h+\nu)^3}(h+\nu)k||\nabla(\frac{e_1^{h,n+1}-e_1^{h,n}}{k})||^2[(h+\nu)k||\nabla u_1^{h,n+1}||^2\\
&+(h+\nu)k||\nabla u_1^{h,n}||^2]\\
&+\frac{1}{8\mu(h+\nu)^2}kC_{\nabla u_t}^2[(h+\nu)k||\nabla u_1^{h,n+1}||^2+(h+\nu)k||\nabla u_1^{h,n}||^2],\\
&\text{where } C_{\nabla u_t}=||\nabla(\frac{u^{n+1}-u^n}{k})||^2
\end{aligned}
\tag{1.8.3}
$$

Cauchy-Schwarz and Young's inequalities with $\mu = 1/10$ *give*

$$\frac{1}{2k}(||u_2^{h,n+1}||^2 - ||u_2^{h,n}||^2) + \frac{1}{2}(h+\nu)||\nabla u_2^{h,n+1}||^2$$
$$\leq \frac{5}{2(h+\nu)}||\frac{f(t_{n+1}) - f(t_n)}{2}||_{-1}^2$$
$$+\frac{5\nu^2k^2}{4(h+\nu)}C_{\nabla u_t}^2 + \frac{5\nu^2k}{4(h+\nu)^2}k(h+\nu)||\nabla(\frac{e_1^{n+1} - e_1^n}{k})||^2$$
$$+\frac{5h^2}{2(h+\nu)^2}(h+\nu)||\nabla u_1^{h,n+1}||^2 \tag{1.8.4}$$
$$+\frac{5}{4(h+\nu)^3}(h+\nu)k||\nabla(\frac{e_1^{h,n+1} - e_1^{h,n}}{k})||^2[(h+\nu)k||\nabla u_1^{h,n+1}||^2$$
$$+(h+\nu)k||\nabla u_1^{h,n}||^2]$$
$$+\frac{5}{4(h+\nu)^2}kC_{\nabla u_t}^2[(h+\nu)k||\nabla u_1^{h,n+1}||^2 + (h+\nu)k||\nabla u_1^{h,n}||^2]$$

Multiplying inequality by 2k and summing over all time levels followed by Lemma (6) and Theorem (9) give

$$
\begin{aligned}
&||u_2^{h,n+1}||^2 + \sum_{i=1}^{n+1}(h+\nu)||\nabla u_2^{h,i}||^2 \\
&\leq ||u_0^s||^2 + \frac{5}{(h+\nu)}k\sum_{i=1}^{n+1}||\frac{f(t_i)-f(t_{i-1})}{2}||_{-1}^2 \\
&+\frac{5\nu^2k^3}{2(h+\nu)}C_{\nabla u_t}^2 + \frac{5\nu^2k^2}{2(h+\nu)^2}C(h^{2m}+h^2+k^2) \\
&+\frac{5h^2}{(h+\nu)^2}(||u_0^s||^2 - ||u_1^{h,n+1}||^2 + \frac{1}{h+\nu}k\sum_{i=1}^{n+1}||f(t_i)||_{-1}^2) \\
&+\frac{5}{2(h+\nu)^2}(\frac{(h^{2m}+h^2+k^2)}{(h+\nu)} + k^2C_{\nabla u_t}^2)[2||u_0^s||^2 \\
&+\frac{1}{h+\nu}k\sum_{i=1}^{n+1}||f(t_i)||_{-1}^2 + \frac{1}{h+\nu}k\sum_{i=1}^{n+1}||f(t_i)||_{-1}^2]
\end{aligned}
\tag{1.8.5}
$$

After some algebraic manipulation, we have the following inequality

$$
\begin{aligned}
&||u_2^{h,n+1}||^2 + \frac{5h^2}{(h+\nu)^2}||u_1^{h,n+1}||^2 + \sum_{i=1}^{n+1}(h+\nu)||\nabla u_2^{h,i}||^2 \\
&\leq ||u_0^s||^2 + \frac{5}{(h+\nu)}k\sum_{i=1}^{n+1}||\frac{f(t_i)-f(t_{i-1})}{2}||_{-1}^2 \\
&+\frac{5\nu^2k^3}{2(h+\nu)}C_{\nabla u_t}^2 + \frac{5\nu^2k^2}{2(h+\nu)^2}C(h^{2m}+h^2+k^2) \\
&+C(||u_0^s||^2 + \frac{1}{h+\nu}k\sum_{i=1}^{n+1}||f(t_i)||_{-1}^2)
\end{aligned}
\tag{1.8.6}
$$

The last inequality implies the theorem statement.

The result of Theorem (10), combined with the result Proposition (4), proves the unconditional stability of both $u_1^{h,i}$ and $u_2^{h,i}$ for any $i \geq 0$.

Next we will prove the error estimate of correction step approximation.

1.9 Error Estimate of CS Approximation

Theorem 11 *Let the assumptions of Theorem (9) be satisfied. Let*

$$k < \frac{h+\nu}{(h+\nu)C_{\nabla u} + 2C_u^2 + (h+\nu)Ch^{m-1} + 2Ch^{2m}}.$$

Then there exists a constant $C = C(\Omega, T, u, p, f, h+\nu)$, such that

$$\max_{1\leq i\leq N} ||u(t_i) - u_2^{h,i}|| + (k\sum_{i=0}^{n}(h+\nu)||\nabla(u(t_i) - u_2^{h,i})||^2)^{1/2}$$
$$\leq C(h^m + h^2 + k^2 + hk).$$

Proof 8 *By Taylor expansion around $t = \frac{t_{n+1}+t_n}{2}$, we have $\frac{u^{n+1}-u^n}{k} - \frac{u_t^{n+1}+u_t^n}{2} = k^2\rho^{n+1}$, where $\rho^{n+1} = \frac{u_{ttt}^{n+\frac{1}{2}}}{8}$.*

Summing variational formulations of NSE at $t = t_n$ and at $t = t_{n+1}$, and then, dividing by 2, we have the following equation.

$$
\begin{aligned}
(\frac{u^{n+1}-u^n}{k},v)+\frac{\nu}{2}(\nabla(\frac{u^{n+1}+u^n}{2}),\nabla v)+\frac{1}{2}b^*(u^{n+1},u^{n+1},v)& \\
+\frac{1}{2}b^*(u^n,u^n,v)-(\frac{p^{n+1}+p^n}{2},\nabla.v)& \\
=(\frac{f(t_{n+1})+f(t_n)}{2},v)-(\frac{u_t^{n+1}+u_t^n}{2},v)+(\frac{u^{n+1}-u^n}{k},v)&
\end{aligned}
\tag{1.9.1}
$$

Subtracting (1.1.4) from the equation (1.9.1) and using error decomposition (1.2.8), we have

$$
\begin{aligned}
(\frac{\phi_2^{h,n+1}-\phi_2^{h,n}}{k},\phi_2^{h,n+1})+(h+\nu)(\nabla\phi_2^{h,n+1},\nabla\phi_2^{h,n+1})& \\
=\frac{\nu}{2}k(\nabla(\frac{e_1^{h,n+1}-e_1^{h,n}}{k}),\nabla\phi_2^{h,n+1})+(\frac{p^{h,n+1}+p^{h,n}}{2}-p_2^{n+1},\nabla.\phi_2^{h,n+1})& \\
-b^*(u^{n+1},\phi_2^{h,n+1},\phi_2^{h,n+1})+b^*(u^{n+1},\eta_2^{n+1},\phi_2^{h,n+1})& \\
-b^*(\phi_2^{h,n+1},u_2^{h,n+1},\phi_2^{h,n+1})+b^*(\eta_2^{n+1},u_2^{h,n+1},\phi_2^{h,n+1})& \\
+\frac{1}{2}kb^*(\frac{u^{n+1}-u^n}{k},e_1^{h,n},\phi_2^{h,n+1})+\frac{1}{2}kb^*(u^{n+1},\frac{e_1^{h,n+1}-e_1^{h,n}}{k},\phi_2^{h,n+1})& \\
+\frac{1}{2}kb^*(e_1^{h,n+1},\frac{u_1^{h,n+1}-u_1^{h,n}}{k},\phi_2^{h,n+1})+\frac{1}{2}kb^*(\frac{e_1^{h,n+1}-e_1^{h,n}}{k},u_1^{h,n},\phi_2^{h,n+1})& \\
h(\nabla e_1^{h,n+1},\nabla\phi_2^{h,n+1})+k^2(\rho^{n+1},\phi_2^{h,n+1})+(\frac{\eta_2^{n+1}-\eta_2^n}{k},\phi_2^{h,n+1})& \\
+(h+\nu)(\nabla\eta_2^{n+1},\nabla\phi_2^{h,n+1})&
\end{aligned}
\tag{1.9.2}
$$

We bound the nonlinear terms on the right hand side of (1.9.2), starting now with the second, fifth and sixth terms. Use the bound (1.2.4), regularity assumption of u

and Young's inequality to obtain

$$|b^*(u^{n+1},\eta_2^{n+1},\phi_2^{h,n+1})| \le \mu(h+\nu)||\nabla\phi_2^{h,n+1}||^2 + \frac{C_{\nabla u}^2}{4\mu(h+\nu)}||\nabla\eta_2^{n+1}||^2 \tag{1.9.3}$$

$$|\frac{1}{2}kb^*(\frac{u^{n+1}-u^n}{k},e_1^{h,n},\phi_2^{h,n+1})| \le \mu(h+\nu)||\nabla\phi_2^{h,n+1}||^2 + \frac{k^2C_{\nabla u_t}^2}{16\mu(h+\nu)}||\nabla e_1^{h,n}||^2 \tag{1.9.4}$$

$$|\frac{1}{2}kb^*(u^{n+1},\frac{e_1^{h,n+1}-e_1^{h,n}}{k},\phi_2^{h,n+1})| \le \mu(h+\nu)||\nabla\phi_2^{h,n+1}||^2 + \frac{k^2C_{\nabla u}^2}{16\mu(h+\nu)}||\nabla(\frac{e_1^{h,n+1}-e_1^{h,n}}{k})||^2 \tag{1.9.5}$$

In order to obtain bounds on the third and the fourth terms, we use the error decomposition (1.2.8), triangle inequality, bound (2), regularity assumption of u and Young's inequality

$$
\begin{aligned}
|b^*(\phi_2^{h,n+1}, u_2^{h,n+1}, \phi_2^{h,n+1})| &\le |b^*(\phi_2^{h,n+1}, u^{h,n+1}, \phi_2^{h,n+1})| \\
&\quad + |b^*(\phi_2^{h,n+1}, \eta_2^{n+1}, \phi_2^{h,n+1})| \\
&\le 2\mu(h+\nu)||\nabla \phi_2^{h,n+1}||^2 \\
+||\phi_2^{h,n+1}||^2 &(\frac{C_{\nabla u}}{2} + \frac{C_u^2}{16\mu(h+\nu)} + \frac{1}{2}||\nabla \eta_2^{n+1}|| + \frac{1}{16\mu(h+\nu)}||\nabla \eta_2^{n+1}||^2)
\end{aligned} \tag{1.9.6}
$$

$$
\begin{aligned}
|b^*(\eta_2^{n+1}, u_2^{h,n+1}, \phi_2^{h,n+1})| &\le |b^*(\eta_2^{n+1}, u^{h,n+1}, \phi_2^{h,n+1})| + |b^*(\eta_2^{n+1}, \eta_2^{n+1}, \phi_2^{h,n+1})| \\
&\le 2\mu(h+\nu)||\nabla \phi_2^{h,n+1}||^2 \\
&\quad + \frac{1}{4\mu(h+\nu)}||\nabla \eta_2^{n+1}||^2 (C_{\nabla u}^2 + ||\nabla \eta_2^{n+1}||^2)
\end{aligned} \tag{1.9.7}
$$

For the bounds on the seventh and the eighth terms, we use the error decomposition $u_1^{h,n} = u^n - e_1^{h,n}$*, triangle inequality, bound (1.2.4), regularity assumptions of* u *and Young's inequality*

$$
\begin{aligned}
|\frac{1}{2}kb^*(e_1^{h,n+1}, \frac{u_1^{h,n+1} - u_1^{h,n}}{k}, \phi_2^{h,n+1})| &\le |\frac{1}{2}kb^*(e_1^{h,n+1}, \frac{e_1^{h,n+1} - e_1^{h,n}}{k}, \phi_2^{h,n+1})| \\
+|\frac{1}{2}kb^*(e_1^{h,n+1}, \frac{u^{n+1} - u^n}{k}, \phi_2^{h,n+1})| &\le 2\mu(h+\nu)||\nabla \phi_2^{h,n+1}||^2 \\
+\frac{1}{16\mu(h+\nu)}||\nabla e_1^{h,n+1}||^2 &(k^2 C_{\nabla u_t}^2 + k^2||\nabla(\frac{e_1^{h,n+1} - e_1^{h,n}}{k})||^2)
\end{aligned} \tag{1.9.8}
$$

$$
\begin{aligned}
|\frac{1}{2}kb^*(\frac{e_1^{h,n+1}-e_1^{h,n}}{k},u_1^{h,n},\phi_2^{h,n+1})| \leq |\frac{1}{2}kb^*(\frac{e_1^{h,n+1}-e_1^{h,n}}{k},u^n,\phi_2^{h,n+1})| \\
+|\frac{1}{2}kb^*(\frac{e_1^{h,n+1}-e_1^{h,n}}{k},e_1^{h,n},\phi_2^{h,n+1})| \leq 2\mu(h+\nu)||\nabla\phi_2^{h,n+1}||^2 \\
+\frac{1}{16\mu(h+\nu)}||\nabla(\frac{e_1^{h,n+1}-e_1^{h,n}}{k})||^2(k^2C_{\nabla u}^2+k^2||\nabla e_1^{h,n}||^2)
\end{aligned}
\tag{1.9.9}
$$

Apply the Cauchy-Schwarz and Young's inequality to (1.9.2). Since $||\nabla.\phi_2^{h,n+1}||^2 \leq d||\nabla\phi_2^{h,n+1}||^2$ *for all* $\mu > 0$

$$
\begin{aligned}
&\frac{||\phi_2^{h,n+1}||^2-||\phi_2^{h,n}||^2}{2k}+(1-16\mu)(h+\nu)||\nabla\phi_2^{h,n+1}||^2\\
&\leq \frac{d}{4\mu(h+\nu)}\inf_{q^h\in Q^h}||\frac{p^{h,n+1}+p^{h,n}}{2}-q^{h,n+1}||^2\\
&+\frac{\nu^2k^2}{16\mu(h+\nu)}||\nabla(\frac{e_1^{h,n+1}-e_1^{h,n}}{k})||^2\\
&+\frac{h^2}{4\mu(h+\nu)}||\nabla e_1^{h,n+1}||^2+\frac{k^4}{4\mu(h+\nu)}||\rho^{n+1}||_{-1}^2\\
&+\frac{1}{4\mu(h+\nu)}||\frac{\eta_2^{n+1}-\eta_2^n}{k}||_{-1}^2+\frac{h+\nu}{4\mu}||\nabla\eta_2^{n+1}||^2+\frac{C_{\nabla u}^2}{4\mu(h+\nu)}||\nabla\eta_2^{n+1}||^2\\
&+\frac{k^2C_{\nabla u_t}^2}{16\mu(h+\nu)}||\nabla e_1^{h,n}||^2+\frac{k^2C_{\nabla u}^2}{16\mu(h+\nu)}||\nabla(\frac{e_1^{h,n+1}-e_1^{h,n}}{k})||^2\\
&+||\phi_2^{h,n+1}||^2(\frac{C_{\nabla u}}{2}+\frac{C_u^2}{16\mu(h+\nu)}+\frac{1}{2}||\nabla\eta_2^{n+1}||+\frac{1}{16\mu(h+\nu)}||\nabla\eta_2^{n+1}||^2)\\
&+\frac{1}{4\mu(h+\nu)}||\nabla\eta_2^{n+1}||^2(C_{\nabla u}^2+||\nabla\eta_2^{n+1}||^2)\\
&+\frac{k^2}{16\mu(h+\nu)}||\nabla e_1^{h,n+1}||^2(C_{\nabla u_t}^2+||\nabla(\frac{e_1^{h,n+1}-e_1^{h,n}}{k})||^2)\\
&+\frac{k^2}{16\mu(h+\nu)}||\nabla(\frac{e_1^{h,n+1}-e_1^{h,n}}{k})||^2(C_{\nabla u}^2+||\nabla e_1^{h,n}||^2)
\end{aligned}
\tag{1.9.10}
$$

Take $\mu=1/32$, multiply (1.9.10) by 2k and sum over all time levels. It follows from the regularity assumptions of theorem that

$$
k\sum_{i=0}^{n}||\rho^{i+1}||_{-1}^2k^4\leq Ck\sum_{i=0}^{n}||\rho^{i+1}||^2k^4\leq Ck^4
$$

Therefore we obtain

$$
\begin{aligned}
||\phi_2^{h,n+1}||^2 + (h+\nu)k\sum_{i=0}^{n}||\nabla\phi_2^{h,i+1}||^2 \\
\leq \frac{C}{h+\nu}k\sum_{i=0}^{n}\Big[\inf_{q^h\in Q^h}||\frac{p^{h,i+1}+p^{h,i}}{2} - q^{h,i+1}||^2 \\
k^2||\nabla(\frac{e_1^{i+1}-e_1^{i+1}}{k})||^2 + h^2||\nabla e_1^{i+1}||^2 + k^4 + ||\frac{\eta_2^{i+1}-\eta_2^i}{k}||_{-1}^2 \\
+||\nabla\eta_2^{i+1}||^2 + k^2||\nabla e_1^{i+1}||^2 + ||\nabla\eta_2^{i+1}||^4 \\
+k||\nabla(\frac{e_1^{i+1}-e_1^{i+1}}{k})||^2(k||\nabla e_1^{i+1}||^2 + k||\nabla e_1^i||^2) \\
+k\sum_{i=0}^{n}||\phi_2^{h,i+1}||^2\Big[\frac{C_{\nabla u}}{2} + \frac{2C_u^2}{(h+\nu)} + \frac{1}{2}||\nabla\eta_2^{i+1}|| \\
+\frac{2}{h+\nu}||\nabla\eta_2^{i+1}||^2\Big] + ||\phi_2^{h,0}||^2
\end{aligned}
\tag{1.9.11}
$$

Take $\tilde{u}^i$ in the error decomposition (1.2.8) to be the L^2-projection onto V^h, for $i \geq 1$. Take $\tilde{u}^0$ to be u_0^s. This gives $\phi_2^{h,0} = 0$ and $e_1^0 = \eta_2^0$. Also it follows from the Proposition (5) that $||\eta_2^0|| \leq Ch^m$; under the assumption of the theorem applying the discrete Gronwall's lemma (3) and using bounds in theorems (7), (9), give

$$
\begin{aligned}
&||\phi_2^{h,n+1}||^2 + (h+\nu)k\sum_{i=0}^{n}||\nabla\phi_2^{h,i+1}||^2 \\
&\leq \frac{C}{h+\nu}k\sum_{i=0}^{n}\Big[\inf_{q^h\in Q^h}||\frac{p^{h,i+1}+p^{h,i}}{2}-q^{h,i+1}||^2 \\
&\quad +\frac{k^2}{h+\nu}(h^2+k^2)+\frac{h^2}{h+\nu}(h^2+k^2)+k^4 \\
&\quad +||\frac{\eta_2^{i+1}-\eta_2^i}{k}||_{-1}^2+||\nabla\eta_2^{i+1}||^2+||\nabla\eta_2^{i+1}||^4 \\
&\quad +\frac{k}{(h+\nu)^2}(h^2+k^2)(h^2+k^2)\Big]+Ch^{2m}
\end{aligned}
\tag{1.9.12}
$$

Use the approximation properties of X^h, Q^h. Since the mesh nodes do not depend upon the time level, it follows from (1.2.5), (1.2.6) that

$$
\begin{aligned}
k\sum_{i=0}^{n}\inf_{q^h\in Q^h}||\frac{p^{h,i+1}+p^{h,i}}{2}-q^{h,i+1}||^2 &\leq Ch^{2m}, \\
k\sum_{i=0}^{n}||\frac{\eta_2^{i+1}-\eta_2^i}{k}||_{-1}^2 \leq Ck\sum_{i=0}^{n}||\frac{\eta_2^{i+1}-\eta_2^i}{k}||^2 &\leq Ch^{2m}, \\
k\sum_{i=0}^{n}||\eta_2^{i+1}||^2 &\leq Ch^{2m}.
\end{aligned}
\tag{1.9.13}
$$

Bounds (1.9.12) and (1.9.13) give the following result

$$
\begin{aligned}
&||\phi_2^{h,n+1}||^2 + (h+\nu)k\sum_{i=0}^{n}||\nabla\phi_2^{h,i+1}||^2 \\
&\leq \frac{C}{(h+\nu)^2}(h^{2m}+h^4+k^4+h^2k^2).
\end{aligned}
\tag{1.9.14}
$$

Using the error decomposition and triangle inequality with (1.9.14), we obtain

$$
\begin{aligned}
&||e_2^{h,n+1}|| + ((h+\nu)k\sum_{i=0}^{n}||\nabla e_2^{h,i+1}||^2)^{\frac{1}{2}} \\
&\leq \frac{C}{(h+\nu)}(h^m+h^2+k^2+hk).
\end{aligned}
\tag{1.9.15}
$$

This proves the Theorem (11). Thus, we derived the error estimates, that agree with the general theory of the defect and deferred correction methods. Briefly, the Correction Step approximation u_2^h is improved by an order of h in space and of k in time, compared to the Artificial Viscosity approximation u_1^h.

Next, we will give some computational results.

1.10 Computational Tests

We perform one quantitative and one qualitative test of the proposed regularization procedure. In both tests the non-homogeneous Dirichlet boundary conditions are implemented, and the computational results support the theoretical findings.

1.11 Quantitative Test

For the quantitative assessment, consider a two-dimensional problem with a known exact solution. The traveling wave solution of the NSE in $\Omega = [0.5, 1]^2$ is given by

$$u = \begin{pmatrix} 0.75 + 0.25\cos(2\pi(x-t))\sin(2\pi(y-t))exp(-8\pi^2 t\nu) \\ 0.75 - 0.25\sin(2\pi(x-t))\cos(2\pi(y-t))exp(-8\pi^2 t\nu) \end{pmatrix}, \tag{1.11.1}$$
$$p = -\frac{1}{64}(\cos(4\pi(x-t)) + \cos(4\pi(y-t)))exp(-16\pi^2 t\nu),$$

and the right-hand side f and initial condition u_0 are computed so that (1.11.1) satisfies (4.1.1). The final time in the computations is taken to be $T = 1$.

In order to verify the theoretical claims on the convergence rates, we take the time step equal to the mesh diameter, $\Delta t = h$.

For $\nu = \frac{1}{100}$ the calculated convergence rates in Tables 1.1 and 1.2 confirm what is predicted by Theorems (7) and (11) for (P_2, P_1) Taylor-Hood finite elements: the convergence rates are doubled after the correction step. Notice also the asymptotic character of convergence, typical of the defect correction methods.

Table 1.1
AV approximation, $\nu = 0.01$.

N	$\|\| u - u_1^h \|\|_{L^2(0,T;L^2(\Omega))}$	rate	$\|\| u - u_1^h \|\|_{L^2(0,T;H^1(\Omega))}$	rate
8	0.0139742	-	0.23282	-
16	0.00945258	0.56	0.179798	0.37
32	0.00580328	0.70	0.123682	0.54
64	0.00331349	0.81	0.0766837	0.69
128	0.00178142	0.90	0.0433087	0.82
256	0.000922772	0.95	0.0228883	0.92

Table 1.2
Correction step approximation, $\nu = 0.01$.

N	$\| u - u_2^h \|_{L^2(0,T;L^2(\Omega))}$	rate	$\| u - u_2^h \|_{L^2(0,T;H^1(\Omega))}$	rate
8	0.0106313	-	0.189918	-
16	0.0060028	0.83	0.128519	0.56
32	0.00272105	1.14	0.0710604	0.86
64	0.000993846	1.45	0.0314236	1.18
128	0.000302142	1.72	0.0111824	1.49
256	0.0000817667	1.89	0.00336761	1.73

As the viscosity coefficient ν decreases, the convergence rates improve slower - see the results for the flow at $\nu = \frac{1}{2000}$ in Tables 1.3 and 1.4.

Table 1.3
AV approximation, $\nu = 0.0005$.

N	$\| u - u_1^h \|_{L^2(0,T;L^2(\Omega))}$	rate	$\| u - u_1^h \|_{L^2(0,T;H^1(\Omega))}$	rate
8	0.0262208	-	0.439399	-
16	0.0188948	0.47	0.367997	0.26
32	0.0125722	0.59	0.291022	0.34
64	0.00776946	0.69	0.2206	0.40
128	0.00443914	0.81	0.159449	0.49
256	0.00237518	0.9	0.108957	0.55

Table 1.4
Correction step approximation, $\nu = 0.0005$.

N	$\| u - u_2^h \|_{L^2(0,T;L^2(\Omega))}$	rate	$\| u - u_2^h \|_{L^2(0,T;H^1(\Omega))}$	rate
8	0.0217697	-	0.396863	-
16	0.0141143	0.63	0.32536	0.29
32	0.00777988	0.86	0.249133	0.39
64	0.0036525	1.09	0.178223	0.48
128	0.00152888	1.26	0.118064	0.59
256	0.000597594	1.36	0.0709845	0.73

To further comment on the asymptotic nature of convergence of defect correction methods, notice that the a priori error estimates have the term $(h+\nu)^{-1}$ in the right hand side. This decreases the convergence rates on the coarse meshes, where $h >> \nu$. The term that contains $\nabla(u-u_i^h), i=1,2$ in the left hand side is also proportional to $(h+\nu)$, which further decreases the convergence rates in the H^1-seminorm on coarse meshes for problems with high Reynolds number. We also ran the same tests (not shown here) with $\Delta t = h^2$ and obtained the convergence rates very similar to those presented above, which indicates that the reduced convergence rates are due to the asymptotic behaviour of the defect correction, and not the deferred correction part of the error.

1.12 Qualitative Test

For the qualitative assessment, consider the 2-D flow past an obstacle, at high Reynolds number $Re = 600$. The von Karman vortex street is expected to be seen for a fully resolved flow; on a coarse mesh with $h \sim \frac{1}{32}$ the true solution demonstrates the oscillatory behavior past the obstacle (Figure 1.1). Note that the solution is known to depend on the Reynolds number in the following manner: for $1 < Re < 10$ the flow is no longer symmetric behind the obstacle, for $10 < Re < 100$ re-circulation areas appear in the wake behind the obstacle and, as the Reynolds number grows beyond $Re = 100$, these vortices develop and start to oscillate. Roughly at $Re = 1000$

turbulence develops and the coherent structures in the flow disappear.

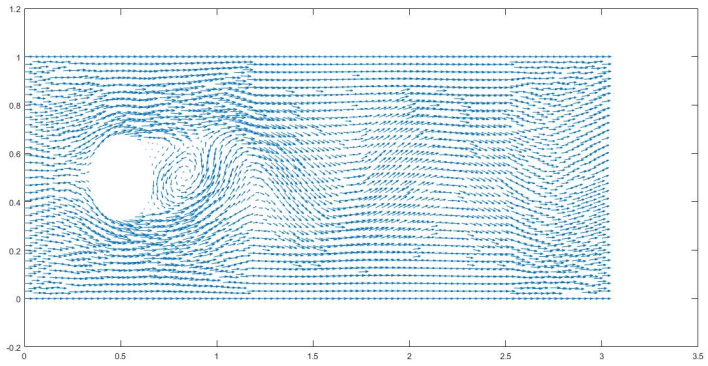

Figure 1.1: DNS velocity field u

We compute the defect step solution u_1 and the corrected solution u_2 on the same coarse mesh with 32 nodes per unit boundary ($h \sim \frac{1}{32}$). The domain is $\Omega = [0,1] \times [0,3]$ with a circle of radius 0.15, centered at $(0.5, 0.5)$, cut out of Ω. The parabolic inflow on the left boundary is introduced, with zero forcing. The results were computed with $Re = 600$, $T = 20$, $\Delta t = h$.

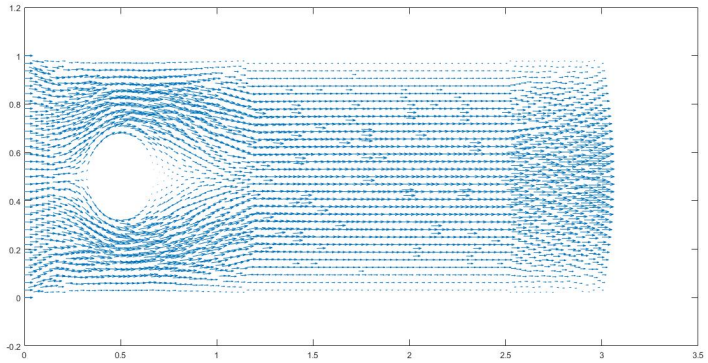

Figure 1.2: AV Approximation u_1^h

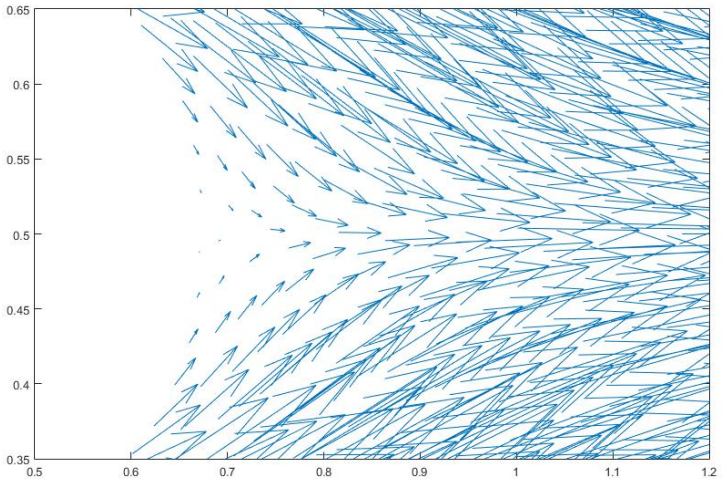

Figure 1.3: AV Approximation zoomed in

As seen in Figures 1.2 and 1.3, artificial viscosity approximation gives a result that cannot capture the flow pattern due to high viscosity coefficient and low accuracy of the AV approximation.

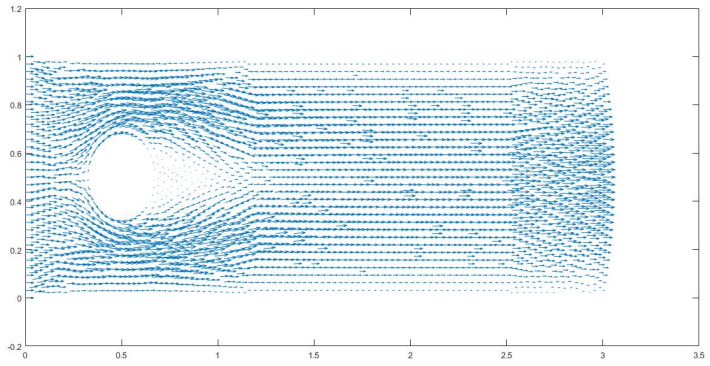

Figure 1.4: CS Approximation u_2^h

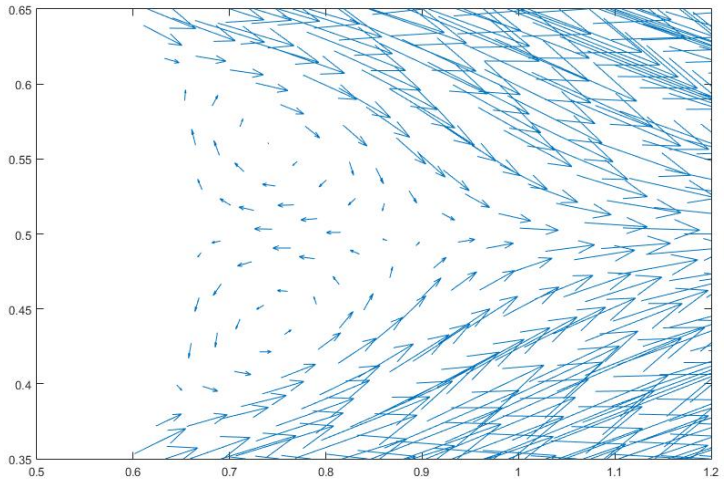

Figure 1.5: CS Approximation Zoomed in

Although the correction solution is computed with the same viscosity coefficient as the AV approximation, it gives some qualitative features of the flow pattern even on the coarse mesh - one can clearly see the re-circulation regions in the wake. This demonstrates the qualitative behavior of the correction step solution: it behaves as if the Reynolds number of the flow was increased, although the matrix of the system remains the same as in the AV case. Thus, the benefits of using the correction procedure are clear: for virtually no extra cost (when the parallelization is implemented) one can model turbulent flows at increasing Reynolds numbers (the interesting possibility that two or three correction steps would deepen this effect is yet to be explored).

Chapter 2

Two Approaches to Creating a Turbulence Model with Increased Temporal Accuracy

2.1 Introduction

The motion of incompressible fluid flow in the flow domain $\Omega = (0, L)^d$ is governed by the Navier-Stokes equations: find the velocity-pressure pair $u : \Omega \times [0, T] \ \rightarrow \mathbb{R}^d \, (d =$

2, 3) and $p : \Omega \times (0, T] \to \mathbb{R}$ satisfying

$$u_t + u \cdot \nabla u - \nu \Delta u + \nabla p = f, \text{ for } x \in \Omega, 0 < t \leq T \tag{2.1.1}$$

$$\nabla \cdot u = 0, \ x \in \Omega, \text{ for } 0 \leq t \leq T,$$

$$u(x, 0) = u_0(x), \text{ for } x \in \Omega,$$

with the normalization condition $\int_\Omega p(x, t)\ dx = 0$ for $0 < t \leq T$. Throughout this paper, we consider the case of periodic boundary conditions.

According to the Kolmogorov $K41$ theory, there exists a continuum of scales in turbulent fluid flow, with the smallest scales (in the case of a $3 - D$ flow) being of the order $O(Re^{-3/4})$, where the Reynolds number Re is inverse proportional to the viscosity coefficient ν. Thus, capturing all the small structures in a turbulent flow requires the number of mesh points in space for each time step to be $O(Re^{9/4})$ for three-dimensional problems. It is not uncommon to have $Re \sim O(10^8 - 10^12)$ in real-life applications.

Hence, the direct numerical simulation (DNS) of a $3 - D$ turbulent flow is often not computationally economical or even feasible. On the other hand, the largest structures in the flow (containing most of the energy in the flow) are responsible

for much of the mixing and most of the momentum transport. This observation led to several numerical regularizations; one of these is Large Eddy Simulation (LES) [41, 42, 43] which is based on the idea that the flow can be represented by a collection of scales with different sizes, and instead of trying to approximate all of them down to the smallest one, one defines a filter width $\delta > 0$ and computes only the scales of size bigger than δ (large scales), whereas the effect of the small scales on the large scales is modeled. This reduces the number of degrees of freedom in a simulation and accurately represents the large structures in the flow.

If $(\cdot)^\delta$ denotes a local, spacing averaging operator that commutes with differentiation, then averaging (4.1.1) gives the following non-closed equations for $\overline{u}^\delta$ and $\overline{p}^\delta$ in $(0,T)\times\Omega$:

$$\overline{u}_t^\delta + \nabla\cdot(\overline{u}^\delta\overline{u^T}^\delta) - \nu\Delta\overline{u}^\delta + \nabla\overline{p}^\delta + \nabla\cdot(\overline{uu^T}^\delta - \overline{u}^\delta\overline{u^T}^\delta) = \overline{f}^\delta, \tag{2.1.2a}$$

$$\nabla\cdot\overline{u}^\delta = 0. \tag{2.1.2b}$$

An LES model arises when one tries to close the system (2.1.2) by choosing an approximation to the last term on the left-hand side of (2.1.2a). Many different LES regularizations have been proposed and studied; we consider the family of Approximate Deconvolution Models (ADMs) that allow for arbitrarily high spatial accuracy. These models were introduced by Stolz and Adams in [1] and extensively studied;

see, e.g., [2, 3, 4, 5, 6, 8]. Given the family of Approximate Deconvolution operators G_N defined in Section 2, the Approximate Deconvolution Model for turbulent Navier-Stokes equations is given by

$$w_t + \nabla \cdot \overline{(G_N w)(G_N w)^T}^{\delta} - \nu \Delta w + \nabla \overline{q}^{\delta} = \overline{f}^{\delta}, \tag{2.1.3a}$$

$$\nabla \cdot w = 0, \tag{2.1.3b}$$

subject to $w(0,x) = \overline{u}_0^{\delta}(x)$ and periodic boundary conditions (with zero means).

We begin by introducing the simplest approximate deconvolution model of turbulence; see, e.g., [3]. To this end, a filtering operator needs to be chosen that commutes with differentiation under periodic boundary conditions. Throughout this paper, we shall use the self-adjoint filtering operator $A^{-1} = (I - \delta^2 \Delta)^{-1}$ defined in Section 2.2.

The zeroth ($N = 0$) ADM, written in the traditional variational formulation (and with the exact deconvolution operator A applied to both sides of (2.1.3a)), seeks $(w, q) \in ((X \bigcap H^2(\Omega)), Q)$ such that for any $(v, \chi) \in (X, Q)$

$$(Aw_t, v) + \nu(A\nabla w, \nabla v) + b^*(w, w; v) - (q, \nabla \cdot v) = (f, v), \tag{2.1.4}$$

$$(\nabla \cdot w, \chi) = 0,$$

where the pair of model variables (w, q) approximates the averaged velocity $\bar{u}$ and the pressure p of the Navier-Stokes equations. Note, however, that with the given choice of the filtering operator A we get a fourth order term $\nu\delta^2(\Delta w, \Delta v)$ in (2.1.4). In order to avoid using C^1 elements, we follow [3] and employ the mixed variational formulation: find $(w^h, \zeta^h, q^h) \in (X^h, X^h, Q^h)$ such that for any $(v^h, \xi^h, \chi^h) \in (X^h, X^h, Q^h)$

$$\begin{aligned}(w_t^h, v^h) + \delta^2(\nabla w_t^h, \nabla v^h) + \nu(\nabla w^h, \nabla v^h) + \nu\delta^2(\nabla \zeta^h, \nabla v^h) \\ +b^*(w^h, w^h; v^h) - (q^h, \nabla \cdot v^h) = (f, v^h), \\ (\nabla w^h, \nabla \xi^h) = (\zeta^h, \xi^h), \\ (\nabla \cdot w^h, \chi^h) = 0.\end{aligned} \tag{2.1.5}$$

The velocity space X and the pressure space Q are defined in Section 2.2, along with the corresponding velocity-pressure finite element spaces X^h, Q^h.

In addition to having other advantages, the ADMs were applied in different areas, including magnetohydrodynamics and the compressible Navier-Stokes equations. High spatial accuracy is achieved, but the time discretization was always performed by a low-order backward Euler or Crank-Nicolson method which introduces non-physical

oscillations. But because solving the Navier-Stokes equations is computationally expensive even with turbulence models, one usually cannot choose the time step significantly smaller than the mesh size. Hence, one of the main advantages of the ADMs, the increased spatial accuracy, cannot be taken full advantage of unless it is combined with a high-accuracy time discretization. The proposed method also needs to be stable and allow for explicit-implicit implementations with different time scales.

To that end, [71] employs the spectral deferred correction (SDC) method, proposed for stiff ODEs by Dutt et al., [39], and further developed by Minion et al.; see [34, 36, 106] and the references therein. SDC methods were studied and compared to intrinsically high-order methods such as additive Runge-Kutta methods and linear multistep methods based on BDFs, with the conclusion that the SDC methods are at least comparable to the latter. In addition, achieving high accuracy for the turbulent NSE using Runge-Kutta-based methods is very expensive, and the BDF-based methods typically do not perform well in problems where relevant time scales associated with different terms in the equation are widely different; see, e.g., [36] for an example of an advection-diffusion-reaction problem for which the SDC is the best choice for high-accuracy temporal discretization.

It is also important to notice that in some situations there aren't many obvious approaches to increasing the temporal accuracy, with deferred correction being the only choice. For example, when one seeks a method to decouple a complex system

in a stable way, one typically develops a first order accurate method; increasing the accuracy of such a method through deferred correction might be possible - see, e.g., [38]. In fact, the atmosphere-ocean-type setting, discussed in [38], was the main motivating factor for the authors. When one or both of the flows in the fluid-fluid coupling become turbulent, the researcher must find a decoupling method which has to be stable, preferably accurate, and allow for a built-in turbulence model. The first step in that direction is the combination of a turbulence model (ADM chosen here) and a deferred correction technique - simply because there is currently no result, other than [38], that allows for a decoupled, stable and higher order accurate approximation.

The two-step deferred correction method for ADM, introduced and studied in [71], computes (w_1^h, q_1^h) and (w_2^h, q_2^h), two consecutive approximations for the averaged velocity and pressure $(\bar{u}, p)$. These approximations satisfy the following equations for $(w_1^{h,n+1}, \zeta_1^{h,n+1}, q_1^{h,n+1})$, $(w_2^{h,n+1}, \zeta_2^{h,n+1}, q_2^{h,n+1}) \in (X^h, X^h, Q^h), \forall (v^h, \xi^h, \chi^h) \in$

(X^h, X^h, Q^h) at $t = t_{n+1}$, $n \geq 0$, with $k := \Delta t = t_{i+1} - t_i$:

$$(\frac{w_1^{h,n+1} - w_1^{h,n}}{k}, v^h) + \delta^2(\nabla(\frac{w_1^{h,n+1} - w_1^{h,n}}{k}), \nabla v^h) + \nu(\nabla w_1^{h,n+1}, \nabla v^h) \tag{2.1.6a}$$

$$+ \nu\delta^2(\nabla\zeta_1^{h,n+1}, \nabla v^h) + b^*(w_1^{h,n+1}, w_1^{h,n+1}, v^h) - (q_1^{h,n+1}, \nabla \cdot v^h) = (f(t_{n+1}), v^h),$$

$$(\frac{w_2^{h,n+1} - w_2^{h,n}}{k}, v^h) + \delta^2(\nabla(\frac{w_2^{h,n+1} - w_2^{h,n}}{k}), \nabla v^h) + \nu(\nabla w_2^{h,n+1}, \nabla v^h) \tag{2.1.6b}$$

$$+ \nu\delta^2(\nabla\zeta_2^{h,n+1}, \nabla v^h) + b^*(w_2^{h,n+1}, w_2^{h,n+1}, v^h) - (q_2^{h,n+1}, \nabla \cdot v^h)$$

$$= (\frac{f(t_{n+1}) + f(t_n)}{2}, v^h) + \frac{\nu}{2}k(\nabla(\frac{w_1^{h,n+1} - w_1^{h,n}}{k}), \nabla v^h) - \frac{1}{2}k(\frac{q_1^{h,n+1} - q_1^{h,n}}{k}, \nabla \cdot v^h)$$

$$+ \frac{\nu}{2}\delta^2 k(\nabla(\frac{\zeta_1^{h,n+1} - \zeta_1^{h,n}}{k}), \nabla v^h) + \frac{1}{2}(b^*(w_1^{h,n+1}, w_1^{h,n+1}, v^h) - b^*(w_1^{h,n}, w_1^{h,n}, v^h)),$$

$$(\nabla w_j^{h,n+1}, \nabla \xi^h) = (\zeta_j^{h,n+1}, \xi^h), \ j = 1, 2, \tag{2.1.6c}$$

$$(\nabla \cdot w_j^{h,n+1}, \chi^h) = 0, \ j = 1, 2, \tag{2.1.6d}$$

where $b^*(\cdot, \cdot, \cdot)$ is the explicitly skew-symmetrized trilinear form, defined below. Note that the second step utilizes the same backward Euler time discretization as in the first step; only the right-hand side is modified by a known quantity, i.e, a known solution from the first step. This results in the computational attractiveness of the method: computing two low-order accurate approximations is much less costly (especially for very stiff problems) than computing a single higher-order approximation. We will refer to this method as ADM-DCM.

Unfortunately, the accuracy of the ADMs comes at a price: the mixed formulation (2.1.6) introduces an extra variable, which increases the size of the system. In some

areas (uncertainty quantification, control, etc.) it is vital to save as much computational time as possible, while trying not to ruin the quality of a solution. To that end, we propose a new method, which replaces (2.1.6a) with a less computationally expensive equation, saving up to 35% of CPU time needed for the ADM-DCM, when the method is run sequentially.

The paper is organized as follows. In Section 2.2, we introduce the necessary notations and preliminary results. The new method is introduced in section 2.3 and the stability and accuracy results are given. The numerical tests, given in Section 2.4, compare the proposed method to the one from [71] - quantitatively, qualitatively, and in terms of the required computational resources.

2.2 Mathematical preliminaries and notations

Throughout this paper, the norm $\|\cdot\|$ denotes the usual $L^2(\Omega)$-norm of scalars, vectors, and tensors, induced by the usual L^2 inner-product, denoted by $(\cdot,\cdot)$. The space that the velocity (at time t) belongs to is given by

$$X = H^1_{per}(\Omega)^d = \{v \in L^2(\Omega)^d : \nabla v \in L^2(\Omega)^{d\times d} \text{ and } v \text{ is periodic with period } L\}$$

equipped with the norm $\|v\|_X = \|\nabla v\|$. The space dual to X is equipped with the norm

$$\|f\|_{-1} = \sup_{v \in X} \frac{(f, v)}{\|\nabla v\|}.$$

The pressure (at time t) is sought in the space

$$Q = L^2_{per}(\Omega) = \{q : q \in L^2(\Omega), \int_\Omega q(x)dx = 0, q \text{ periodic with period } L\}.$$

Also introduce the space of weakly divergence-free functions

$$X \supset V = \{v \in X : (\nabla \cdot v, q) = 0, \forall q \in Q\}.$$

For measurable $v : [0, T] \to X$, we define

$$\|v\|_{L^p(0,T;X)} = (\int_0^T \|v(t)\|_X^p dt)^{\frac{1}{p}}, \ 1 \leq p < \infty$$

and

$$\|v\|_{L^\infty(0,T;X)} = ess \sup_{0\le t\le T} \|v(t)\|_X.$$

Define the trilinear form on $X \times X \times X$

$$b(u,v,w) = \int_\Omega u \cdot \nabla v \cdot w dx.$$

The following lemma is also necessary for the analysis

Lemma 12 *There exist finite constants $M = M(d)$ and $N = N(d)$ such that $M \ge N$ and*

$$M = \sup_{u,v,w\in X} \frac{b(u,v,w)}{\|\nabla u\|\|\nabla v\|\|\nabla w\|} < \infty \ , \ N = \sup_{u,v,w\in V} \frac{b(u,v,w)}{\|\nabla u\|\|\nabla v\|\|\nabla w\|} < \infty.$$

The proof can be found, for example, in [32]. The corresponding constants M^h and N^h are defined by replacing X by the finite element space $X^h \subset X$ and V by $V^h \subset X$, which will be defined below. Note that $M \ge \max(M^h, N, N^h)$ and that as $h \to 0$,

$N^h \to N$ and $M^h \to M$; see [32].

Throughout the paper, we shall assume that the velocity-pressure finite element spaces $X^h \subset X$ and $Q^h \subset Q$ are conforming, have typical approximation properties of finite element spaces commonly in use, and satisfy the discrete inf-sup, or LBB^h, condition

$$\inf_{q^h \in Q^h} \sup_{v^h \in X^h} \frac{(q^h, \nabla \cdot v^h)}{\|\nabla v^h\| \|q^h\|} \geq \beta^h > 0, \tag{2.2.1}$$

where β^h is bounded away from zero uniformly in h. Examples of such spaces can be found in [32]. We shall consider $X^h \subset X$, $Q^h \subset Q$ to be spaces of continuous piecewise polynomials of degree r and $r-1$, respectively, with $r \geq 1$.

The space of discretely divergence-free functions is defined as follows

$$V^h = \{v^h \in X^h : (q^h, \nabla \cdot v^h) = 0, \forall q^h \in Q^h\}.$$

The idea of approximate deconvolution modeling is based on the definition and properties of the following operator.

Definition 3 (Approximate Deconvolution Operator) *For a fixed finite N, define the Nth approximate deconvolution operator G_N by*

$$G_N\phi = \sum_{n=0}^{N}(I - A_\delta^{-1})^n\phi,$$

where the averaging operator A_δ^{-1} is the differential filter: given $\phi \in L^2(\Omega)$, $\overline{\phi}^\delta \in H^2(\Omega)$ is the unique solution of

$$A_\delta\overline{\phi}^\delta := -\delta^2\Delta\overline{\phi}^\delta + \overline{\phi}^\delta = \phi \quad \text{in } \Omega, \tag{2.2.2}$$

subject to periodic boundary conditions. Under periodic boundary conditions, this averaging operator commutes with differentiation.

Lemma 13 *The operator G_N^i is compact, positive, and is an asymptotic inverse to the filter A_δ^{-1}, i.e., for very smooth ϕ and as $\delta \to 0$, it satisfies*

$$\phi = G_N\overline{\phi}^\delta + (-1)^{N+1}\delta^{2N+2}\Delta^{N+1}A_\delta^{-(N+1)}\phi. \tag{2.2.3}$$

The proof of Lemma 13 can be found in [8].

We also define the following norm, induced by the deconvolution operator A:

$$\|\phi\|_A^2 = \|\phi\|^2 + \delta^2 \|\nabla\phi\|^2.$$

Define the explicitly skew-symmetrized trilinear form

$$b^*(u, v, w) := \frac{1}{2}(u \cdot \nabla v, w) - \frac{1}{2}(u \cdot \nabla w, v).$$

2.3 New Method: Formulation and Theoretical Results

We now propose a modification to the ADM-DCM method (2.1.6), based on the following key observation. In order for the correction step approximation w_2^h of (2.1.6b) to be stable and second order accurate, the defect step approximation w_1^h need not satisfy (2.1.6a)! Instead, the pair w_1^h, q_1^h from the right hand side of (2.1.6b) must be computed by any method, that satisfies the following three requirements:

† The method must be stable (any restrictions on its stability will transfer onto

the corresponding restrictions for the resulting approximation w_2^h).

† The method must be first order accurate in both space and time.

† Finally, the discrete time derivative $\frac{\bar{u}(t_{n+1})-\bar{u}(t_n)}{k}$ of the filtered true solution $\bar{u}(t)$ must be approximated within $O(h,k)$ (in the norm $L^2(0,T;L^2(\Omega))$) by $\frac{w_1^{h,n+1}-w_1^{h,n}}{k}$.

We can use the fact that the first approximation w_1^h need not come from a computationally expensive turbulence model (note that the ADMs use hyperviscosity, and this requires either C^1 finite elements, or the usage of the mixed formulation (2.1.6), which increases the size of the system by introducing extra variables). The simplest method for computing w_1^h, that would satisfy all three of the above requirements, is the well-known artificial viscosity (AV) approximation (see, e.g., [25] and [111] for the theoretical results on stability and accuracy of the AV approximation, and the accuracy of its discrete time derivative) below.

$$(\frac{w_1^{h,n+1}-w_1^{h,n}}{k}, v^h) + (\nu + h)(\nabla w_1^{h,n+1}, \nabla v^h) + b^*(w_1^{h,n+1}, w_1^{h,n+1}, v^h) \qquad (2.3.1)$$
$$-(q_1^{h,n+1}, \nabla \cdot v^h) = (f(t_{n+1}), v^h).$$

In turbulent regimes, when the Reynolds number is prohibitively high, the iterative methods would fail to compute a solution to (2.3.1), if it weren't for the increased viscosity coefficient $(\nu + h)$. A solution (w_1, q_1) of (2.3.1) is usually too crude and over-diffusive, but it does satisfy the three requirements above, and obtaining it is much less computationally expensive, than getting a solution of $(2.1.6a)$.

Combining (2.3.1) with $(2.1.6b) - (2.1.6d)$, we propose the following

Algorithm 2.3.1 *Let $f \in L^2(0,T;H^{-1}(\Omega))$, time step $k > 0$ and end time $T > 0$ be given. Set $M = T/\Delta t$ and $w_1^{h,0} = w_2^{h,0} = \bar{u}(0)$, $q_1^{h,0} = q_2^{h,0} = p(0)$. For all $n = 0, 1, ..., M-1$, compute $w_2^{h,n+1}, q_2^{h,n+1}$ via:*

Step 1: Find $w_1^{h,n+1} \in X_h$, $q_1^{h,n+1} \in Q_h$ satisfying for all $v^h \in X_h, \chi^h \in Q_h$

$$\begin{aligned}(\frac{w_1^{h,n+1} - w_1^{h,n}}{k}, v^h) + (\nu + h)(\nabla w_1^{h,n+1}, \nabla v^h) + b^*(w_1^{h,n+1}, w_1^{h,n+1}, v^h) \qquad (2.3.2)\\ -(q_1^{h,n+1}, \nabla \cdot v^h) = (f(t_{n+1}), v^h),\\ (\nabla \cdot w_1^{h,n+1}, \chi^h) = 0\end{aligned}$$

Step 2: Find $\zeta_1^{h,n+1} \in X_h$ satisfying for all $\xi_h \in X_h$

$$(\nabla w_1^{h,n+1}, \nabla \xi^h) = (\zeta_1^{h,n+1}, \xi^h). \tag{2.3.3}$$

Step 3: Find $w_2^{h,n+1}, \zeta_2^{h,n+1} \in X_h$, $q_2^{h,n+1} \in Q_h$ *satisfying for all* $v^h, \xi^h \in X_h, \chi^h \in Q_h$

$$\begin{aligned}
&(\frac{w_2^{h,n+1} - w_2^{h,n}}{k}, v^h) + \delta^2(\nabla(\frac{w_2^{h,n+1} - w_2^{h,n}}{k}), \nabla v^h) + \nu(\nabla w_2^{h,n+1}, \nabla v^h) \\
&\qquad + \nu\delta^2(\nabla \zeta_2^{h,n+1}, \nabla v^h) + b^*(w_2^{h,n+1}, w_2^{h,n+1}, v^h) - (q_2^{h,n+1}, \nabla \cdot v^h) \\
&= (\frac{f(t_{n+1}) + f(t_n)}{2}, v^h) + \frac{\nu}{2}k(\nabla(\frac{w_1^{h,n+1} - w_1^{h,n}}{k}), \nabla v^h) - \frac{1}{2}k(\frac{q_1^{h,n+1} - q_1^{h,n}}{k}, \nabla \cdot v^h) \\
&\quad + \frac{\nu}{2}\delta^2 k(\nabla(\frac{\zeta_1^{h,n+1} - \zeta_1^{h,n}}{k}), \nabla v^h) + \frac{1}{2}(b^*(w_1^{h,n+1}, w_1^{h,n+1}, v^h) - b^*(w_1^{h,n}, w_1^{h,n}, v^h)), \\
&\qquad (\nabla w_2^{h,n+1}, \nabla \xi^h) = (\zeta_2^{h,n+1}, \xi^h), \\
&\qquad\qquad (\nabla \cdot w_2^{h,n+1}, \chi^h) = 0.
\end{aligned} \tag{2.3.4}$$

The method is easily parallelizable (as is the method (2.1.6) from [71]), because Steps 1 and 3 can be run simultaneously on two cores. No extra core would be needed for Step 2: the time needed to run Steps 1 and 2 sequentially on the same core, is still less than the time needed to do one run of Step 3.

The numerical analysis, performed in [71], along with the corresponding stability and accuracy results of the AV approximation from [25] and [111], provides all the

necessary details for the proofs of the two theorems below. Note that the restriction on the time step could be waved if the model was linearized (one approach is due to Baker '76; see, e.g., [7]).

Theorem 14 (Stability) *Let w_2^h be computed by Algorithm 2.3.1. Let $f \in L^2(0,T;H^{-1}(\Omega))$. Also let $\bar{u} \in L^2(0,T;H^3(\Omega))$ and $\bar{u}_{tt} \in L^2(0,T;H^1(\Omega))$.*

Then, for $n = 0, \ldots, N-1$,

$$\|w_2^{h,n+1}\|_A^2 + \nu k \Sigma_{i=0}^n \|\nabla w_2^{h,i+1}\|^2 + \nu \delta^2 k \Sigma_{i=0}^n \|\zeta_2^{h,i+1}\|^2$$
$$\leq \|w_2^{h,0}\|_A^2 + C\nu^{-2} k \Sigma_{i=0}^n \|\frac{f(t_{i+1}) + f(t_i)}{2}\|_{-1}^2.$$

Theorem 15 (Accuracy) *Let the assumptions of Theorem 14 be satisfied. Let the time step satisfy*

$$k < \frac{\nu^3}{\max_{i=0,1,..,N} \|\nabla \bar{u}(t_i)\|^4}. \tag{2.3.5}$$

Also let $\bar{u}_t \in L^2(0,T;H^3(\Omega))$ and $\bar{u}_{ttt} \in L^2(0,T;H^1(\Omega))$. Then, the error in the

second approximation satisfies

$$\begin{aligned}\|\bar{u}(t_{n+1}) - w_2^{h,n+1}\|_A^2 + \nu k \sum_{i=0}^{n} \|\nabla(\bar{u}(t_{i+1}) - w_2^{h,i+1})\|^2 \\ + \nu\delta^2 k \sum_{i=0}^{n} \|\zeta(t_{i+1}) - \zeta_2^{h,i+1}\|^2 \\ \leq C(\nu, \bar{u})(k^4 + \delta^4 + \delta^2 k \sum_{i=0}^{n} \inf_{\chi \in X^h} \|\zeta(t_i) - \chi^i\|^2 \\ + k \sum_{i=0}^{n} (\inf_{v \in V^h} \|\nabla(\bar{u}(t_i) - v^i)\|^2 + \inf_{q \in Q^h} \|p(t_i) - q^i\|^2)).\end{aligned} \tag{2.3.6}$$

2.4 Numerical Tests

We now compare the ADM-DCM solution of (2.1.6) with the new method, AV-ADM, given by Algorithm 2.3.1. The first comparison will be qualitative: both approaches will be tested on a problem with the known true solution, to verify the claimed second order accuracy of AV-ADM. To that end, we consider $\Omega = [0,1] \times [0,1]$, $T = 1$, and the right hand side chosen so that the true solution is given by

$$u_1 = \quad e^{-8t}(1-x^2-y^2)y,$$

$$u_2 = \quad -e^{-8t}(1-x^2-y^2)x,$$

$$p = \quad 0.$$

First, we try the flow in a laminar regime, with $\nu = 0.1$.

Table 2.1
The first step of AV-ADM, $\nu = 0.1, h = \Delta t = \delta$

N	$\| \bar{u} - w_1^h \|_{L^2(0,T;L^2(\Omega))}$	rate	$\| \bar{u} - w_1^h \|_{L^2(0,T;H^1(\Omega))}$	rate
4	0.00555074	-	0.0568668	-
8	0.00583349	-	0.0556956	0.03
16	0.00452737	0.37	0.0422693	0.40
32	0.00293495	0.63	0.0272595	0.63
64	0.00169471	0.79	0.0157943	0.79

Table 2.2
The correction step of AV-ADM, $\nu = 0.1, h = \Delta t = \delta$

N	$\| \bar{u} - w_2^h \|_{L^2(0,T;L^2(\Omega))}$	rate	$\| \bar{u} - w_2^h \|_{L^2(0,T;H^1(\Omega))}$	rate
4	0.00674305	-	0.053864	-
8	0.00416039	0.70	0.0325734	0.73
16	0.00165678	1.33	0.0134262	1.28
32	0.000492286	1.75	0.00422331	1.67
64	0.000130285	1.92	0.00118431	1.83

Table 2.3
The first step of ADM-DCM, $\nu = 0.1, h = \Delta t = \delta$

N	$\| \bar{u} - w_1^h \|_{L^2(0,T;L^2(\Omega))}$	rate	$\| \bar{u} - w_1^h \|_{L^2(0,T;H^1(\Omega))}$	rate
4	0.00562277	-	0.0454994	-
8	0.00350465	0.68	0.031502	0.53
16	0.00283339	0.31	0.0285787	0.14
32	0.00202803	0.48	0.0208906	0.45
64	0.00118028	0.78	0.0123171	0.76

Table 2.4
The correction step of ADM-DCM, $\nu = 0.1, h = \Delta t = \delta$

N	$\| \bar{u} - w_2^h \|_{L^2(0,T;L^2(\Omega))}$	rate	$\| \bar{u} - w_2^h \|_{L^2(0,T;H^1(\Omega))}$	rate
4	0.00828015	-	0.0638702	-
8	0.00464303	0.83	0.0347793	0.88
16	0.0017667	1.39	0.0135634	1.36
32	0.000519078	1.77	0.0041831	1.70
64	0.000137056	1.92	0.00116371	1.85

The results in Tables 1-4 demonstrate that both methods achieve the claimed convergence rates, when modeling a laminar flow. As expected for the deferred correction-type methods, the convergence is asymptotic in $h, \Delta t$. Next, we apply the methods to the flow in a turbulent regime, $\nu = 10^{-5}$.

Table 2.5
The first step of AV-ADM, $\nu = 0.00001, h = \Delta t = \delta$

N	$\| \bar{u} - w_1^h \|_{L^2(0,T;L^2(\Omega))}$	rate	$\| \bar{u} - w_1^h \|_{L^2(0,T;H^1(\Omega))}$	rate
4	0.00746608	-	0.0759235	-
8	0.0093729	-	0.091114	-
16	0.00927388	0.02	0.0898472	0.02
32	0.00786712	0.24	0.0785126	0.19
64	0.00578672	0.44	0.0616183	0.35
128	0.00376394	0.62	0.044508	0.47

Table 2.6
The correction step of AV-ADM, $\nu = 0.00001, h = \Delta t = \delta$

N	$\| \bar{u} - w_2^h \|_{L^2(0,T;L^2(\Omega))}$	rate	$\| \bar{u} - w_2^h \|_{L^2(0,T;H^1(\Omega))}$	rate
4	0.0338806	-	0.280109	-
8	0.0200362	0.76	0.174428	0.68
16	0.00802842	1.32	0.082568	1.08
32	0.00250324	1.68	0.0336661	1.29
64	0.000690117	1.86	0.0131069	1.36
128	0.000179588	1.94	0.00498518	1.39

Table 2.7
The first step of ADM-DCM, $\nu = 0.00001, h = \Delta t = \delta$

N	$\| \bar{u} - w_1^h \|_{L^2(0,T;L^2(\Omega))}$	rate	$\| \bar{u} - w_1^h \|_{L^2(0,T;H^1(\Omega))}$	rate
4	0.0274338	-	0.233568	-
8	0.0214227	0.36	0.229293	-
16	0.020055	0.10	0.259242	-
32	0.0147868	0.44	0.243666	0.09
64	0.00890914	0.73	0.206143	0.24
128	0.00482633	0.88	0.164244	0.33

Table 2.8
The correction step of ADM-DCM, $\nu = 0.00001, h = \Delta t = \delta$

N	$\| \bar{u} - w_2^h \|_{L^2(0,T;L^2(\Omega))}$	rate	$\| \bar{u} - w_2^h \|_{L^2(0,T;H^1(\Omega))}$	rate
4	0.0338833	-	0.280133	-
8	0.0200413	0.76	0.17445	0.68
16	0.00803423	1.32	0.0825819	1.08
32	0.00250582	1.68	0.036317	1.30
64	0.000691374	1.86	0.0129472	1.37
128	0.000180689	1.94	0.0049732	1.38

The results of the comparison of the two methods show their agreement in both the sizes of the errors and the convergence rates - see Tables 6 and 8 for the comparison of the correction step results. Thus, at least quantitatively, a solution based on the computationally cheap AV approximation behaves just as well as the one based on the ADM solution.

Next we try the qualitative test: we check that the AV-ADM solution is able to capture the coherent structures of a turbulent flow past the step. This would demonstrate, that the correction step solution of AV-ADM, although based on a much less "sophisticated" AV approximation, than the solution of ADM-DCM, still is not too dissipative to miss any of the important physical characteristics of the flow.

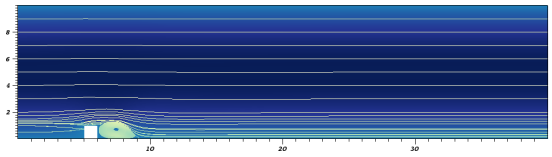

(a) ADM-ADM, $T = 10$

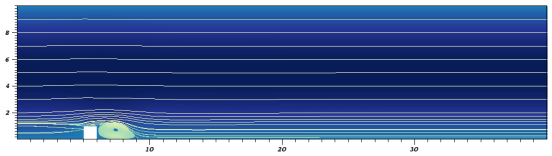

(b) AV-ADM, $T = 10$

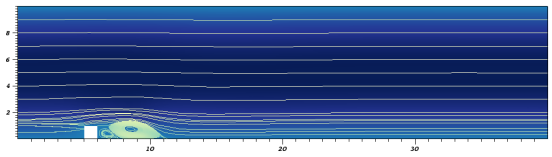

(c) ADM-DCM, $T = 20$

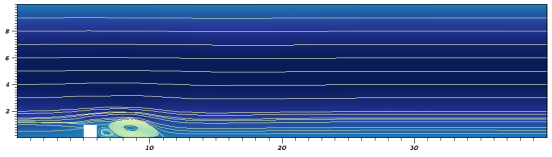

(d) AV-ADM, $T = 20$

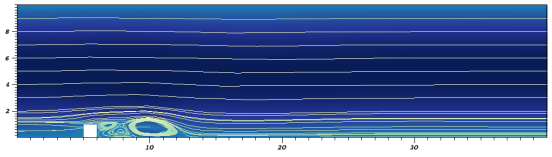

(e) ADM-ADM, $T = 30$

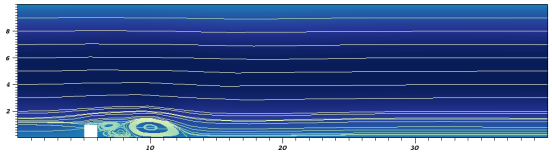

(f) AV-ADM, $T = 30$

Figure 2.1: Flow past forward backward-facing step streamlines, $\nu = 1/600$

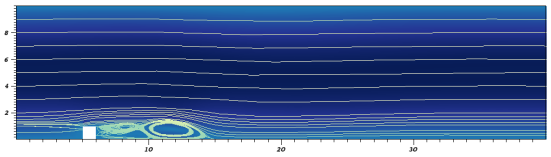

(a) ADM-DCM, $T = 40$

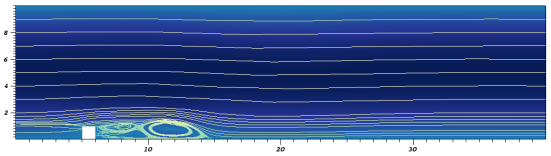

(b) AV-ADM, $T = 40$

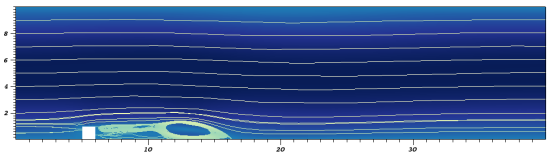

(c) ADM-DCM, $T = 50$

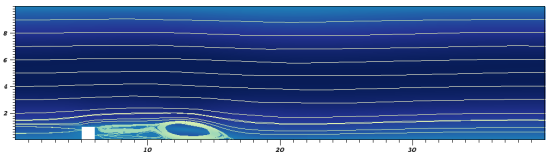

(d) AV-ADM, $T = 50$

Figure 2.2: Flow past forward backward-facing step streamlines, $\nu = 1/600$

Figures 1 and 2 show that both methods are able to capture equally well the formation, shedding and traveling of the eddies. Thus, qualitatively, as well as quantitatively, the methods are in excellent agreement - and they both produce the expected results.

Now to the main reason for possibly choosing AV-ADM instead of ADM-DCM: the

computational attractiveness. We compare the computational time that it took the methods to produce the pictures above. The table below shows two cases: when both methods are run sequentially (time marching to compute the defect step approximations, then compute all the correction step approximations on the same core) and in parallel (with $w_1^{h,n+1}$ and w_2^n computed at the same time on two different cores). The results clearly demonstrate the effectiveness of the proposed new approach - but only in the sequential setting. When each of the methods is parallelized, the computational time needed for the correction step becomes the leading factor for both methods; this correction step involves resolving an approximate deconvolution model (with the right hand sides being different for both methods) - and so in the parallelized versions these methods require the same amount of computational resources.

Table 2.9
Computational Times for the Qualitative Testing

	ADM-ADM	AV-ADM
Parallel	2584	2590
Sequential	4530	3043

For one extra qualitative comparison of the methods we consider the two-dimensional flow between two offset circles; see, e.g., [136], [137], [138]. The domain is a circle with an interior off-center circle obstacle.

Let $r_1 = 1$, $r_2 = 0.1$, $c_1 = 0.5$, and $c_2 = 0$. The domain is then given by

$$\Omega = \{(x, y) : x^2 + y^2 \leq r_1^2\} \cap \{(x, y) : (x - c_1)^2 + (y - c_2)^2 \geq r_2^2\}.$$

Zero initial conditions and no-slip boundary conditions have been chosen for both cases. The flow is driven by the counterclockwise rotational body force

$$f(x, y, t) = \big(- 4y(1 - x^2 - y^2), 4x(1 - x^2 - y^2)\big)^T.$$

All computations have been performed using deal.II — a general-purpose object-oriented finite element library [128]. For all of the computations below, $\Delta t = \delta = H = 0.025$.

To verify the accuracy of AV-ADM and ADM-ADM methods, we plot the velocity fields, as is done in [138], and vorticity contours at the final time $T = 5$. In addition, we give two plots for the model energy $||w||^2 + \delta^2||\nabla w||^2$ and enstrophy $\frac{1}{2}||\nabla \times w||^2 + \frac{\delta^2}{2}||\Delta w||^2$. As seen in figures 2.3, 2.4 and 2.5, computational results are consistent both within ADM-DCM and AV-ADM, and they are also consistent with [138].

Figure 2.3: The difference between velocity fields at the final time T = 5 of ADM-DCM (on the left) and AV-ADM (on the right) approximations ($\nu = 1/200$).

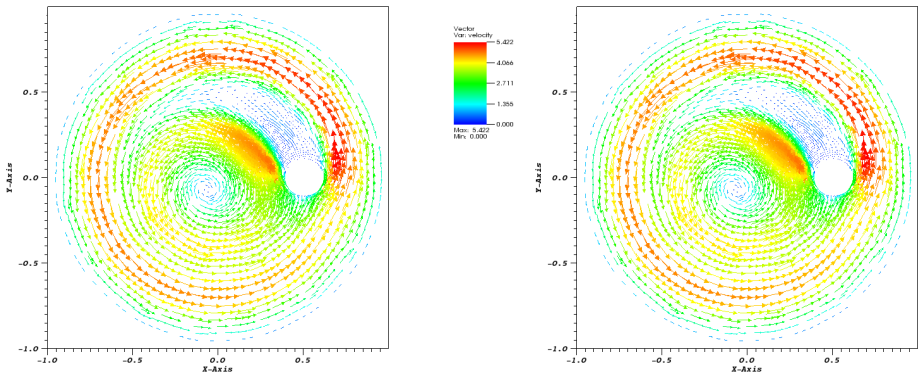

Figure 2.4: The difference between vorticities at the final time T = 5 of ADM-DCM (on the left) and AV-ADM (on the right) approximations ($\nu = 1/200$).

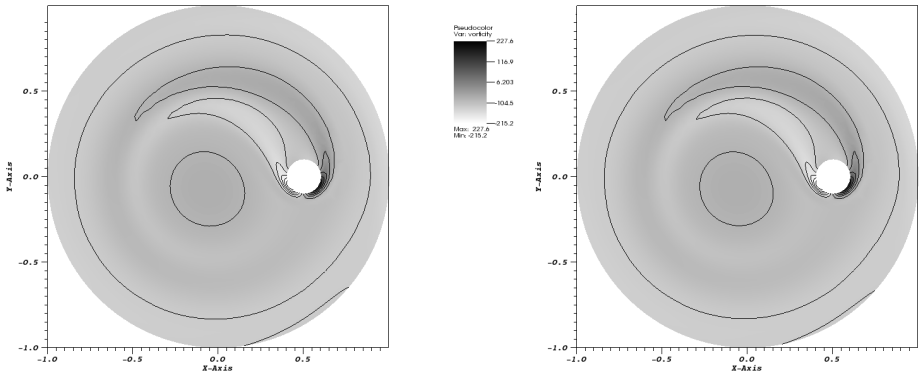

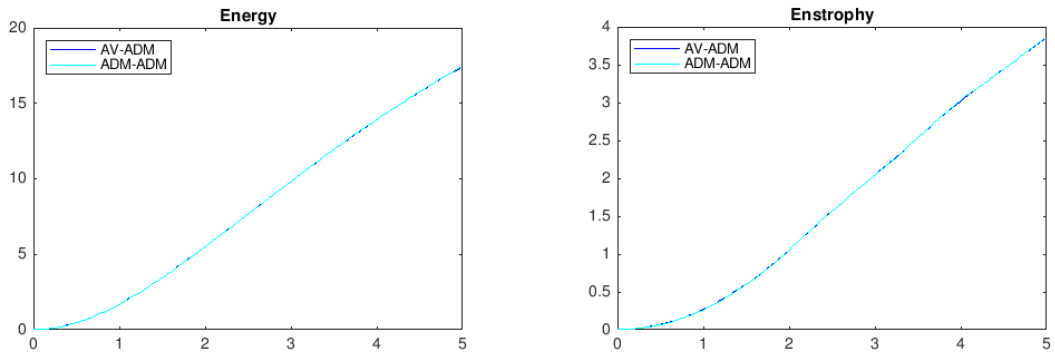

(a) The difference between energies

(b) The difference between enstrophies

Figure 2.5: Time Evolutions of Energy and Enstrophy ($\nu = 1/200$)

Chapter 3

A Defect-Deferred Correction Method for Fluid-Fluid Interaction

3.1 Introduction

Global climate and regional weather simulations often require the resolution of phenomena related to atmosphere-ocean interaction (AOI), such as hurricanes, monsoons, and climate variability like El Niño-Southern Oscillation and the Madden-Julian Oscillation [77, 113, 114, 115]. The most common numerical approach is to pass fluxes (across the fluid interface) of conserved quantities between an ocean code and an atmosphere code with some prescribed frequency, such as every simulated day. The

ocean and atmosphere codes otherwise view each other as black boxes. Each code is optimized to resolve the dynamics of the respective physical system. For example, energy in the atmosphere remains significant at smaller time scales and larger spatial scales than in the ocean, so different time steps and grids are often used for each system. This intuitive approach is now well-established, with numerous codes in existence. Some examples are the so-called *global circulation models* (GCMs) used to assess climate change by the Intergovernmental Panel on Climate Change (IPCC) [98], as well as coupled Weather Research and Forecasting (WRF) and Regional Oceanic Models (ROMS) [94, 96, 107, 108].

We consider an approach to improve two numerical aspects of typical AOI simulations: artificial diffusion (or viscosity) processes, and the coupling across the fluid interface. Viscosity and diffusion parameterizations are included in simulations to control numerical noise and to model subscale mixing processes; we provide some details in Section 3.1.2. But the net effect can be to overdiffuse (formally) and impact model resolution. For example, reduction of viscosity parameters in the ocean alone have been shown to improve some simulation outputs for both the ocean and atmosphere [99], but remain larger than physical parameter values in order to control numerical noise. Meanwhile, typical coupling methods induce time-consistency errors (with rare exceptions; coupling details are discussed below). Some studies indicate sensitivity with respect to this error, demonstrating that improved coupling methods could translate to better simulation results in many cases [84, 96].

There is an abundance of literature regarding the physics behind surface fluxes and the preservation of flux conservation properties when mapping between different computational grids. In contrast, the literature that addresses the temporal aspects of flux calculations in the context of AOI is somewhat sparse. The method in [85] exemplifies the approach used for climate models, while approaches for regional coupled models may be found in [76, 109]. The common feature we point out is that the time consistency is always formally first-order with respect to the size of time interval between coupling air and sea components. An exception is the recent method in [95, 96], which employs iteration to achieve second-order consistency; further details are discussed below. Generally, the development of flux-passing algorithms is complicated by technical issues of numerical stability and consistency. Numerical analysis of algorithms can illustrate the challenges and provide insight for future developments, but few examples of this sort of analysis exist that address time-dependent issues. To our knowledge, the papers are [78, 91, 92, 95, 116]. Our approach is investigated for a simple model of two viscous fluids that retains the key aspect of their coupling; the ensuing algorithms are amenable to a rigorous mathematical analysis.

Consider the d-dimensional domain Ω in space that consists of two subdomains Ω_1 and Ω_2, coupled across an interface I, for times $t \in [0, T]$. The problem is: *given* $\nu_i > 0$, $f_i : [0, T] \to H^1(\Omega_i)^d, u_i(0) \in H^1(\Omega_i)^d$ *and* $\kappa \in \mathbb{R}$, *find (for* $i = 1, 2$*)*

$u_i : \Omega_i \times [0,T] \to \mathbb{R}^d$ *and* $p_i : \Omega_i \times [0,T] \to \mathbb{R}$ *satisfying (for* $0 < t \leq T$*)*

$$
\begin{aligned}
u_{i,t} &= \nu_i \Delta u_i - u_i \cdot \nabla u_i - \nabla p_i + f_i, \quad \text{in } \Omega_i, && (3.1.1)\\
-\nu_i \hat{n}_i \cdot \nabla u_i \cdot \tau &= \kappa |u_i - u_j|(u_i - u_j) \cdot \tau, \quad \text{on } I,\ i,j = 1,2\,,\ i \neq j\,, && (3.1.2)\\
u_i \cdot \hat{n}_i &= 0 \quad \text{on } I, i = 1,2 && (3.1.3)\\
\nabla \cdot u_i &= 0, \quad \text{in } \Omega_i && (3.1.4)\\
u_i(x,0) &= u_i^0(x), \quad \text{in } \Omega_i, && (3.1.5)\\
u_i &= 0, \quad \text{on } \Gamma_i = \partial\Omega_i \setminus I. && (3.1.6)
\end{aligned}
$$

The vectors $\hat{n}_i$ are the unit normals on $\partial\Omega_i$, and τ is any vector such that $\tau \cdot \hat{n}_i = 0$. The parameters ν_i represent kinematic viscosities. We include generic body forces f_i, for generality. This model for fluid velocities, u_i, and pressures, p_i, was studied in [91], initially.

The coupling condition (3.1.2) represents the flux of momentum across a boundary layer region near the fluid interface. The interface is modelled as being flat (just a line segment for $d = 2$). The bulk fluids slide past each other across the boundary layers. The action of the fluid in the layer region is modelled as imparting a horizontal frictional drag force that scales quadratically with the jump in velocities across the

layers. The constant $\kappa > 0$ is a friction parameter. A discussion of the full equations of the atmosphere and ocean and their mathematical analysis is provided in the work of Lions, Temam and Wang [103]. Our condition (3.1.2) is analogous to the coupling equations in [103], up to scaling constants.

In application, momentum flux is not calculated using simultaneous values of the ocean and air velocities, as would be required to satisfy (3.1.2). Fluxes are averaged locally in time to remove aliasing effects and computed using explicit or semi-implicit methods, so that the ocean and atmosphere codes may be run independently; sequentially, or even in parallel. This introduces a consistency error in time. A review of numerical coupling strategies is provided in the work of Lemarié, Blayo and Debreu [95], where an alternative coupling method is proposed and analyzed that is second-order consistent in time, and could be extended to higher order. In contrast, the methods in most codes, and in [78, 91, 92, 116], are only first-order time accurate. The approaches in [78, 95] advocate iterating between the fluid solvers until convergence. These methods are flux-conservative and stable. In particular, the method of [95] applies to a general class of flux computations encountered in application codes.

In this chapter, we develop a method that is unconditionally stable and second-order time accurate, with exactly two solves per time step; further iterations are not required for stability or (formal) consistency. It is desirable to minimize iterations as much as possible, since in practice these require the execution of expensive physics subroutines

and additional parallel communication. However, further iterations (in the manner of [95]) might still be justified for accuracy when fluxes become large. We also provide a correction for the use of viscosity parameterizations. Our goal is to outline a broad methodology, but also provide a specific algorithm with a full mathematical analysis, and computational examples to illustrate the theory. The coupling method we focus on is not flux-conservative or time-averaged, as one encounters in application codes. More general flux calculations will be handled in future work.

3.1.1 Improvement of time consistency via spectral deferred correction

The main advantage of the deferred correction approach is that a simple low-order method can be employed, and the recovered solution is of high-order accuracy, due to a sequence of deferred correction equations. The classical deferred correction approach could be seen, e.g., in [69]. However, in 2000 a modification of the classical deferred correction approach was introduced by Dutt, Greengard and Rokhlin, [39]. This allowed the construction of stable and high-order accurate *spectral deferred correction* (SDC) methods.

In [105], Minion discusses these SDC methods in application to an initial value ODE.

For clarity, that discussion is adapted here to explain the application to our problem. Assume a method-of-lines approach in each fluid domain; application of a given discrete method in space for (3.1.1)-(3.1.6) generates a semi-discrete problem of the form

$$\begin{aligned} \phi_i'(t) &= F_i(t, \phi_1(t), \phi_2(t)),\ t \in (0, T] \\ \phi_i(0) &= \phi_i^0, \end{aligned} \tag{3.1.7}$$

for $i = 1, 2$. Here, $\phi_i \in \mathbb{R}^{N_i}$ is a vector of unknowns to approximate, for example, all fluid variables at grid points in space, and $F_i : (0, T] \times \mathbb{R}^{N_1} \times \mathbb{R}^{N_2} \to \mathbb{R}^{N_i}$. Boundary conditions are already included in the operator F_i. The simultaneous flux conditions (3.1.2) are applied on I, which is the reason that both ϕ_1 and ϕ_2 are required as inputs for F_i. The above formulation does not assume that the same methods are applied to the equations in both fluid domains.

Let $\mathbf{u} = (u_1, u_2)$ and define $[\mathbf{u}] \equiv u_1 - u_2$. Our base (low-order) numerical method is derived by applying a backward-Euler method to approximate (3.1.7), but with the

following semi-implicit modification to the coupling conditions:

$$
\begin{aligned}
-\nu_i \hat{n}_i \cdot \nabla u_i(t^{n+1}) \cdot \tau \approx{}& \kappa |[\mathbf{u}](t^n)| u_i(t^{n+1}) \cdot \tau \\
&- \kappa \sqrt{|[\mathbf{u}](t^n)|} \sqrt{|[\mathbf{u}](t^{n-1})|} u_j(t^n) \cdot \tau, \qquad \text{on } I,\ i,j = 1,2\,,\ i \neq j. \quad (3.1.8)
\end{aligned}
$$

When using a finite element formulation in space, this treatment of the coupling was shown to be unconditionally stable in [91]. Without the geometric averaging in (3.1.8), the coupling is known to exhibit less stable behavior for large enough time steps; see [116]. Since the data $u_j(t^{n+1})$ is not used in the coupling, the result is a system of fully-discrete equations of the form

$$
\begin{aligned}
\frac{\phi_i^{n+1} - \phi_i^n}{\Delta t} &= \tilde{F}_i(\phi_i^{n+1}, \phi_i^n, \phi_i^{n-1}, \phi_j^n, \phi_j^{n-1}) \\
&= F_i(t^{n+1}, \phi_1(t^{n+1}), \phi_2(t^{n+1})) + \mathcal{O}(\Delta t),
\end{aligned} \tag{3.1.9}
$$

where $\phi_i^n \approx \phi_i(t^n)$, for $i = 1, 2$ and $i \neq j$. The variables ϕ_1^{n+1} and ϕ_2^{n+1} are thus "decoupled", enabling solvers for each to run in parallel. We note that other coupling methods and time discretizations could be represented in an analogous form in order to explore extensions to applications. The time step size Δt represents the length of time between coupling of the fluid models. Typically, subcycling of the atmosphere is performed due to the faster dynamics compared to the ocean. In mathematical terminology, this is known as *multirate time stepping*.

In the deferred correction approach, the formal accuracy of (3.1.9) is increased to

order Δt^k through a series of $k-1$ additional correction steps. We focus on the case of $k=2$, so we define one correction step. In the derivation of the correction equations, one introduces an abstract continuum reconstruction in time of the data ϕ_i^n, say $\tilde{\phi}_i : [0,T] \to \mathbb{R}^{N_i}$, such that $\tilde{\phi}_i(t^n) = \phi_i^n$ for $i = 1,2$ and all n. Corrections are found by approximating the error function $\delta_i(t) \equiv \phi_i(t) - \tilde{\phi}_i(t)$. One notes first that we may eliminate ϕ_i by inserting $\phi_i = \tilde{\phi}_i + \delta_i$ in (3.1.7) and integrating to yield

$$\tilde{\phi}_i(t) + \delta_i(t) = \phi_i^0 + \int_0^t F_i(\tau, \tilde{\phi}_1 + \delta_1, \tilde{\phi}_2 + \delta_2)\, d\tau.$$

The following functions are one measure of error in $\tilde{\phi}_i$:

$$E_i(t, \tilde{\phi}_1(t), \tilde{\phi}_2(t)) \equiv \phi_i^0 + \int_0^t F_i(\tau, \tilde{\phi}_1, \tilde{\phi}_2)\, d\tau - \tilde{\phi}_i(t).$$

An equation for the error is then

$$\delta_i(t) = \int_0^t \left\{ F_i(\tau, \tilde{\phi}_1 + \delta_1, \tilde{\phi}_2 + \delta_2) - F_i(\tau, \tilde{\phi}_1, \tilde{\phi}_2) \right\} d\tau + E_i(t, \tilde{\phi}_1(t), \tilde{\phi}_2(t)),$$

from which one sees that

$$\begin{aligned} \frac{\delta_i(t^{n+1}) - \delta_i(t^n)}{\Delta t} = \frac{1}{\Delta t} \int_{t^n}^{t^{n+1}} \left\{ F_i(\tau, \tilde{\phi}_1 + \delta_1, \tilde{\phi}_2 + \delta_2) - F_i(\tau, \tilde{\phi}_1, \tilde{\phi}_2) \right\} d\tau \\ + \frac{E_i(t^{n+1}, \tilde{\phi}_1^{n+1}, \tilde{\phi}_2^{n+1}) - E_i(t^n, \tilde{\phi}_1^n, \tilde{\phi}_2^n)}{\Delta t}. \end{aligned} \tag{3.1.10}$$

The E_i-terms satisfy

$$\frac{E_i(t^{n+1}, \tilde{\phi}_1^{n+1}, \tilde{\phi}_2^{n+1}) - E_i(t^n, \tilde{\phi}_1^n, \tilde{\phi}_2^n)}{\Delta t} = \frac{1}{\Delta t} \int_{t^n}^{t^{n+1}} F_i(\tau, \tilde{\phi}_1, \tilde{\phi}_2)\, d\tau - \frac{\tilde{\phi}_i^{n+1} - \tilde{\phi}_i^n}{\Delta t}.$$

In order to achieve the desired (second-order) accuracy, the deferred correction method requires this latter integral to be evaluated using a second-order quadrature rule. We apply the trapezoidal rule in this research.

A benefit of the deferred correction approach is that the same base discretization method may be applied to the remaining terms in (3.1.10), so we apply our semi-discrete method and approximate F_i by $\tilde{F}_i$. The error approximations are denoted by $\delta_i^n \approx \delta_i(t^n)$, which are added to ϕ_i^n to get the corrected approximations, say

$$\eta_i^n \equiv \phi_i^n + \delta_i^n = \phi_i(t^n) + \mathcal{O}(\Delta t^2).$$

After applying the discretization method to (3.1.10) and eliminating the values δ_i^n, the method for the corrected approximation is

$$\begin{aligned} \frac{\eta_i^{n+1} - \eta_i^n}{\Delta t} = &\left\{ \tilde{F}_i(\eta_i^{n+1}, \eta_i^n, \eta_i^{n-1}, \eta_j^n, \eta_j^{n-1}) - \tilde{F}_i(\phi_i^{n+1}, \phi_i^n, \phi_i^{n-1}, \phi_j^n, \phi_j^{n-1}) \right\} \\ &+ \frac{1}{2} \left\{ F_i(t^{n+1}, \phi_1^{n+1}, \phi_2^{n+1}) + F_i(t^n, \phi_1^n, \phi_2^n) \right\}. \end{aligned} \tag{3.1.11}$$

Note that η_j^{n+1} is not needed to compute η_i^{n+1} for $i \neq j$. The data ϕ_i^{n+1} and some terms in (3.1.11) are already computed in the predictor step. The correction step

is equivalent to performing the predictor step with some extra source terms and an algebraic change to the approximation of the momentum flux. This property of the deferred correction approach makes it potentially viable for application codes, since the existing code structure (the implementation of the predictor step) could be leveraged quite heavily to implement the corrector step.

3.1.2 Reduction of numerical diffusion effects via defect correction

The general idea of defect correction and deferred correction methods for solving partial differential equations has been known for a long time. For a survey, see [81]. Defect correction has been proven computationally attractive in fluid applications; see, e.g., [25, 53, 64, 73, 100] and references therein. Initial approaches to using the defect-deferred correction ideas for AOI were tested in [111, 112], where the method was successfully applied to the Navier-Stokes equations in one domain ([111]) and convection-diffusion equations in the two-domain setting (with the coupling condition introduced as a linearized version of rigid lid) in [112]. The general idea of any *defect correction method* (DCM) can be formulated as follows (see, e.g., [68, 81]). Given an

operator $\tilde{G}$ to approximate $Gx = 0$, build an iterative procedure:

$$\tilde{G}x_1 = 0, \tag{3.1.12}$$

$$\tilde{G}x_{i+1} = \tilde{G}x_i - Gx_i, i \geq 1.$$

The choice of a particular approximation $\tilde{G}$ determines the defect correction method in use. In this chapter, the "defect" will represent numerical viscosity, which we represent using the additional (constant) parameters $H_i > 0$ to obtain an effective viscosity coefficient of $\nu_i + H_i$, $i = 1, 2$. The operator $\tilde{G}$ in (3.1.12) may be interpreted as using the effective viscosity in the construction of the operator $\tilde{F}_i$. Then G represents a corresponding operator that does not use numerical viscosity. In the deferred correction step (3.1.11), this translates to using the viscosity coefficient ν_i alone in the construction of the operator F_i.

In summary, the combined defect-deferred correction (DDC) method is equivalent to using the following viscous terms when constructing the operators in (3.1.9)

and (3.1.11):

$$(\nu_i + H_i)\Delta\eta_i^{n+1} \Leftrightarrow \tilde{F}_i(\eta_i^{n+1}, \eta_i^n, \eta_i^{n-1}, \eta_j^n, \eta_j^{n-1})$$

$$(\nu_i + H_i)\Delta\phi_i^{n+1} \Leftrightarrow \tilde{F}_i(\phi_i^{n+1}, \phi_i^n, \phi_i^{n-1}, \phi_j^n, \phi_j^{n-1})$$

$$\nu_i\Delta\phi_i^j \Leftrightarrow F_i(t^j, \phi_1^j, \phi_2^j),\ j = n, n+1.$$

The DDC method constitutes an easy way to enhance the deferred correction algorithm by reducing the impact of artificial viscosity. This approach preserves an important attribute of deferred correction: that the code structure used to implement the predictor step may be leveraged to implement the corrector step.

Constant-coefficient mixing-length models are used to some extent in codes, but a number of more sophisticated parameterizations also exist. For sake of brevity, we refer to the atmosphere and ocean components of the Community Earth Systems Model (see [88, 110]) and focus on the dissipation of momentum. In the atmosphere code, divergent modes in horizontal transport may be controlled with different options. Harmonic mixing $\nabla \cdot \alpha\nabla$ is one; another is to use the more scale-selective biharmonic mixing like $\nabla \cdot \nu\nabla\Delta$, again with constant coefficient in lower model layers for all cases. In upper model layers, the constants are allowed monotonically-increasing values (up to about four times the bulk value) due to the different dynamics near the top of the atmosphere.

Vertical dynamics are time-split from the horizontal, and vertical viscosity is handled using implicit, backward-Euler time stepping with a moist turbulence scheme. One

calculates an eddy-diffusivity parameter $K = l \cdot \sqrt{e} \cdot S$, with l a mixing length, e a diagnostic turbulent kinetic energy, and S a stability parameter. The calculations of these quantities are semi-implicit during the iteration required for the implicit-Euler step, and dependent on many state variables.

The ocean model also provides a range of options for horizontal and vertical viscosity. For horizontal dynamics, both harmonic and biharmonic damping operators may be used, with spatially-varying coefficients. There is an option for anisotropic horizontal viscosity, which is represented as the divergence of a viscous stress tensor that depends linearly on the velocity gradient. The tensor coefficients may vary in space and time in some prescribed way, or may be computed in terms of the strain-rates, nonlinearly, in the manner of Smagorinsky. Vertical viscosity $\partial_z \mu \partial_z$ can be implemented either explicitly or implicitly, with a constant-coefficient option. Another option allows a computation for μ as a function of the local Richardson number. Finally, μ can be computed using the so-called K-profile parameterization (KPP); this is complex and we refer the reader to [101] for details. The Richardson and KPP methods let μ depend on various state variables.

In this chapter, only constant-coefficient harmonic diffusion is used to control the complexity of our full numerical analysis. More sophisticated operators could be explored by changing the definitions of the functions F_i, and various time-stepping approaches, including operator-splitting. These extensions are left for future investigation.

The remainder of this work is organized as follows: in Section 3.2, notation and mathematical preliminaries are given and the two-step DDC method is introduced (Algorithm 3.2.1) using a finite element discretization in space. The unconditional stability of the proposed method and convergence results are proven in Section 3.3. Computations are performed to illustrate the stability and accuracy predictions of the theory in Section 3.4. In our computations we also observe that the corrector step provides a significant improvement to accuracy at the largest tested scales of time step and artificial viscosity parameters. This indicates a potential benefit in application, where time step sizes and artificial viscosity (or diffusion) values are restricted by computational resources. In Section 3.5 we conclude with a summary and discussion of future work.

3.2 Method Description, Notation and Preliminaries

This section presents the numerical schemes for (3.1.1)-(3.1.6), and provides the necessary definitions and lemmas for the stability and convergence analysis. For $D \subset \Omega$, the Sobolev space $H^k(D) = W^{k,2}(D)$ is equipped with the usual norm $\|\cdot\|_{H^k(D)}$, and semi-norm $|\cdot|_{H^k(D)}$, for $1 \leq k < \infty$, e.g., Adams [74]. The L^2 norm is denoted by $\|\cdot\|_D$. For functions $v(x,t)$ defined for almost every $t \in (0,T)$ on a function space

$V(D)$, we define the norms $(1 \leq p \leq \infty)$

$$\|v\|_{L^\infty(0,T;V)} = \operatorname*{ess\,sup}_{0<t<T} \|v(\cdot,t)\|_V \quad \text{and} \quad \|v\|_{L^p(0,T;V)} = \left(\int_0^T \|v\|_V^p dt \right)^{1/p}.$$

The dual space of the Banach space V is denoted V'.

For $i = 1, 2$, let

$$X_i := \{v_i \in H^1(\Omega_i)^d : v_i = 0 \, on \, \Omega_i \setminus I, i = 1, 2, v_i \cdot \hat{n}_i = 0 \, on \, I\}$$

be velocity spaces, with associated pressure spaces

$$Q_i = \{q_i \in L^2(\Omega_i)^d : \int_{\Omega_i} q_i d\Omega_i = 0\}.$$

We denote $\mathbf{u} = (u_1, u_2)$, $\mathbf{f} = (f_1, f_2)$ and $X := \{\mathbf{v} = (v_1, v_2) : v_i \in X_i, i = 1, 2\}$. Similarly, we denote $\mathbf{q} = (q_1, q_2)$ and $Q := \{\mathbf{q} = (q_1, q_2) : q_i \in Q_i, i = 1, 2\}$.

A natural subdomain variational formulation for (3.1.1)-(3.1.6), obtained by multiplying (3.1.1) by v_i, integrating and applying the divergence theorem, is to find (for

$i, j = 1, 2, i \neq j)$ $u_i : [0, T] \to X_i$ and $p_i : [0, T] \to Q_i$ satisfying

$$\begin{aligned}(u_{i,t}, v_i)_{\Omega_i} + \nu_i(\nabla u_i, \nabla v_i)_{\Omega_i} + (u_i \cdot \nabla u_i, v_i)_{\Omega_i} - (p_i, \nabla v_i) \\ + \int_I \kappa(u_i - u_j)|u_i - u_j|v_i ds = (f_i, v_i)_{\Omega_i},\ \forall\, v_i \in X_i, \\ (\nabla \cdot u_i, q_i) = 0,\ \forall\, q_i \in Q_i.\end{aligned} \tag{3.2.1}$$

The natural monolithic variational formulation for (3.1.1)-(3.1.6) is found by summing (3.2.1) over $i, j = 1, 2$ and $i \neq j$ and is to find $\mathbf{u} : [0, T] \to X$ and $\mathbf{p} : [0, T] \to Q$ satisfying

$$\begin{aligned}(\mathbf{u}_t, \mathbf{v}) + \nu(\nabla \mathbf{u}, \nabla \mathbf{v}) + (\mathbf{u} \cdot \nabla \mathbf{u}, \mathbf{v}) - (\mathbf{p}, \nabla \cdot \mathbf{v}) + \int_I \kappa |[\mathbf{u}]||[\mathbf{u}][\mathbf{v}] ds = (\mathbf{f}, \mathbf{v}), \forall v \in X, \\ (\nabla \cdot \mathbf{u}, \mathbf{q}) = 0,\ \forall\, q \in Q\end{aligned} \tag{3.2.2}$$

where $[\cdot]$ denotes the jump of the indicated quantity across the interface I, $(\cdot, \cdot)$ is the $L^2(\Omega_1 \cup \Omega_2)$ inner product and $\nu = \nu_i$ in Ω_i.

Comparing (3.2.2) and (3.2.1) we see that the monolithic problem (3.2.2) has a global energy that is exactly conserved, (in the appropriate sense), (set $\mathbf{v} = \mathbf{u}$ and $\mathbf{q} = \mathbf{p}$ in (3.2.2)). The subdomain sub-problems (3.2.1) do not possess a subdomain energy which behaves similarly due to energy transfer back and forth across the interface I. It is possible for decoupling strategies to become unstable due to the input of non-physical energy as a numerical artifact; see [90, 91].

Let the domain $\Omega \subset \mathbb{R}^d$ (typically $d = 2, 3$) have convex, polygonal subdomains Ω_i for $i = 1, 2$ with $\partial\Omega_1 \cap \partial\Omega_2 = \Omega_1 \cap \Omega_2 = I$. Let Γ_i denote the portion of $\partial\Omega_i$ that is not on I, i.e. $\Gamma_i = \partial\Omega_i \backslash I$. For $i = 1, 2$, let $X_i = \left\{ v \in H^1(\Omega_i)^d \mid v|_{\Gamma_i} = g_i, v \cdot \hat{n}_i = 0 \, on \, I \right\}$, let $(\cdot, \cdot)_{\Omega_i}$ denote the standard L^2 inner product on Ω_i, and let $(\cdot, \cdot)_{X_i}$ denote the standard H^1 inner product on Ω_i. Define $X = X_1 \times X_2$ and $L^2(\Omega) = L^2(\Omega_1) \times L^2(\Omega_2)$. For $\mathbf{u}, \mathbf{v} \in X$ with $\mathbf{u} = [u_1, u_2]^T$ and $\mathbf{v} = [v_1, v_2]^T$, define the L^2 inner product

$$(\mathbf{u}, \mathbf{v}) = \sum_{i=1,2} \int_{\Omega_i} u_i \cdot v_i \, dx \, ,$$

and H^1 inner product

$$(\mathbf{u}, \mathbf{v})_X = \sum_{i=1,2} \left(\int_{\Omega_i} u_i \cdot v_i \, dx + \int_{\Omega_i} \nabla u_i : \nabla v_i \, dx \right) \, ,$$

and the induced norms $\|\mathbf{v}\| = (\mathbf{v}, \mathbf{v})^{1/2}$ and $\|\mathbf{v}\|_X = (\mathbf{v}, \mathbf{v})_X{}^{1/2}$, respectively. The case where $g_i = 0, i = 1, 2$ will be considered here, and can be easily extended to the case of nonhomogeneous Dirichlet conditions on $\partial\Omega_i \setminus I$.

The inf-sup stable pair of velocity-pressure spaces (P_m, P_{m-1}) will be chosen with $m \geq 2$.

For functions $u, v, w \in X_i$, $i = 1, 2$ we define the expilicitly skew-symmetrized non-linear form on Ω_i by

$$c_i(u; v, w) = \frac{1}{2}(u \cdot \nabla v, w)_{\Omega_i} - \frac{1}{2}(u \cdot \nabla w, v)_{\Omega_i} \tag{3.2.3}$$

Lemma 16 *$(X, \|\cdot\|_X)$ is a Hilbert space.*

Proof 9 *The choice of boundary conditions for X_1 and X_2 will ensure $X_i \subset H^1(\Omega_i)$, $i = 1, 2$ are closed subspaces. Hence by the definitions of $(\cdot, \cdot)_X$ and $\|\cdot\|_X$, $(X, \|\cdot\|_X)$ is a Hilbert space.* ■

The following discrete Gronwall's lemma and its modified version from [70] will be utilized in the subsequent analysis.

Lemma 17 *(Gronwall's lemma) Let k, M, and $a_\mu, b_\mu, c_\mu, \gamma_\mu$, for integers $\mu > 0$, be nonnegative numbers such that*

$$a_n + k \sum_{\mu=0}^{n} b_\mu \leq k \sum_{\mu=0}^{n} \gamma_\mu a_\mu + k \sum_{\mu=0}^{n} c_\mu + M \text{ for } n \geq 0. \tag{3.2.4}$$

Suppose that $k\gamma_\mu < 1$, for all μ, and set $\sigma_\mu \equiv (1 - k\gamma_\mu)^{-1}$. Then,

$$a_n + k \sum_{\mu=0}^{n} b_\mu \leq exp\left(k \sum_{\mu=0}^{n} \sigma_\mu \gamma_\mu\right) \left\{k \sum_{\mu=0}^{n} c_\mu + M\right\} \text{ for } n \geq 0. \tag{3.2.5}$$

Lemma 18 *(Modified Gronwall's lemma) Let k, M, and $a_\mu, b_\mu, c_\mu, \gamma_\mu$,*

for integers $\mu > 0$, be nonnegative numbers such that

$$\begin{aligned} & a_n + k \sum_{\mu=0}^{n} b_\mu \\ & \leq k \sum_{\mu=0}^{n-1} \gamma_\mu a_\mu + k \sum_{\mu=0}^{n} c_\mu + M \text{ for } n \geq 0. \end{aligned} \tag{3.2.6}$$

Then, with $\sigma_\mu \equiv (1 - k\gamma_\mu)^{-1}$,

$$\begin{aligned} & a_n + k \sum_{\mu=0}^{n} b_\mu \\ & \leq exp\left(k \sum_{\mu=0}^{n-1} \sigma_\mu \gamma_\mu \right) \left\{ k \sum_{\mu=0}^{n} c_\mu + M \right\} \text{ for } n \geq 0. \end{aligned} \tag{3.2.7}$$

Lemma 19 *Let $v \in H^1_\Omega$. Then there exists $C = C(\Omega) > 0$,*

a finite constant such that

$$\|v\|_{L^3(\partial\Omega)} \leq C(\|v\|^{1/4}_{L^2(\Omega)} \|\nabla v\|^{3/4}_{L^2(\Omega)} + \|v\|^{1/6}_{L^2(\Omega)} \|\nabla v\|^{5/6}_{L^2(\Omega)}), \tag{3.2.8}$$

$$\|v\|_{L^2(\partial\Omega)} \leq C\|v\|^{1/2}_{L^2(\Omega)}\|\nabla v\|^{1/2}_{L^2(\Omega)}, \tag{3.2.9}$$

$$\|v\|_{L^4(\partial\Omega)} \leq C\|\nabla v\|_{L^2(\Omega)} \tag{3.2.10}$$

Proof 10 *See [72], Theorem II.*4.1*, pg. 63.* ■

Lemma 20 *Let $u, v, w \in H^1(\Omega_i)$ for $i = 1, 2$. Then there exists $C = C(\Omega_i) > 0$, a finite constant such that*

$$c_i(u; v, w) \leq C\|u\|^{1/2}_{\Omega_i}\|\nabla u\|^{1/2}_{\Omega_i}\|\nabla v\|_{\Omega_i}\|\nabla w\|_{\Omega_i} \tag{3.2.11}$$

Proof 11 *The proof can be found in [91].* ■

The following constants and assumptions on the problem data (written here as assumptions on the true solution $\mathbf{u}$) will be used in the proofs below.

Definition 4 *Let $i = 1, 2$.*

$$C_u := \|\mathbf{u}(x,t)\|_{L^\infty(0,T;L^\infty(\Omega))},$$

$$C_{u_{i,t}} := \|\mathbf{u}_{i,t}(x,t)\|_{L^\infty(0,T;L^\infty(\Omega))},$$

$$C_{\nabla u_{i,t}} := \|\nabla \mathbf{u}_{i,t}(x,t)\|_{L^\infty(0,T;L^\infty(\Omega))}$$

Assumption 1 *$\exists \alpha > 0$, such that $\alpha \leq |[\mathbf{u}(\vec{x},t)]|$, $\forall \vec{x} \in I$, $\forall t \in (0,T]$.*

Assumption 2 *Let the true solution u satisfy*

$$\left|\frac{\partial}{\partial t}(|\mathbf{u}_i(t)|)\right| \leq C\Delta t^{1/4}, \text{for } i = 1, 2, 0 < t \leq \Delta t, \forall \vec{x} \in I. \tag{3.2.12}$$

3.2.1 Discrete Formulation

Let $\mathcal{T}_i$ be a triangulation of Ω_i and $\mathcal{T}_h = \mathcal{T}_1 \cup \mathcal{T}_2$. Take $X_i^h \subset X_i$ to be conforming finite element spaces for $i = 1, 2$, and define $X^h = X_1^h \times X_2^h \subset X$. It follows that $X^h \subset X$ is a Hilbert space with corresponding inner product and induced norm. We shall consider X_i^h to be spaces of continuous piecewise polynomials of degree $m \geq 2$.

For $t_k \in [0,T]$, $\hat{\mathbf{u}}^{\mathbf{k}}$, $\tilde{\mathbf{u}}^{\mathbf{k}}$ will denote the discrete approximations (defect step and correction step, respectively) to $\mathbf{u}(t_k)$.

Every defect/deferred correction method is based on a lower-order accurate method, which still possesses some desirable characteristics. In our case, it is the geometric averaging-based data passing scheme from [91].

Let $\Delta t > 0$, $f_i \in L^2(\Omega_i)$. For each $M \in \mathbb{N}, M \leq \frac{T}{\Delta t}$, given $u_i^n \in X_{i,h}$ and $p_i^n \in Q_{i,h}$, $n = 0, 1, 2, \cdots, M-1$, solve on each subdomain (for $i, j = 1, 2, i \neq j$) to find $u_i^{n+1} \in X_{i,h}$ satisfying

$$\begin{aligned}\left(\frac{u_i^{n+1}-u_i^n}{\Delta t}, v_i\right) + \nu_i(\nabla u_i^{n+1}, \nabla v_i) + \kappa \int_I u_i^{n+1}|u_i^n - u_j^n| v_i \, ds \\ - \kappa \int_I u_j^n |u_i^n - u_j^n|^{1/2} |u_i^{n-1} - u_j^{n-1}|^{1/2} v_i \, ds \\ + c_i(u_i^{n+1}; u_i^{n+1}, v_i) - (p_i^{n+1}, \nabla \cdot v_i) = (f_i(t^{n+1}), v_i), \ \forall v_i \in X_{i,h}\,. \\ (\nabla \cdot u_i^{n+1}, q_i) = 0, \ \forall\, q_i \in Q_{i,h}. \quad (3.2.13)\end{aligned}$$

This scheme was extensively studied in [91] and was proven to be unconditionally stable and first order accurate. The variational formulation of the two-step DDC method is obtained by combining the defect and deferred correction techniques, as described in Sections 3.1.1-3.1.2.

Algorithm 3.2.1 (Two Step DDC) *Let $\Delta t > 0$, $M = \frac{T}{\Delta t}$, $f_i \in L^2(\Omega_i)$. Given $\hat{u}_i^n$, find $\hat{u}_i^{n+1} \in X_i^h$, $i, j = 1, 2, i \neq j$, $n = 0, 1, 2, \cdots, M-1$, satisfying*

$$\left(\frac{\hat{u}_i^{n+1} - \hat{u}_i^n}{\Delta t}, v_i\right) + (\nu_i + H_i)\left(\nabla \hat{u}_i^{n+1}, \nabla v_i\right) + \kappa \int_I |[\hat{u}^n]| \hat{u}_i^{n+1} v_i ds$$
$$- \kappa \int_I \hat{u}_j^n |[\hat{u}^n]|^{1/2} |[\hat{u}^{n-1}]|^{1/2} v_i ds$$
$$- (\hat{p}_i^{n+1}, \nabla \cdot v_i) + c_i\left(\hat{u}_i^{n+1}; \hat{u}_i^{n+1}, v_i\right) = \left(f_i^{n+1}, v_i\right), \ \forall v_i \in X_{i,h} \quad (3.2.14)$$

Then, given $\hat{u}_i^{n+1}$ and $\tilde{u}_i^n$, find $\tilde{u}_i^{n+1} \in X_i^h$ satisfying

$$\left(\frac{\tilde{u}_i^{n+1} - \tilde{u}_i^n}{\Delta t}, v_i\right) + (\nu_i + H_i)\left(\nabla \tilde{u}_i^{n+1}, \nabla v_i\right) - \kappa \int_I \tilde{u}_j^n |[\tilde{u}^n]|^{1/2} |[\tilde{u}^{n-1}]|^{1/2} v_i ds - (\tilde{p}_i^{n+1}, \nabla \cdot v_i)$$
$$+ \kappa \int_I |[\tilde{u}^n]| \tilde{u}_i^{n+1} v_i ds + c_i\left(\tilde{u}_i^{n+1}; \tilde{u}_i^{n+1}, v_i\right) = \left(\frac{f_i^{n+1} + f_i^n}{2}, v_i\right)$$
$$+ \frac{\Delta t(\nu_i + H_i)}{2}\left(\nabla(\frac{\hat{u}_i^{n+1} - \hat{u}_i^n}{\Delta t}), \nabla v_i\right) + \frac{\kappa}{2}\Delta t \int_I |[\hat{u}^n]|(\frac{\hat{u}_i^{n+1} - \hat{u}_i^n}{\Delta t}) v_i ds$$
$$- \frac{\kappa}{2}\Delta t \int_I \hat{u}_i^{n+1}(\frac{|[\hat{u}^{n+1}]| - |[\hat{u}^n]|}{\Delta t}) v_i ds + H_i\left(\nabla(\frac{\hat{u}_i^{n+1} + \hat{u}_i^n}{2}), \nabla v_i\right)$$
$$- \kappa \int_I \hat{u}_j^n |[\hat{u}^n]|^{1/2} |[\hat{u}^{n-1}]|^{1/2} v_i ds + \frac{\kappa}{2} \int_I |[\hat{u}^{n+1}]| \hat{u}_j^{n+1} v_i ds + \frac{\kappa}{2} \int_I |[\hat{u}^n]| \hat{u}_j^n v_i ds$$
$$+ \frac{1}{2} c_i(\hat{u}_i^{n+1}; \hat{u}_i^{n+1}, v_i) - \frac{1}{2} c_i(\hat{u}_i^n; \hat{u}_i^n, v_i) - \left(\frac{\hat{p}_i^{n+1} - \hat{p}_i^n}{2}, \nabla \cdot v_i\right), \ \forall v_i \in X_{i,h}. \quad (3.2.15)$$

The structure of the left hand side (and therefore the matrix of the system) is identical for (3.2.14) and (3.2.15); thus, a simple and computationally cheap artificial viscosity data-passing approximation is computed twice to achieve higher accuracy while maintaining the unconditional stability.

3.3 Proof of Stability and Convergence analysis

In this section we prove the unconditional stability of both the defect step and the correction step approximations. Also we show the accuracy of defect, correction and time derivative steps.

Lemma 21 *(Stability of Defect approximation) Let* $\hat{u}_i^j \in X_{i,h}$ *satisfy (3.2.14) for each* $j \in \left\{0, 1, 2, \cdots, \frac{T}{\Delta t} - 1\right\}$, $i = 1, 2$. *Then* $\exists C > 0$ *independent of* h, Δt *such that* $\hat{\mathbf{u}}^{n+1}$ *satisfies:*

$$\left\|\hat{\mathbf{u}}^{n+1}\right\|^2 + \sum_{j=1}^{n} \left\|\hat{\mathbf{u}}^{j+1} - \hat{\mathbf{u}}^{j}\right\|^2 + \Delta t \sum_{j=1}^{n} \left[(\nu_1 + H_1) \|\nabla u_1^{j+1}\|_{\Omega_1}^2 + (\nu_2 + H_2) \|\nabla u_2^{j+1}\|_{\Omega_2}^2 \right]$$
$$+ \kappa \Delta t \int_I |[\hat{\mathbf{u}}^n]| (|u_1^{n+1}|^2 + |u_2^{n+1}|^2) ds \ + \kappa \Delta t \sum_{j=1}^{n} \int_I |u_1^{j+1}| [\hat{\mathbf{u}}^j]|^{1/2} - u_2^j |[\hat{\mathbf{u}}^{j-1}]|^{1/2}|^2 ds$$
$$+ \kappa \Delta t \sum_{j=1}^{n} \int_I |u_2^{j+1}| [\hat{\mathbf{u}}^j]|^{1/2} - u_1^j |\hat{\mathbf{u}}^{j-1}|^{1/2}|^2 ds \leq \|\mathbf{u}^1\|^2 + \kappa \Delta t \int_I |[\mathbf{u}^0]| (|u_1^1|^2 + |u_2^1|^2) ds$$
$$+ \sum_{j=1}^{n} \left[\frac{\Delta t}{\nu_1 + H_1} \|f_1^{j+1}\|_{-1}^2 + \frac{\Delta t}{\nu_2 + H_2} \|f_2^{j+1}\|_{-1}^2 \right]. \quad (3.3.1)$$

Proof 12 *Replace ν_1 and ν_2 with $\nu_1 + H_1$ and $\nu_2 + H_2$, respectively, in the proof of Lemma 3.1 in [91].* ■

The accuracy result for the defect solution u is obtained in a manner very similar to Theorem 3.2 in [91].

Theorem 22 *(Accuracy of Defect Solution) Let $\hat{u}_i^k \in X_{i,h}$ satisfy (3.2.14) for each $k \in 2, \cdots, n \leq N-1$. Let $\tilde{\nu} = max\{\nu_1^{-1}, \nu_2^{-1}\}$, $\hat{\nu} = max\{\nu_1, \nu_2\}$, and let $D^{n+1} = \tilde{\nu}^3(1+\kappa^4 E^{n+1} + \|\nabla \mathbf{u}^{n+1}\|^4)$, where $E^{n+1} = max_{j=0,1,\cdots,n+1}\{\|\mathbf{u}^j\|_I^4\}$. Assume $\Delta t \leq \frac{1}{D^{n+1}}$, and that $(\mathbf{u}, \mathbf{p})$ is a strong solution of the coupled NSE system (3.1.1)–(3.1.6) with $\mathbf{u}_t \in L^2(0,T;X)$ and $\mathbf{u}_{tt} \in L^2(0,T;L^2(\Omega))$. Then the solution $\hat{\mathbf{u}}^{n+1}$ of (3.2.14) satisfies:*

$$\|\mathbf{u}^{n+1}-\hat{\mathbf{u}}^{n+1}\|^2+\frac{\Delta t}{2}\Bigg[(\nu_1+H_1)\sum_{k=1}^{n}\|\nabla(u_1^{k+1}-\hat{u}_1^{k+1})\|_{\Omega_1}^2$$
$$+(\nu_2+H_2)\sum_{k=1}^{n}\|\nabla(u_2^{k+1}-\hat{u}_2^{k+1})\|_{\Omega_2}^2\Bigg]$$
$$\leq Cexp\left\{\Delta t\sum_{n=1}^{j}\frac{D^{n+1}}{1-\Delta tD^{n+1}}\right\}\Bigg[\|\mathbf{u}^1-\hat{\mathbf{u}}^1\|^2+\inf_{\mathbf{v}^1\in V_h}\|\mathbf{u}^1-\mathbf{v}^1\|^2$$
$$+\Delta t(\nu_1+H_1)(\|\nabla(u_1^1-\hat{u}_1^1)\|_{\Omega_1}^2$$
$$+\frac{1}{2}\|\nabla(u_1^0-\hat{u}_1^0)\|_{\Omega_1}^2+\inf_{v_1^1\in V_{1,h}}\|\nabla(u_1^1-v_1^1)\|_{\Omega_1}^2+\frac{1}{2}\inf_{v_1^0\in V_{1,h}}\|\nabla(u_1^0-v_1^0)\|_{\Omega_1}^2)$$
$$+\Delta t(\nu_2+H_2)(\|\nabla(u_2^1-\hat{u}_2^1)\|_{\Omega_2}^2+\frac{1}{2}\|\nabla(u_2^0-\hat{u}_2^0)\|_{\Omega_2}^2+\inf_{v_2^1\in V_{2,h}}\|\nabla(u_2^1-v_2^1)\|_{\Omega_2}^2$$
$$+\frac{1}{2}\inf_{v_2^0\in V_{2,h}}\|\nabla(u_2^0-v_2^0)\|_{\Omega_2}^2)+\Delta t^2\|\mathbf{u}_{tt}\|_{L^2(0,T;L^2(\Omega))}^2+\inf_{\mathbf{v}\in V_h}\|(\mathbf{u}-\mathbf{v})_t\|_{L^2(0,T;L^2(\Omega))}^2$$
$$+\inf_{\mathbf{q}\in Q_h}\|\mathbf{p}-\mathbf{q}\|_{L^2(0,T;L^2(\Omega))}^2+\kappa^2\Delta t^2\|\mathbf{u}_t\|_{L^2(0,T;X)}^2$$
$$+T\max_{k=2,\cdots,n+1}(\inf_{\mathbf{v}^k\in V_h}\|\nabla(\mathbf{u}^k-\mathbf{v}^k)\|^2)+\frac{H_1^2}{\nu_1+H_1}C_{\nabla u_1}^2+\frac{H_2^2}{\nu_2+H_2}C_{\nabla u_2}^2\Bigg] \quad (3.3.2)$$

where C has the following dependence on κ , ν_1 and ν_2: $C = O(max\{\tilde{\nu}, \hat{\nu}, (1 + \Delta t\kappa^4)\tilde{\nu}^3, \kappa^2\})$.

Proof 13 *The proof can be found in [91], replacing ν_1 and ν_2 with $\nu_1 + H_1$ and $\nu_2 + H_2$, respectively. The extra term $H_i(\nabla u_i^{n+1}, \nabla v_i)$ is treated by applying the Cauchy-Schwarz and Young's inequalities to obtain the accuracy of $O(H_1^2 + H_2^2)$.* ■

Corollary 3.3.1 *Let the problem data be smooth enough; let the discrete velocity-pressure spaces consist of continuous piecewise polynomials of degrees m and $m-1$, respectively ($m \geq 2$). Then there exists a constant C independent of $h, H, \Delta t$, s.t.*

$$\begin{aligned}\|\mathbf{u}^{n+1} - \hat{\mathbf{u}}^{n+1}\|^2 + \frac{\Delta t}{2}\Bigg[&(\nu_1 + H_1)\sum_{k=1}^{n}\|\nabla(u_1^{k+1} - \hat{u}_1^{k+1})\|_{\Omega_1}^2 \\ &+(\nu_2 + H_2)\sum_{k=1}^{n}\|\nabla(u_2^{k+1} - \hat{u}_2^{k+1})\|_{\Omega_2}^2\Bigg] \\ &\leq C(h^{2m} + \Delta t^2 + H_1^2 + H_2^2). \end{aligned} \tag{3.3.3}$$

In order to show the improved accuracy for the correction approximation, we will need the following result; the proof will be given in full detail here, because typically the most challenging part of proving the accuracy of the correction step of DDC methods has to do with the theorem below. Consider $e_i^j = u_i^j - \hat{u}_i^j$, $i = 1, 2$, $j = 0, 1, 2, \cdots, M$.

Theorem 23 *(Accuracy of Time Derivative of the Error in the Defect Step) Let $u_i(\Delta t) \in H^2(\Omega_i)$, $\Delta \mathbf{u} \in L^2(0, T; L^2(\Omega))$ and $\mathbf{u}_{tt}, \mathbf{u}_t, \mathbf{u} \in L^2(0, T; L^2(\Omega))$. Let $min(h, \Delta t) < C(\frac{\nu_i + h_i}{\kappa})$.*

Let also $max(h, \Delta t, H_1, H_2) \leq \frac{\alpha}{4\sqrt{C_f}}$, where α is the constant introduced in Assumption 1, and C_f is the constant from (3.3.3).

Then $\exists C > 0$ *independent of* h, H_i, Δt *such that for any* $n \in \{0, 1, 2, \cdots, M-1 = \frac{T}{\Delta t} - 1\}$ *, the discrete time derivative of the error* $\frac{e_i^{n+1}-e_i^n}{\Delta t}$ *satisfies*

$$\|\frac{\mathbf{e}^{n+1}-\mathbf{e}^n}{\Delta t}\|^2+(\nu_1+H_1)\Delta t\sum_{j=1}^{n}\|\nabla\left(\frac{e_1^{j+1}-e_1^j}{\Delta t}\right)\|^2+(\nu_2+H_2)\Delta t\sum_{j=1}^{n}\|\nabla\left(\frac{e_2^{j+1}-e_2^j}{\Delta t}\right)\|^2$$
$$\leq C\left(h^{2m}+(\Delta t)^2+H^2\right). \quad (3.3.4)$$

Proof 14 *Focusing on* Ω_1 *first, write* (3.2.1) *at time* t_{n+1} *to obtain*

$$\left(\frac{u_1^{n+1}-u_1^n}{\Delta t}, v_1\right)+(\nu_1+H_1)(\nabla u_1^{n+1}, \nabla v_1)+c_1(u_1^{n+1}; u_1^{n+1}, v_1)-(p_1^{n+1}, \nabla\cdot v_1)$$
$$+\kappa\int_I u_1^{n+1}|[u^{n+1}]|v_1 ds-\kappa\int_I u_2^{n+1}|[u^{n+1}]|^{1/2}|[u^{n+1}]|^{1/2}v_1 ds$$
$$=(f_1^{n+1}, v_1)+H_1(\nabla u_1^{n+1}, \nabla v_1)+\left(\frac{u_1^{n+1}-u_1^n}{\Delta t}-u_{1,t}^{n+1}, v_1\right) \quad (3.3.5)$$

Denote $\frac{u_1^{n+1}-u_1^n}{\Delta t}-u_{1,t}^{n+1}\equiv\rho_1^{n+1}$*. Subtract* (3.2.14) *from* (3.3.5) *to obtain the equation for the error,* $e_i^{n+1}=u_i^{n+1}-\hat{u}_i^{n+1}, i=1,2$*. For any* $v_1\in X_1^h$

$$\left(\frac{e_1^{n+1}-e_1^n}{\Delta t}, v_1\right)+(\nu_1+H_1)(\nabla e_1^{n+1}, \nabla v_1)$$
$$+c_1(u_1^{n+1}; u_1^{n+1}, v_1)-c_1(\hat{u}_1^{n+1}; \hat{u}_1^{n+1}, v_1)$$
$$-(p_1^{n+1}-\hat{p}_1^{n+1}, \nabla\cdot v_1)+\kappa\int_I u_1^{n+1}|[u^{n+1}]|v_1 ds-\kappa\int_I \hat{u}_1^{n+1}|[\hat{u}^n]|v_1 ds \quad (3.3.6)$$
$$-\kappa\int_I u_2^{n+1}|[u^{n+1}]|v_1 ds+\kappa\int_I \hat{u}_2^{n}|[\hat{u}^n]|^{1/2}|[\hat{u}^{n-1}]|^{1/2}v_1 ds$$
$$=H_1(\nabla u_1^{n+1}, \nabla v_1)+(\rho_1^{n+1}, v_1)$$

Decompose $e_1^i = u_1^i - \hat{u}_1^i = (\breve{u}_1^i - \hat{u}_1^i) - (\breve{u}_1^i - u_1^i) = \phi_1^i - \eta_1^i$, *for some* $\breve{u}_1^i \in X_1^h$. *Taking* $v_1 = \frac{\phi_1^{n+1} - \phi_1^n}{\Delta t} \in X_{1,h}$ *in (3.3.6) leads to*

$$\begin{aligned}
&\left(\frac{e_1^{n+1} - e_1^n}{\Delta t}, \frac{\phi_1^{n+1} - \phi_1^n}{\Delta t}\right) + (\nu_1 + H_1)(\nabla e_1^{n+1}, \nabla \frac{\phi_1^{n+1} - \phi_1^n}{\Delta t}) \\
&\qquad + c_1(u_1^{n+1}; u_1^{n+1}, \frac{\phi_1^{n+1} - \phi_1^n}{\Delta t}) - c_1(u_1^{n+1}; u_1^{n+1}, \frac{\phi_1^{n+1} - \phi_1^n}{\Delta t}) \\
&-(p_1^{n+1} - \hat{p}_1^{n+1}, \nabla \cdot \frac{\phi_1^{n+1} - \phi_1^n}{\Delta t}) + \kappa \int_I u_1^{n+1} |[u^{n+1}]| \frac{\phi_1^{n+1} - \phi_1^n}{\Delta t} ds \\
&-\kappa \int_I \hat{u}_1^{n+1} |[\hat{u}^n]| \frac{\phi_1^{n+1} - \phi_1^n}{\Delta t} ds - \kappa \int_I u_2^{n+1} |[u^{n+1}]| \frac{\phi_1^{n+1} - \phi_1^n}{\Delta t} ds \\
&\qquad + \kappa \int_I \hat{u}_2^n |[\hat{u}^n]|^{1/2} |[\hat{u}^{n-1}]|^{1/2} \frac{\phi_1^{n+1} - \phi_1^n}{\Delta t} ds \\
&\qquad = H_1(\nabla u_1^{n+1}, \nabla \frac{\phi_1^{n+1} - \phi_1^n}{\Delta t}) + (\rho_1^{n+1}, \frac{\phi_1^{n+1} - \phi_1^n}{\Delta t})
\end{aligned} \tag{3.3.7}$$

Also, take $v_1 = \frac{\phi_1^{n+1} - \phi_1^n}{\Delta t}$ *in (3.3.6) at the previous time level, and subtract the resulting equation from (3.3.7). Denoting* $s_1^{n+1} \equiv \frac{\phi_1^{n+1} - \phi_1^n}{\Delta t}$,*we obtain for* $n \geq 1$

$$
\begin{aligned}
&\|s_1^{n+1}\|^2 - (s_1^{n+1}, s_1^n) + (\nu_1 + H_1)\Delta t\|\nabla s_1^{n+1}\|^2 + c_1(u_1^{n+1}; u_1^{n+1}, s_1^{n+1}) \\
&-c_1(u_1^n; u_1^n, s_1^{n+1}) - c_1(\hat{u}_1^{n+1}; \hat{u}_1^{n+1}, s_1^{n+1}) + c_1(\hat{u}_1^n; \hat{u}_1^n, s_1^{n+1}) \\
&+\Delta t\left(\frac{p_1^{n+1} - p_1^n}{\Delta t} - \frac{\hat{p}_1^{n+1} - \hat{p}_1^n}{\Delta t}, \nabla \cdot s_1^{n+1}\right) + \kappa \int_I u_1^{n+1}|[u^{n+1}]|s_1^{n+1} ds \\
&-\kappa \int_I u_1^n|[u^n]|s_1^{n+1} ds - \kappa \int_I \hat{u}_1^{n+1}|[\hat{u}^n]|s_1^{n+1} ds + \kappa \int_I \hat{u}_1^n|[\hat{u}^{n-1}]|s_1^{n+1} ds \\
&-\kappa \int_I u_2^{n+1}|[u^{n+1}]|s_1^{n+1} ds + \kappa \int_I u_2^n|[u^n]|s_1^{n+1} ds \\
&+\kappa \int_I \hat{u}_2^n|[\hat{u}^n]|^{1/2}|[\hat{u}^{n-1}]|^{1/2} s_1^{n+1} ds - \kappa \int_I \hat{u}_2^{n-1}|[\hat{u}^{n-1}]|^{1/2}|[\hat{u}^{n-2}]|^{1/2} s_1^{n+1} ds \\
&= H_1\Delta t\left(\nabla(\frac{u_1^{n+1} - u_1^n}{\Delta t}), \nabla s_1^{n+1}\right) + \Delta t\left(\frac{\rho_1^{n+1} - \rho_1^n}{\Delta t}, s_1^{n+1}\right) \\
&+\Delta t\left(\frac{\eta_1^{n+1} - 2\eta_1^n + \eta_1^{n-1}}{(\Delta t)^2}, s_1^{n+1}\right) + (\nu_1 + H_1)\Delta t\left(\nabla(\frac{\eta_1^{n+1} - \eta_1^n}{\Delta t}), \nabla s_1^{n+1}\right)
\end{aligned}
\tag{3.3.8}
$$

Special treatment is required for the interface and nonlinear terms. Consider the nonlinear terms

$$
c_1(u_1^{n+1}; u_1^{n+1}, s_1^{n+1}) - c_1(\hat{u}_1^{n+1}; \hat{u}_1^{n+1}, s_1^{n+1}) - c_1(u_1^n; u_1^n, s_1^{n+1}) + c_1(\hat{u}_1^n; \hat{u}_1^n, s_1^{n+1}). \tag{3.3.9}
$$

Add and subtract $c_1(u_1^{n+1}; \hat{u}_1^{n+1}, s_1^{n+1})$ *for the first pair,* $c_1(u_1^n; \hat{u}_1^n, s_1^{n+1})$ *for the second pair:*

$$
c_1(u_1^{n+1}; e_1^{n+1}, s_1^{n+1}) - c_1(u_1^n; e_1^n, s_1^{n+1}) - c_1(e_1^{n+1}; \hat{u}_1^{n+1}, s_1^{n+1}) - c_1(e_1^n; \hat{u}_1^n, s_1^{n+1}). \tag{3.3.10}
$$

Again, add and subtract $c_1(u_1^n; e_1^{n+1}, s_1^{n+1})$ for the first pair, $c_1(e_1^n; \hat{u}_1^{n+1}, s_1^{n+1})$ for the second pair:

$$\Delta t c_1(\frac{u_1^{n+1}-u_1^n}{\Delta t}; e_1^{n+1}, s_1^{n+1}) + \Delta t c_1(u_1^n; \frac{e_1^{n+1}-e_1^n}{\Delta t}, s_1^{n+1}) \\ + \Delta t c_1(\frac{e_1^{n+1}-e_1^n}{\Delta t}; \hat{u}_1^{n+1}, s_1^{n+1}) + \Delta t c_1(e_1^n; \frac{\hat{u}_1^{n+1}-\hat{u}_1^n}{\Delta t}, s_1^{n+1}). \quad (3.3.11)$$

After writing $\phi_1^i - \eta_1^i$ instead of e_1^i we get

$$\Delta t c_1(\frac{u_1^{n+1}-u_1^n}{\Delta t}; \phi_1^{n+1}, s_1^{n+1}) - \Delta t c_1(\frac{u_1^{n+1}-u_1^n}{\Delta t}; \eta_1^{n+1}, s_1^{n+1}) \\ + \Delta t c_1(u_1^n; s_1^{n+1}, s_1^{n+1}) - \Delta t c_1(u_1^n; \frac{\eta_1^{n+1}-\eta_1^n}{\Delta t}, s_1^{n+1}) \\ + \Delta t c_1(s_1^{n+1}; \hat{u}_1^{n+1}, s_1^{n+1}) - \Delta t c_1(\frac{\eta_1^{n+1}-\eta_1^n}{\Delta t}; \hat{u}_1^{n+1}, s_1^{n+1}) \\ + \Delta t c_1(\phi_1^n; \frac{\hat{u}_1^{n+1}-\hat{u}_1^n}{\Delta t}, s_1^{n+1}) - \Delta t c_1(\eta_1^n; \frac{\hat{u}_1^{n+1}-\hat{u}_1^n}{\Delta t}, s_1^{n+1}). \quad (3.3.12)$$

Note $\Delta t c_1(u_1^n; s_1^{n+1}, s_1^{n+1}) = 0$ (skew-symmetry). Replace all $\hat{u}_1^i$ terms with $u_1^i - e_1^i$. After that, bound them by applying the Cauchy-Schwarz and Young's inequalities.

Consider the first 4 interface terms

$$\kappa \int_I u_1^{n+1} |[u^{n+1}]| s_1^{n+1} ds - \kappa \int_I \hat{u}_1^{n+1} |[\hat{u}^n]| s_1^{n+1} ds \\ -(\kappa \int_I u_1^n |[u^n]| s_1^{n+1} ds - \kappa \int_I \hat{u}_1^n |[\hat{u}^{n-1}]| s_1^{n+1} ds) = F_1 - F_2.$$

Write F_1 as

$$\begin{aligned}
F_1 &= \kappa \int_I u_1^{n+1} |[u^{n+1}]| s_1^{n+1} ds - \kappa \int_I \hat{u}_1^{n+1} |[u^{n+1}]| s_1^{n+1} ds \\
&+\kappa \int_I \hat{u}_1^{n+1} |[u^{n+1}]| s_1^{n+1} ds - \kappa \int_I \hat{u}_1^{n+1} |[u^n]| s_1^{n+1} ds \\
&+\kappa \int_I \hat{u}_1^{n+1} |[u^n]| s_1^{n+1} ds - \kappa \int_I \hat{u}_1^{n+1} |[\hat{u}^n]| s_1^{n+1} ds \\
&= \kappa \int_I e_1^{n+1} |[u^{n+1}]| s_1^{n+1} ds + \kappa \int_I \hat{u}_1^{n+1} (|[u^{n+1}]| - |[u^n]|) s_1^{n+1} ds \\
&+\kappa \int_I \hat{u}_1^{n+1} |[e^n]| s_1^{n+1} ds = \kappa \int_I e_1^{n+1} |[u^{n+1}]| s_1^{n+1} ds \\
&+\kappa \int_I u_1^{n+1} (|[u^{n+1}]| - |[u^n]|) s_1^{n+1} ds - \kappa \int_I e_1^{n+1} (|[u^{n+1}]| - |[u^n]|) s_1^{n+1} ds \\
&+\kappa \int_I u_1^{n+1} |[e^n]| s_1^{n+1} ds - \kappa \int_I e_1^{n+1} |[e^n]| s_1^{n+1} ds.
\end{aligned}$$

In order to treat the five terms above, apply the same arguments for F_2 and subtract the result from F_1. Let $F_1 - F_2 = F_{12,1} + F_{12,2} + F_{12,3} + F_{12,4} + F_{12,5}$, defined as follows

$$\begin{aligned}
F_{12,1} &= \kappa \int_I (e_1^{n+1} - e_1^n) |[u^{n+1}]| s_1^{n+1} ds + \kappa \int_I e_1^n (|[u^{n+1}]| - |[u^n]|) s_1^{n+1} ds \qquad (3.3.13) \\
&= \kappa \Delta t \int_I |[u^{n+1}]| |s_1^{n+1}|^2 ds + \kappa \Delta t \int_I e_1^n \frac{|[u^{n+1}]| - |[u^n]|}{\Delta t} s_1^{n+1} ds \\
&+\kappa \Delta t \int_I \frac{\eta_1^{n+1} - \eta_1^n}{\Delta t} |[u^{n+1}]| s_1^{n+1} ds
\end{aligned}$$

The term $\kappa \int_I \Delta t |[u^{n+1}]||s_1^{n+1}|^2 ds$ *is non-negative and it stays in the left hand side. The Cauchy-Schwarz and Young's inequalities are used to bound the two remaining terms in the right hand side of* (3.3.13).

The term

$$\begin{aligned} F_{12,2} = \kappa \int_I u_1^{n+1}(|[u^{n+1}]| - |[u^n]|)s_1^{n+1} ds - \kappa \int_I u_1^n(|[u^n]| - |[u^{n-1}]|)s_1^{n+1} ds \\ = \kappa \int_I \Delta t \frac{u_1^{n+1} - u_1^n}{\Delta t}(|[u^{n+1}]| - |[u^n]|)s_1^{n+1} ds \\ + \kappa \int_I u_1^n(|[u^{n+1}]| - 2|[u^n]| + |[u^{n-1}]|)s_1^{n+1} ds \end{aligned}$$

is bounded by using Assumption 1 for the second integral in the right hand side and then applying the Cauchy-Schwarz and Young's inequalities.

Similarly, the Cauchy-Schwarz and Young's inequalities are used to derive the $O(H^2 + H\Delta t + \Delta t^2)$ *bounds for* $F_{12,3}, F_{12,4}, F_{12,5}$.

$$\begin{aligned} -F_{12,3} = \kappa \int_I e_1^{n+1}(|[u^{n+1}]| - |[u^n]|)s_1^{n+1} ds - \kappa \int_I e_1^n(|[u^n]| - |[u^{n-1}]|)s_1^{n+1} ds \\ = \kappa \int_I \Delta t(|[u^{n+1}]| - |[u^n]|)|s_1^{n+1}|^2 ds + \kappa \int_I \Delta t \frac{\eta_1^{n+1} - \eta_1^n}{\Delta t}(|[u^{n+1}]| - |[u^n]|)s_1^{n+1} ds \\ + \kappa \int_I e_1^n(|[u^{n+1}]| - 2|[u^n]| + |[u^{n-1}]|)s_1^{n+1} ds, \end{aligned}$$

$$F_{12,4} = \kappa \int_I u_1^{n+1} |[e^n]| s_1^{n+1} ds - \kappa \int_I u_1^n |[e^{n-1}]| s_1^{n+1} ds$$
$$= \kappa \int_I \frac{u_1^{n+1} - u_1^n}{\Delta t} \Delta t |[e^n]| s_1^{n+1} ds + \kappa \int_I u_1^n (|[e^n]| - |[e^{n-1}]|) s_1^{n+1} ds,$$

and

$$-F_{12,5} = \kappa \int_I e_1^{n+1} |[e^n]| s_1^{n+1} ds - \kappa \int_I e_1^n |[e^{n-1}]| s_1^{n+1} ds$$
$$= \kappa \int_I \Delta t |[e^n]| |s_1^{n+1}|^2 ds + \kappa \int_I \Delta t \frac{\eta_1^{n+1} - \eta_1^n}{\Delta t} |[e^n]| s_1^{n+1} ds$$
$$+ \kappa \int_I e_1^n (|[e^n]| - |[e^{n-1}]|) s_1^{n+1} ds.$$

We now proceed with the bounds on the remainder of the interface terms.

$$\kappa \int_I \hat{u}_2^n |[\hat{u}^n]|^{1/2} |[\hat{u}^{n-1}]|^{1/2} s_1^{n+1} ds - \kappa \int_I u_2^{n+1} |[u^{n+1}]| s_1^{n+1} ds$$
$$-(\kappa \int_I \hat{u}_2^{n-1} |[\hat{u}^{n-1}]|^{1/2} |[\hat{u}^{n-2}]|^{1/2} s_1^{n+1} ds - \kappa \int_I u_2^n |[u^n]| s_1^{n+1} ds) = B_1 - B_2.$$

For B_1,

$$\kappa \int_I \hat{u}_2^n (|[\hat{u}^n]|^{1/2} |[\hat{u}^{n-1}]|^{1/2} - \frac{1}{2}(|[\hat{u}^n]| + |[\hat{u}^{n-1}]|)) s_1^{n+1} ds - \kappa \int_I u_2^{n+1} |[u^{n+1}]| s_1^{n+1} ds$$
$$+\frac{\kappa}{2} \int_I \hat{u}_2^n (|[\hat{u}^n]| - |[\hat{u}^{n-1}]|) s_1^{n+1} ds + \kappa \int_I \hat{u}_2^n |[u^{n+1}]| s_1^{n+1} ds - \kappa \int_I \hat{u}_2^n |[u^{n+1}]| s_1^{n+1} ds$$
$$= \kappa \int_I \hat{u}_2^n (|[\hat{u}^n]|^{1/2} |[\hat{u}^{n-1}]|^{1/2} - \frac{1}{2}(|[\hat{u}^n]| + |[\hat{u}^{n-1}]|)) s_1^{n+1} ds - \kappa \int_I e_2^n |[u^{n+1}]| s_1^{n+1} ds$$
$$+\kappa \int_I \hat{u}_2^n (\frac{|[\hat{u}^n]| + |[\hat{u}^{n-1}]|}{2} - |[u^{n+1}]|) s_1^{n+1} ds.$$

Treating B_2 in the same way, we get

$$
\begin{aligned}
B_1 - B_2 = \kappa \int_I \hat{u}_2^n (|[\hat{u}^n]|^{1/2} |[\hat{u}^{n-1}]|^{1/2} \\
- \frac{1}{2}(|[\hat{u}^n]| + |[\hat{u}^{n-1}]|)) s_1^{n+1} ds \\
-\kappa \int_I \hat{u}_2^{n-1} (|[\hat{u}^{n-1}]|^{1/2} |[\hat{u}^{n-2}]|^{1/2} - \frac{1}{2}(|[\hat{u}^{n-1}]| + |[\hat{u}^{n-2}]|)) s_1^{n+1} ds \\
-\kappa \int_I e_2^n |[u^{n+1}]| s_1^{n+1} ds + \kappa \int_I e_2^{n-1} |[u^n]| s_1^{n+1} ds \\
+\kappa \int_I \hat{u}_2^n (\frac{|[\hat{u}^n]| + |[\hat{u}^{n-1}]|}{2} - |[u^{n+1}]|) s_1^{n+1} ds \\
-\kappa \int_I \hat{u}_2^{n-1} (\frac{|[\hat{u}^{n-1}]| + |[\hat{u}^{n-2}]|}{2} - |[u^n]|) s_1^{n+1} ds.
\end{aligned}
$$

Let

$$
\begin{aligned}
a &= |[\hat{u}^n]|^{1/2} |[\hat{u}^{n-1}]|^{1/2} - \frac{1}{2}(|[\hat{u}^n]| + |[\hat{u}^{n-1}]|) \\
a_p &= |[\hat{u}^{n-1}]|^{1/2} |[\hat{u}^{n-2}]|^{1/2} - \frac{1}{2}(|[\hat{u}^{n-1}]| + |[\hat{u}^{n-2}]|).
\end{aligned}
$$

Denote

$$I_1 = \kappa \int_I \hat{u}_2^n a s_1^{n+1} ds - \kappa \int_I \hat{u}_2^{n-1} a_p s_1^{n+1} ds$$

$$I_2 = -\kappa \int_I e_2^n |[u^{n+1}]| s_1^{n+1} ds + \kappa \int_I e_2^{n-1} |[u^n]| s_1^{n+1} ds$$

$$I_3 = \kappa \int_I \hat{u}_2^n (\frac{|[\hat{u}^n]| + |[\hat{u}^{n-1}]|}{2} - |[u^{n+1}]|) s_1^{n+1} ds$$

$$-\kappa \int_I \hat{u}_2^{n-1} (\frac{|[\hat{u}^{n-1}]| + |[\hat{u}^{n-2}]|}{2} - |[u^n]|) s_1^{n+1} ds.$$

.

The integrals in I_1 are treated as follows

$$\begin{aligned} I_1 &= \kappa \int_I \hat{u}_2^n a s_1^{n+1} ds - \kappa \int_I \hat{u}_2^{n-1} a_p s_1^{n+1} ds \\ &= \kappa \int_I \hat{u}_2^n a s_1^{n+1} ds - \kappa \int_I u_2^n a s_1^{n+1} ds \\ &+ \kappa \int_I u_2^n a s_1^{n+1} ds - \kappa \int_I u_2^{n-1} a s_1^{n+1} ds \\ &+ \kappa \int_I u_2^{n-1} a_p s_1^{n+1} ds - \kappa \int_I u_2^n a_p s_1^{n+1} ds \\ &+ \kappa \int_I u_2^{n-1} a s_1^{n+1} ds - \kappa \int_I \hat{u}_2^{n-1} a_p s_1^{n+1} ds. \end{aligned}$$

Denoting $x = |[\hat{u}^n]|^{1/2}$ *and* $y = |[\hat{u}^{n-1}]|^{1/2}$, *we write*

$$|a| = |xy - \frac{1}{2}(x^2+y^2)| = |-\frac{1}{2}(-2xy+x^2+y^2)| = |-\frac{1}{2}(x-y)^2| \qquad (3.3.14)$$
$$\leq \frac{1}{2}|x-y|(x+y) = \frac{1}{2}|x^2-y^2| = \frac{1}{2}|[\hat{u}^n - \hat{u}^{n-1}]|.$$

Then

$$|a| \leq \frac{1}{2}|[\hat{u}^n - \hat{u}^{n-1}]| \leq \frac{1}{2}|[e^n - e^{n-1}] - [u^n - u^{n-1}]|$$
$$\leq \frac{1}{2}|[\phi^n - \phi^{n-1}]| + \frac{1}{2}|[\eta^n - \eta^{n-1}]| + \frac{\Delta t}{2}\left|\left[\frac{u^n - u^{n-1}}{\Delta t}\right]\right|$$
$$\leq \frac{1}{2}\Delta t|s_1^n| + \frac{1}{2}\Delta t|s_2^n| + \frac{1}{2}\Delta t\left|\left[\frac{\eta^n - \eta^{n-1}}{\Delta t}\right]\right| + \frac{1}{2}\Delta t\left|\left[\frac{u^n - u^{n-1}}{\Delta t}\right]\right|.$$

Since a *is bounded, we can bound each line in* I_1*:*

$$\kappa\int_I \hat{u}_2^n a s_1^{n+1} ds - \kappa\int_I u_2^n a s_1^{n+1} ds$$
$$\leq C\kappa\int_I |e_2^n|\Delta t\left[|s_1^n| + |s_1^n| + \left|\frac{\eta^n - \eta^{n-1}}{\Delta t}\right| + \left|[\frac{u^n - u^{n-1}}{\Delta t}]\right|\right]|s_1^{n+1}|ds.$$

$$\kappa \int_I u_2^n a s_1^{n+1} ds - \kappa \int_I u_2^{n-1} a s_1^{n+1} ds \leq C\kappa \int_I \Delta t^2 \left| \frac{u_2^n - u_2^{n-1}}{\Delta t} \right| |a| |s_1^{n+1}| ds.$$

$$\kappa \int_I u_2^{n-1} a_p s_1^{n+1} ds - \kappa \int_I \hat{u}_2^{n-1} a_p s_1^{n+1} ds \leq C\kappa \int_I |e_2^{n-1}| \Delta t |a| |s_1^{n+1}| ds.$$

Instead of trying to show the second order of smallness of $|a - a_p|$*, we will show that* a *(and therefore* a_p*) is small enough. Each of the last two terms in* I_1*, is bounded using Assumption* 1*, as follows*

$$|\kappa \int_I u_2^n (|[\hat{u}^n]|^{1/2} - |[\hat{u}^{n-1}]|^{1/2})^2 s_1^{n+1} ds|$$
$$\leq \kappa \int_I (u_2^n/\alpha) |[u^n]| (|[\hat{u}^n]|^{1/2} - |[\hat{u}^{n-1}]|^{1/2})^2 |s_1^{n+1}| ds = A.$$

$$
\begin{aligned}
&|[u^n]|(|[\hat{u}^n]|^{1/2} - |[\hat{u}^{n-1}]|^{1/2})^2 \\
&= \frac{1}{4}\left[4|[u^n]| - (|[\hat{u}^n]|^{1/2} + |[\hat{u}^{n-1}]|^{1/2})^2 + (|[\hat{u}^n]|^{1/2} + |[\hat{u}^{n-1}]|^{1/2})^2\right](|[\hat{u}^n]|^{1/2} - |[\hat{u}^{n-1}]|^{1/2})^2 \\
&= \frac{1}{4}\left[4|[u^n]| - 2|[\hat{u}^n]| - 2|[\hat{u}^{n-1}]| + (|[\hat{u}^n]|^{1/2} - |[\hat{u}^{n-1}]|^{1/2})^2 + (|[\hat{u}^n]|^{1/2} + |[\hat{u}^{n-1}]|^{1/2})^2\right](|[\hat{u}^n]|^{1/2} \\
&- |[\hat{u}^{n-1}]|^{1/2})^2 = \frac{1}{4}\left[2(|[u^n]| - |[\hat{u}^n]|) + 2(|[u^n]| - |[u^{n-1}]|) + 2(|[u^{n-1}]| - |[\hat{u}^{n-1}]|)\right](|[\hat{u}^n]|^{1/2} \\
&\qquad - |[\hat{u}^{n-1}]|^{1/2})^2 + \frac{1}{4}(|[\hat{u}^n]|^{1/2} - |[\hat{u}^{n-1}]|^{1/2})^4 + \frac{1}{4}(|[\hat{u}^n]| - |[\hat{u}^{n-1}]|)^2.
\end{aligned}
$$

Thus,

$$
\begin{aligned}
A \leq \kappa \int_I \frac{1}{\alpha} |u_2^n||s_1^{n+1}| \Bigg[&\left(\Delta t \left| \left[\frac{u^n - u^{n-1}}{\Delta t} \right] \right| + |[\eta^n]| + |[\phi^n]| \right. \\
&\left. + |[\eta^{n-1}]| + |[\phi^{n-1}]| \right) \left[\Delta t \left| \left[\frac{u^n - u^{n-1}}{\Delta t} \right] \right| \right. \\
&\left. + \Delta t \left| \left[\frac{\eta^n - \eta^{n-1}}{\Delta t} \right] \right| + \Delta t |[s^n]| \right] + \Delta t^2 \left| \left[\frac{u^n - u^{n-1}}{\Delta t} \right] \right|^2 \\
&+ \Delta t^2 \left| \left[\frac{\eta^n - \eta^{n-1}}{\Delta t} \right] \right|^2 + \Delta t^2 |[s^n]|^2 \Bigg] ds. \quad (3.3.15)
\end{aligned}
$$

We will now show how to bound the terms in the right hand side of (3.3.15).

$$\kappa \int_I \frac{1}{\alpha}|u_2^n||s_1^{n+1}|\Delta t^2 \left|\left[\frac{\eta^n-\eta^{n-1}}{\Delta t}\right]\right|^2 ds \leq C\Delta t^2 \|\nabla s_1^{n+1}\| \left\|\left[\frac{\nabla\eta^n-\nabla\eta^{n-1}}{\Delta t}\right]\right\|^2$$
$$\leq \epsilon(\nu_1+H_1)\Delta t\|\nabla s_1^{n+1}\|^2 + C\Delta t^2\Delta t \left\|\left[\frac{\nabla\eta^n-\nabla\eta^{n-1}}{\Delta t}\right]\right\|^4. \tag{3.3.16}$$

The following term is bounding in exactly the same manner as (3.3.16).

$$\kappa \int_I \frac{1}{\alpha}|u_2^n||s_1^{n+1}|\Delta t^2 \left\|\left[\frac{u^n-u^{n-1}}{\Delta t}\right]\right\|^2 ds.$$

The next term is bounded in two different ways, depending on the relationship between the mesh diameter and the time step.

$$\kappa \int_I \frac{1}{\alpha}|u_2^n||s_1^{n+1}||\phi_1^n|\Delta t|s_1^n|ds \leq C\Delta t\|\phi_1^n\|^{1/2}\|\nabla\phi_1^n\|^{1/2}\|\nabla s_1^n\|\|\nabla s_1^{n+1}\|$$
$$\leq \epsilon(\nu_1+H_1)\Delta t\|\nabla s_1^{n+1}\|^2 + \frac{C}{\nu_1+H_1}\Delta t\|\phi_1^n\|\|\nabla\phi_1^n\|\|\nabla s_1^n\|^2. \tag{3.3.17}$$

$$\leq \begin{cases} \epsilon(\nu_1+H_1)\Delta t\|\nabla s_1^{n+1}\|^2 + \frac{C}{\nu_1+H_1}\Delta t h^{-1}(h^2+\Delta t^2)\|\nabla s_1^n\|^2 & if \Delta t < h \\ \epsilon(\nu_1+H_1)\Delta t\|\nabla s_1^{n+1}\|^2 + \frac{C}{\nu_1+H_1}(h+\Delta t)\Delta t^{1/2}(h+\Delta t)\|\nabla s_1^n\|^2 & \\ \leq \epsilon(\nu_1+H_1)\Delta t\|\nabla s_1^{n+1}\|^2 + \frac{C}{\nu_1+H_1}\Delta t^{3/2}\Delta t\|\nabla s_1^n\|^2 & if h < \Delta t. \end{cases}$$

Given that, $max(h, \Delta t) \leq \frac{\epsilon(\nu_1+H_1)^2}{C}$*, the terms in the right-hand side of* (3.3.17) *are small enough to either be subsumed in the left-hand side, or to provide the necessary accuracy.*

Two more terms from the right hand side of (3.3.15) *are bounded below.*

$$\kappa \int_I \frac{1}{\alpha}|u_2^n||s_1^{n+1}||\phi_1^n|\Delta t \left\| \left[\frac{u^n - u^{n-1}}{\Delta t} \right] \right\|^2 ds \leq C\Delta t \|\nabla \phi_1^n\| \|\nabla s_1^{n+1}\|^2$$
$$\leq \epsilon(\nu_1 + H_1)\Delta t \|\nabla s_1^{n+1}\|^2 + \frac{C}{\nu_1 + H_1}\Delta t \|\nabla \phi_1^n\|^2. \quad (3.3.18)$$

The next bound is obtained in a manner, similar to (3.3.17).

$$\kappa \int_I \frac{1}{\alpha}|u_2^n||s_1^{n+1}|\Delta t^2 |s_1^n|^2 ds \leq C\Delta t^2 \|s_1^n\|^{1/2} \|\nabla s_1^n\|^{3/2} \|\nabla s_1^{n+1}\|$$
$$\leq \epsilon(\nu_1 + H_1)\Delta t \|\nabla s_1^{n+1}\|^2 + \frac{C}{\nu_1 + H_1}\Delta t^3 \|s_1^n\| \|\nabla s_1^n\|^3$$
$$\leq \epsilon(\nu_1 + H_1)\Delta t \|\nabla s_1^{n+1}\|^2 + \frac{C}{\nu_1 + H_1}\|\phi_1^n\| \|\nabla \phi_1^n\| \Delta t \|\nabla s_1^n\|^2. \quad (3.3.19)$$

The remainder of the terms in (3.3.15) are bounded, using the Cauchy-Schwarz and Young's inequalities, similar to (3.3.16)-(3.3.19).

Add and subtract $\kappa \int e_2^n |[u^n]| s_1^{n+1} ds$ *for* I_2 *and* $\kappa \int \hat{u}_2^n (\frac{|[\hat{u}^{n-1}]|+|[\hat{u}^{n-2}]|}{2} - |[u^n]|) s_1^{n+1} ds$ *for* I_3*. The goal, as usual, is to get the second order of smallness in each of the interface*

terms; for most of them, applying the Cauchy-Schwarz and Young's inequalities is straightforward. The only problematic term is the one remaining from I_3*:*

$$\kappa \int_I u_2^n \left(|[\hat{\mathbf{u}}^n]| - |[\hat{\mathbf{u}}^{n-1}]| - |[\mathbf{u}^n]| + |[\mathbf{u}^{n-1}]| \right) s_1^{n+1} ds. \tag{3.3.20}$$

The second order of smallness for the interface term (3.3.20) *is achieved as follows. Notice that here lies the reason for us restricting the proof to the* $2-D$ *problems; the rest of the proof of this theorem (and others) is also valid in* $3-D$*.*

$$\begin{aligned} &|[\hat{\mathbf{u}}^n]| - |[\hat{\mathbf{u}}^{n-1}]| - |[\mathbf{u}^n]| + |[\mathbf{u}^{n-1}]| \\ &= \left((|[\hat{\mathbf{u}}^n]|^{\frac{1}{2}} - |[\mathbf{u}^{n-1}]|^{\frac{1}{2}})^2 - (|[\mathbf{u}^n]|^{\frac{1}{2}} - |[\hat{\mathbf{u}}^{n-1}]|^{\frac{1}{2}})^2 \right) \\ &+2 \left(|[\hat{\mathbf{u}}^n]|^{\frac{1}{2}} |[\mathbf{u}^{n-1}]|^{\frac{1}{2}} - |[\mathbf{u}^n]|^{\frac{1}{2}} |[\hat{\mathbf{u}}^{n-1}]|^{\frac{1}{2}} \right) = G + 2L. \end{aligned} \tag{3.3.21}$$

The second order of smallness of G follows from an argument given in (3.3.15). *With* $h + \Delta t \leq C\alpha$, *we have*

$$[\hat{\mathbf{u}}^n] = [\mathbf{u}^n] - [\mathbf{e}^n] => |[\hat{\mathbf{u}}^n]| \geq |[\mathbf{u}^n]| - |[\mathbf{e}^n]| \geq \frac{\alpha}{2}.$$

Then,

$$\begin{aligned} |L| &\leq \frac{1}{\alpha}|L| \left(|[\hat{\mathbf{u}}^n]|^{\frac{1}{2}} |[\mathbf{u}^{n-1}]|^{\frac{1}{2}} + |[\mathbf{u}^n]|^{\frac{1}{2}} |[\hat{\mathbf{u}}^{n-1}]|^{\frac{1}{2}} \right) \\ &\leq \frac{1}{\alpha} ||[\hat{\mathbf{u}}^n]| |[\mathbf{u}^{n-1}]| - |[\mathbf{u}^n]| |[\hat{\mathbf{u}}^{n-1}]|| = \frac{1}{\alpha}|D|. \end{aligned} \tag{3.3.22}$$

At the same time,

$$|[\hat{\mathbf{u}}^n][\mathbf{u}^{n-1}] - [\mathbf{u}^n][\hat{\mathbf{u}}^{n-1}]| = \quad |[\mathbf{u}^n][\mathbf{u}^{n-1}] - [\mathbf{e}^n][\mathbf{u}^{n-1}] - [\mathbf{u}^n][\mathbf{u}^{n-1}] + [\mathbf{u}^n][\mathbf{e}^{n-1}]|$$

$$\leq \qquad |[\mathbf{e}^n]|\Delta t|\tfrac{\mathbf{u}^n - \mathbf{u}^{n-1}}{\Delta t}| + |\mathbf{u}^n||[\mathbf{e}^n] - [\mathbf{e}^{n-1}]|. \quad (3.3.23)$$

In $2-D$*: for any* $i, j = 1, 2$*,* $\hat{u}_i \cdot n = u_j \cdot n = 0$ *on* I*, therefore* $\hat{u}_i || u_j$ *on* I*.*

Thus, in $2-D$

$$|[\hat{\mathbf{u}}^n]||[\mathbf{u}^{n-1}]| = |[\hat{\mathbf{u}}^n][\mathbf{u}^{n-1}]| \text{ and } |[\mathbf{u}^n]||[\hat{\mathbf{u}}^{n-1}]| = |[\mathbf{u}^n][\hat{\mathbf{u}}^{n-1}]|.$$

Putting it together, it follows from (3.3.21)-(3.3.23) *that*

$$|L| \leq \frac{1}{\alpha}|D| \leq \frac{1}{\alpha}|[\hat{\mathbf{u}}^n]||[\mathbf{u}^{n-1}] - [\mathbf{u}^n]||[\hat{\mathbf{u}}^{n-1}]| \quad (3.3.24)$$

$$\leq \frac{1}{\alpha}\left(\Delta t|[\mathbf{e}^n]||\frac{[\mathbf{u}^n] - [\mathbf{u}^{n-1}]}{\Delta t}| + \Delta t|[\mathbf{u}^n]||\frac{[\eta^n] - [\eta^{n-1}]}{\Delta t}| + \Delta t|[\mathbf{u}^n]||[s^n]|\right).$$

The last term in (3.3.24) *will be dealt with by using the Gronwall's lemma, and the rest of the terms are* $O(\Delta t(h+\Delta t))$.

Combining all the bounds together leads to

$$\frac{\|s_1^{n+1}\|^2-\|s_1^n\|^2}{2}+(\nu_1+H_1)\Delta t\|\nabla s_1^{n+1}\|^2\le\epsilon\Delta t(\nu_1+H_1)\|\nabla s_1^{n+1}\|^2$$
$$+\frac{d\Delta t}{4\epsilon(\nu_1+H_1)}\inf_{q_1\in Q_1^h}\|\frac{p_1^{n+1}-p_1^n}{\Delta t}-q_1\|^2+\frac{\Delta tH_1^2}{4\epsilon(\nu_1+H_1)}C^2_{\nabla u_{1t}}+\frac{\Delta t}{4\epsilon(\nu_1+H_1)}\|\frac{\rho_1^{n+1}-\rho_1^n}{\Delta t}\|^2_{-1}$$
$$\frac{\Delta tC_{PF}}{4\epsilon(\nu_1+H_1)}\|\frac{\eta_1^{n+1}-2\eta_1^n+\eta_1^{n-1}}{\Delta t^2}\|^2_{-1}+\frac{\Delta t(\nu_1+H_1)}{4\epsilon}\|\nabla(\frac{\eta_1^{n+1}-\eta_1^n}{\Delta t})\|^2$$
$$+\frac{C^2_{\nabla u_{1t}}\Delta t}{4\epsilon(\nu_1+H_1)}\|\nabla\phi_1^{n+1}\|^2+\frac{C^2_{\nabla u_{1t}}\Delta t}{4\epsilon(\nu_1+H_1)}\|\nabla\eta_1^{n+1}\|^2+\frac{C^2_{\nabla u_1}\Delta t}{4\epsilon(\nu_1+H_1)}\|\nabla(\frac{\eta_1^{n+1}-\eta_1^n}{\Delta t})\|^2$$
$$+\Delta t(\frac{C^2_{\nabla u_{1t}}}{2}+\frac{C^2_{u_1}}{16\epsilon(\nu_1+H_1)})\|s_1^{n+1}\|^2+\frac{4\Delta t}{\epsilon^3(\nu_1+H_1)^3}\|\nabla\phi_1^{n+1}\|^4\|s_1^{n+1}\|^2$$
$$+\frac{4\Delta t}{\epsilon^3(\nu_1+H_1)^3}\|\nabla\eta_1^{n+1}\|^4\|s_1^{n+1}\|^2+\frac{\Delta t}{4\epsilon(\nu_1+H_1)}\|\nabla\eta_1^{n+1}\|^2\|\nabla(\frac{\eta_1^{n+1}-\eta_1^n}{\Delta t})\|^2$$
$$+\frac{\Delta t}{4\epsilon(\nu_1+H_1)}\|\nabla\phi_1^{n+1}\|^2\|\nabla(\frac{\eta_1^{n+1}-\eta_1^n}{\Delta t})\|^2+C\frac{\kappa^2}{(\nu_1+H_1)}\Delta t\|\nabla e_1^n\|^2$$
$$+\frac{C\kappa^2}{(\nu_1+H_1)}\Delta t\|\nabla(\frac{\eta_1^{n+1}-\eta_1^n}{\Delta t})\|^2+\frac{C\kappa^2}{(\nu_1+H_1)}\Delta t\Delta t^2+C\kappa\Delta t^2\|\nabla s_1^{n+1}\|^2$$
$$+\frac{C\kappa^2}{(\nu_1+H_1)}\Delta t\Delta t^2\|\nabla(\frac{\eta_1^{n+1}-\eta_1^n}{\Delta t})\|^2+\frac{C\kappa^2}{(\nu_1+H_1)}\Delta t\Delta t^2\|\nabla\eta_1^n\|^2+\frac{C\kappa^2}{(\nu_1+H_1)}\Delta t\|s_1^{n+1}\|^2$$
$$+\epsilon\Delta t(\nu_1+H_1)\|\nabla s_1^n\|^2+\epsilon\Delta t(\nu_1+H_1)\|\nabla s_2^n\|^2+\frac{C\kappa^2}{(\nu_1+H_1)}\Delta t\|s_1^n\|^2+\frac{C\kappa^2}{(\nu_1+H_1)}\Delta t\|s_2^n\|^2$$
$$+\frac{C\kappa}{(\nu_1+H_1)^3}\Delta t\|\nabla e_1^n\|^4\|s_1^{n+1}\|^2+\frac{C\kappa}{(\nu_1+H_1)^3}\Delta t\|\nabla e_2^n\|^4\|s_1^{n+1}\|^2$$
$$+\frac{C\kappa^2}{(\nu_1+H_1)}\Delta t\|\nabla e_1^n\|^2\|\nabla(\frac{\eta_1^{n+1}-\eta_1^n}{\Delta t})\|^2+\frac{C\kappa^2}{(\nu_1+H_1)}\Delta t\|\nabla e_2^n\|^2\|\nabla(\frac{\eta_1^{n+1}-\eta_1^n}{\Delta t})\|^2$$

(to be continued on the next page)

$$+\frac{C\kappa^2}{(\nu_1+H_1)}\Delta t\|\nabla e_1^n\|^2\|[\nabla(\frac{\eta_1^n-\eta_1^{n-1}}{\Delta t})]\|^2$$
$$+\frac{C\kappa^2}{(\nu_1+H_1)^2}\Delta t\|e_1^n\|\|\nabla e_1^n\|\|\nabla s_1^n\|^2(\nu_1+H_1)$$
$$+\frac{C\kappa^2}{(\nu_1+H_1)^2}\Delta t\|e_2^n\|\|\nabla e_2^n\|\|\nabla s_1^n\|^2(\nu_1+H_1)$$
$$+\frac{C\kappa^2}{(\nu_1+H_1)^2}\Delta t\|e_2^n\|\|\nabla e_2^n\|\|\nabla s_2^n\|^2(\nu_1+H_1)$$
$$+\frac{C_{\nabla u_t}^2\kappa^2}{(\nu_1+H_1)}\Delta t\|\nabla e_2^n\|^2+\frac{C\kappa^2}{(\nu_1+H_1)^2}\Delta t\|e_2^{n-1}\|\|\nabla e_2^{n-1}\|\|\nabla s_1^n\|^2(\nu_1+H_1)$$
$$+\frac{C\kappa^2}{(\nu_1+H_1)^2}\Delta t\|e_2^{n-1}\|\|\nabla e_2^{n-1}\|\|\nabla s_2^n\|^2(\nu_1+H_1)+\frac{C_{\nabla u_t}^2\kappa^2}{(\nu_1+H_1)}\Delta t\|\nabla e_2^{n-1}\|^2$$
$$+\frac{C_{\nabla u_{2t}}^2\kappa^2}{4\epsilon(\nu_1+H_1)}\Delta t\Delta t^2\|\nabla s_1^n\|^2+\frac{C_{\nabla u_{2t}}^2\kappa^2}{4\epsilon(\nu_1+H_1)}\Delta t\Delta t^2\|\nabla s_2^n\|^2$$
$$+\frac{C_{\nabla u_{2t}}^2\kappa^2}{4\epsilon(\nu_1+H_1)}\Delta t\Delta t^2\|\nabla(\frac{[\eta^n-\eta^{n-1}]}{\Delta t})\|^2+\frac{C_{\nabla u_{2t}}^2\kappa^2}{4\epsilon(\nu_1+H_1)}\Delta t\Delta t^2C_{\nabla u_t}^2$$
$$+C\Delta t\Delta t^2\|\nabla(\frac{[\eta^n-\eta^{n-1}]}{\Delta t})\|^4+\frac{C}{(\nu_1+H_1)}\Delta t\|\phi_1^n\|\|\nabla\phi_1^n\|\|\nabla s_1^n\|^2$$
$$+\frac{C}{\nu_1+H_1}\Delta t\|\nabla\phi_1^n\|^2+\frac{C}{\epsilon(\nu_1+H_1)}\Delta t^2\Delta t\|\nabla[s^n]\|^4+\frac{C\kappa}{\epsilon(\nu_1+H_1)}\Delta t\|\nabla[s^n]\|^2\|\nabla[\eta^n]\|^2$$

Summing over the time levels, multiplying both sides by 2, letting appropriate ϵ and using the modified Gronwall's lemma gives

$$\|s_1^{n+1}\|^2+(\nu_1+H_1)\Delta t\sum_{j=1}^{n}\|\nabla s_1^{n+1}\|^2\leq C\left(\|s_1^2\|^2+O(h^{2m}+(\Delta t)^2+H^2)\right)$$

In order to be able to finish the proof using the discrete Gronwall's lemma, we will need the following bound

$$\|s_i^2\|^2 + \Delta t\|\nabla s_i^1\|^2 + \Delta t\|\nabla s_i^2\|^2 \leq C(h^2 + (\Delta t)^2)$$

Notice that the method requires two initial conditions, so that we are given $\hat{u}_i^0$ *and* $\hat{u}_i^1$, $i = 1, 2$. *Then we can take* $\tilde{u_i}^0$ *and* $\tilde{u_i}^1$ *to be the* L^2 *projections of* $\hat{u}_i^0$ *and* $\hat{u}_i^1$, *respectively, onto* X^h. *This gives:*

$\phi^0 = \phi^1 = s^1 = 0$, $\|\eta_i^0\| \leq Ch^{m+1}$, $\|\eta_i^1\| \leq Ch^{m+1}$, *with* C *independent of* h, Δt. *In order to get a bound on the* s_i^2*-terms, consider the error equation at* $n = 1$*; take* $v = s_1^2$ *in* Ω_1 *and* $v = s_2^2$ *in* Ω_2. *In* Ω_1 *this gives,*

$$\begin{aligned}
&\|s_1^2\|^2 + \left(\frac{\eta_1^2 - \eta_1^1}{\Delta t}, s_1^2\right) + (\nu_1 + H_1)(\nabla\phi_1^2, \nabla s_1^2) \\
&+(\nu_1 + H_1)(\nabla\eta_1^2, \nabla s_1^2) + c_1(u_1^2; u_1^2, s_1^2) - c_1(\hat{u}_1^2; \hat{u}_1^2, s_1^2) \\
&-(p_1^2 - q, \nabla \cdot s_1^2) + \kappa \int_I [u^2][|u^2|]s_1^2 ds \\
&-\kappa \int_I \hat{u}_1^2 |[\hat{u}^1]| s_1^2 ds + \kappa \int_I \hat{u}_2^1 |[\hat{u}^1]|^{1/2} |[\hat{u}^0]|^{1/2} s_1^2 ds \\
&= H_1(\nabla u_1^2, \nabla s_1^2) + (\rho_1^2, s_1^2) \qquad (3.3.25)
\end{aligned}$$

First, to bound the terms on the on the right hand side (RHS);

$$H_1(\nabla u_1^1, \nabla s_1^2) + H_1\left(\nabla(\frac{u_1^2 - u_1^1}{\Delta t}), \nabla s_1^2\right)\Delta t + (\rho_1^2, s_1^2)$$

$$\leq 2\epsilon\|s_1^2\|^2 + CH_1^2\|\nabla u_1^1\|^2$$

$$+C\|\rho_1^2\|^2 + \epsilon_1(\nu_1 + H_1)\Delta t\|\nabla s_1^2\|^2$$

$$+\frac{C}{\nu_1 + H_1}\Delta t H_1^2\left\|\nabla(\frac{u_1^2 - u_1^1}{\Delta t})\right\|^2$$

For nonlinearity,

$$c_1(u_1^2; u_1^2, s_1^2) - c_1(\hat{u}_1^2; u_1^2, s_1^2) + c_1(\hat{u}_1^2; u_1^2, s_1^2) - c_1(\hat{u}_1^2; \hat{u}_1^2, s_1^2)$$

$$= c_1(\eta_1^2 + \phi_1^2, u_1^2, s_1^2) + c_1(\hat{u}_1^2; \eta_1^2, s_1^2)$$

$$= c_1(\eta_1^2; u_1^2, s_1^2) + c_1(\phi_1^2; u_1^2, s_1^2) + c_1(u_1^2; \eta_1^2, s_1^2)$$

$$-c_1(\eta_1^2; \eta_1^2, s_1^2) - c_1(\phi_1^2; \eta_1^2, s_1^2)$$

Let's bound each of these five terms separately.

$$|c_1(\eta_1^2; u_1^2, s_1^2)| \leq C\|\eta_1^2\|\|\nabla s_1^2\|$$

$$|c_1(\phi_1^2; u_1^2, s_1^2)| \leq C\|\phi_1^2\|\|\nabla s_1^2\| = C\Delta t\|s_1^2\|\|\nabla s_1^2\|$$

$$\leq \epsilon\|s_1^2\|^2 + C\Delta t(\nu_1 + H_1)^{-1}(\nu_1 + H_1)\Delta t\|\nabla s_1^2\|^2$$

$$|c_1(u_1^2; \eta_1^2, s_1^2)| \leq C\|\nabla\eta_1^2\|\|s_1^2\| \leq \epsilon\|s_1^2\|^2 + C\|\nabla\eta_1^2\|^2$$

$$|c_1(\eta_1^2; \eta_1^2, s_1^2)| \leq \epsilon\|\nabla s_1^2\|^2 + Ch^{-2}\|\nabla\eta_1^2\|^4$$

$$|c_1(\phi_1^2; \eta_1^2, s_1^2)| \leq C\Delta t\|s_1^2\|^{1/2}\|\nabla s_1^2\|^{3/2}\|\nabla\eta_1^2\|$$

$$\leq \epsilon\|s_1^2\|^2 + C\|\nabla\eta_1^2\|^{4/3}\Delta t^{1/2}(\nu_1 + H_1)^{-1}\Delta t(\nu_1 + H_1)\|\nabla s_1^2\|^2$$

The pressure term (if $2 \leq m$*);*

$$|(p_1^2 - q, \nabla \cdot s_1^2)| \leq \epsilon\|s_1^2\|^2 + C\|\nabla(p_1^2 - q)\|^2$$

Thus,

$$\|s_1^2\|^2 + (\nu_1 + H_1)\Delta t\|\nabla s_1^2\|^2 \leq O(h^2 + \Delta t^2) + \textit{interface terms}$$

For interface terms;

$$A = \kappa \int_I u_1^2 |[u^2]| s_1^2 ds - \kappa \int_I \hat{u}_1^2 |[\hat{u}^1]| s_1^2 ds$$
$$B = \kappa \int_I u_2^2 |[u^2]| s_1^2 ds - \kappa \int_I \hat{u}_2^1 |[\hat{u}^1]|^{1/2} |[\hat{u}^0]|^{1/2} s_1^2 ds$$

Write A as $A = A_1 + A_2 + A_3$, where

$$A_1 = \kappa \int_I u_1^2 |[u^2]| s_1^2 ds - \kappa \int_I u_1^2 |[u^1]| s_1^2 ds$$
$$A_2 = \kappa \int_I u_1^2 |[u^1]| s_1^2 ds - \kappa \int_I \hat{u}_1^2 |[u^1]| s_1^2 ds$$
$$A_3 = \kappa \int_I \hat{u}_1^2 |[u^1]| s_1^2 ds - \kappa \int_I \hat{u}_1^2 |[\hat{u}^1]| s_1^2 ds$$

A_1 is bounded by

$$|A_1| \leq \kappa \int_I |u_1^2| ||[u^2]| - 2|[u^1]| + |[u^0]|| |s_1^2| ds + \kappa \int_I |u_1^2| ||[u^1]| - |[u^0]|| |s_1^2| ds = A_{11} + A_{12}$$

For a bound on $S = \left| |[u^n]| - 2|[u^{n-1}]| + |[u^{n-2}]| \right|$, consider $g(\vec{x}, t^i) = |[u^i]|$

$$g(\vec{x}, t^n) = g(\vec{x}, t^{n-1}) + \Delta t g_t(\vec{x}, t^{n-1}) + \Delta t^2 g_{tt}(\vec{x}, t^{n-1} + \xi_1 \Delta t), \tag{3.3.26}$$

for some $\xi_1 \in (0, 1)$.

$$g(\vec{x}, t^{n-2}) = g(\vec{x}, t^{n-1}) - \Delta t g_t(\vec{x}, t^{n-1}) + \Delta t^2 g_{tt}(\vec{x}, t^{n-1} - \xi_2 \Delta t), \tag{3.3.27}$$

for some $\xi_2 \in (0, 1)$.

$$S = g(\vec{x}, t^n) - 2g(\vec{x}, t^{n-1}) + g(\vec{x}, t^{n-2}) = \Delta t^2 g_{tt}(\vec{x}, t^{n-1}) + O(\Delta t^3) = O(\Delta t^2),$$

provided that

$$\begin{aligned} |[\mathbf{u}]| &\leq C \\ |[\mathbf{u}_t]| &\leq C \\ |[\mathbf{u}_{tt}]| &\leq C. \end{aligned} \tag{3.3.28}$$

Thus, under the assumptions of the theorem,

$$A_{11} \leq C\|\nabla u_1^2\|\Delta t^2\|\nabla s_1^2\| \leq \epsilon(\nu_1 + H_1)\Delta t\|\nabla s_1^2\|^2 + (\nu_1 + H_1)^{-1}\Delta t C \Delta t^2$$

For A_{12} use Assumption 2,

$$A_{12} \leq C\Delta t^{5/4}\|\nabla u_1^2\|\|s_1^2\|^{1/2}\|\nabla s_1^2\|^{1/2}$$

$$\leq \epsilon(\nu_1 + H_1)\Delta t\|\nabla s_1^2\|^2 + C(\nu_1 + H_1)^{-1/3}\Delta t^{4/3}\|\nabla u_1^2\|^{4/3}\|s_1^2\|^{2/3}$$

$$\leq \epsilon(\nu_1 + H_1)\Delta t\|\nabla s_1^2\|^2 + \epsilon_1\|s_1^2\|^2 + C(\nu_1 + H_1)^{-1/2}\Delta t^2\|\nabla u_1^2\|^2$$

The terms A_2 and A_3 are bounded as

$$|A_2| \leq \kappa\int_I \Delta t|s_1^2|^2|[u^1]|ds + \kappa\int_I \eta_1^2|[u^1]|s_1^2 ds \leq C\Delta t\|s_1^2\|\|\nabla s_1^2\| + Ch^{-1}\|\eta_1^2\|\|s_1^2\|$$

$$\leq \epsilon\|s_1^2\|^2 + C(\nu_1 + H_1)^{-1}\Delta t\Delta t(\nu_1 + H_1)\|\nabla s_1^2\|^2 + \epsilon\|s_1^2\|^2 + Ch^{-2}\|\eta_1^2\|^2$$

and

$$|A_3| \leq \kappa\int_I |\hat{u}_1^2||[\eta^1]||s_1^2|ds$$

$$\leq Ch^{-1}\|[\eta^1]\|\|s_1^2\| + C\|\nabla\phi_1^2\|h^{-3/2}\|[\eta^1]\|\|s_1^2\| + C\|\nabla\eta_1^2\|h^{-3/2}\|[\eta^1]\|\|s_1^2\|$$

Write B as $B = B_1 + B_2 + B_3 + B_4$, where

$$B_1 = \kappa \int_I u_2^2 |[u^2]| s_1^2 ds - \kappa \int_I u_2^2 \frac{1}{2}(|[u^1]| + |[u^0]|) s_1^2 ds$$

$$B_2 = \frac{1}{2}\kappa \int_I u_2^2 (|[u^1]| + |[u^0]|) s_1^2 ds - \frac{1}{2}\kappa \int_I u_2^2 (|[\hat{u}^1]| + |[\hat{u}^0]|) s_1^2 ds$$

$$B_3 = \frac{1}{2}\kappa \int_I u_2^2 (|[\hat{u}^1]| + |[\hat{u}^0]|) s_1^2 ds - \frac{1}{2}\kappa \int_I \hat{u}_2^1 (|[\hat{u}^1]| + |[\hat{u}^0]|) s_1^2 ds$$

$$B_4 = \frac{1}{2}\kappa \int_I \hat{u}_2^1 (|[\hat{u}^1]|^{1/2} - |[\hat{u}^0]|^{1/2})^2 s_1^2 ds$$

To bound B_1;

$$B_1 = \frac{1}{2}\kappa \int_I u_2^2 (|[u^2]| - |[u^1]|) s_1^2 ds + \frac{1}{2}\kappa \int_I u_2^2 (|[u^2]| - |[u^0]|) s_1^2 ds$$

$$= \frac{1}{2}\kappa \int_I u_2^2 (|[u^2]| - |[u^1]|) s_1^2 ds + \frac{1}{2}\kappa \int_I u_2^2 (|[u^2]| - |[u^1]|) s_1^2 ds + \frac{1}{2}\kappa \int_I u_2^2 (|[u^1]| - |[\hat{u}^0]|) s_1^2 ds$$

bounded exactly as we treated A_1.

To bound B_2;

$$B_2 = \frac{1}{2}\kappa \int_I u_2^2 (|[u^1]| - |[\hat{u}^1]|) s_1^2 ds + \frac{1}{2}\kappa \int_I u_2^2 (|[u^0]| - |[\hat{u}^0]|) s_1^2 ds$$

$$|B_2| \leq \frac{1}{2}\kappa \int_I |u_2^2| |[u^1 - \hat{u}^1]| |s_1^2| ds + \frac{1}{2}\kappa \int_I |u_2^2| |[u^0 - \hat{u}^0]| |s_1^2| ds$$

$$\leq Ch^{-3/2} \|\nabla u_2^2\| \|\eta^1\| \|s_1^2\| + Ch^{-3/2} \|\nabla u_2^2\| \|\eta^0\| \|s_1^2\|$$

$$\leq \epsilon_1 \|s_1^2\|^2 + Ch^{-3}(\|\eta^1\|^2 + \|\eta^0\|^2)$$

To bound B_3;

$$B_3 = \frac{1}{2}\kappa \int_I (u_2^2 - u_2^1)(|[\hat{u}^1]| + |[\hat{u}^0]|)s_1^2 ds + \frac{1}{2}\kappa \int_I (u_2^1 - \hat{u}_2^1)(|[\hat{u}^1]| + |[\hat{u}^0]|)s_1^2 ds$$

$$= B_{31} + B_{32}$$

Write

$$|[\hat{u}^1]| + |[\hat{u}^0]| = |[u^1 - \eta^1]| + |[u^0 - \eta^0]| \leq |[u^1]| + |[u^0]| + |[\eta^1]| + |[\eta^0]|, \qquad (3.3.29)$$

use $u_2^1 - \hat{u}_2^1 = \eta_2^1$ and Assumption 2, to bound B_3 similar to the bounds onA_1 and B_2.

For a bound on B_4, use Assumption 1 and follow the way of bounding A interface term.

Finally, using the results , the upper bound on $\|s_1^2\|^2 + \Delta t\|\nabla s_1^2\|^2$ follows from (14):

$$\|s_1^2\|^2 + (\nu_1 + H_1)\Delta t\|\nabla s_1^2\|^2 \leq C(\Delta t^2 + h^{2m-2}).$$

For $2 \leq m$, we get

$$\|s_1^2\|^2 + (\nu_1 + H_1)\Delta t\|\nabla s_1^2\|^2 \leq C(\Delta t^2 + h^2).$$

Terms in domain 2 are treated in exactly the same way. After adding the inequalities for domains 1 and 2 , use the discrete Gronwall's lemma and the triangle inequality, we obtain for $e_j^i = u_j^i - \hat{u}_j^i$ $(j = 1, 2)$*:*

$$\|\frac{\mathbf{e}^{n+1} - \mathbf{e}^n}{\Delta t}\|^2 + (\nu_1 + H_1)\Delta t \sum_{j=1}^{n} \|\nabla \left(\frac{e_1^{j+1} - e_1^j}{\Delta t} \right)\|^2$$

$$+(\nu_2 + H_2)\Delta t \sum_{j=1}^{n} \|\nabla \left(\frac{e_2^{j+1} - e_2^j}{\Delta t} \right)\|^2 \leq C \left(h^2 + (\Delta t)^2 + H_1^2 + H_2^2 \right) . \blacksquare$$

We now proceed to show the stability and increased accuracy of the correction step approximation $\tilde{u}$. The left hand sides of the equations satisfied by $\hat{u}$ and $\tilde{u}$ are the same, so parts of the proofs of stability and accuracy of the defect step approximation can be reused here.

Theorem 24 (Stability of Correction Step of DDC) *Let* $\tilde{\mathbf{u}}^{\mathbf{n+1}} \in \mathbf{X^h}$ *satisfy (3.2.15) for each* $n \in \left\{0, 1, 2, \cdots, \frac{T}{\Delta t} - 1\right\}$*. Then* $\exists C > 0$ *independent of* h, Δt *such that* $\tilde{\mathbf{u}}^{n+1}$ *satisfies:*

$$\left\|\tilde{u}_1^{n+1}\right\|^2+\left\|\tilde{u}_2^{n+1}\right\|^2+(\nu_1+H_1)\Delta t\sum_{k=1}^{n+1}\left\|\nabla\tilde{u}_1^{k}\right\|^2+(\nu_1+H_2)\Delta t\sum_{k=1}^{n+1}\left\|\nabla\tilde{u}_2^{k}\right\|^2$$

$$+\kappa\,\Delta t\int_I\left|\tilde{u}_1^{n+1}|[\tilde{\mathbf{u}}^n]|^{1/2}-\tilde{u}_2^{n}|[\tilde{\mathbf{u}}^{n-1}]|^{1/2}\right|^2ds+\kappa\,\Delta t\int_I\left|\tilde{u}_2^{n+1}|[\tilde{\mathbf{u}}^n]|^{1/2}-\tilde{u}_1^{n}|[\tilde{\mathbf{u}}^{n-1}]|^{1/2}\right|^2ds$$

$$\leq\frac{C\Delta t}{\nu_1+H_1}\sum_{j=1}^{n}\Bigg[\|\nabla e_1^{j+1}\|^2+\|e_2^j\|\|\nabla e_2^j\|\|\nabla e_i^j\|^2$$

$$+\|\nabla e_i^{j+1}\|^2+\|e_1^{j+1}\|\|\nabla e_1^{j+1}\|\|\nabla e_i^j\|^2+\|e_1^j\|\|\nabla e_1^j\|\|\nabla e_i^j\|^2+\|\nabla e_2^j\|^2\Bigg]$$

$$+\frac{\Delta t}{14(\nu_1+H_1)}\sum_{j=1}^{n}(\|\nabla e_2^j\|^2+\|e_2^j\|\|\nabla e_2^j\|\|\nabla e_i^j\|^2)$$

$$+\frac{8\Delta t(\nu_1+H_1)}{19}\sum_{j=1}^{n}\left\{\Delta t^2\|\nabla(\frac{e_1^{j+1}-e_1^j}{\Delta t})\|^2+\Delta t^2C^2_{\nabla\hat{u}_t})\right\}$$

$$+\frac{8\Delta t(\nu_1+H_1)}{19}\sum_{j=1}^{n}\Bigg[\Delta t\|\nabla\hat{u}_1^{j+1}\|^2\Delta t\|\nabla(\frac{e_1^{j+1}-e_1^j}{\Delta t})\|^2$$

$$+\Delta t\|\nabla\hat{u}_1^{j+1}\|^2\Delta tC^2_{\nabla\hat{u}_{1t}}+\Delta t\|\nabla\hat{u}_1^{j}\|^2\Delta t\|\nabla(\frac{e_1^{j+1}-e_1^j}{\Delta t})\|^2+\Delta t\|\nabla\hat{u}_1^{j}\|^2\Delta tC^2_{\nabla\hat{u}_{1t}}\Bigg]$$

$$+\frac{19\Delta t}{(\nu_1+H_1)}\sum_{j=1}^{n}\left[H_1^2\|\nabla\hat{u}_1^{j+1}\|^2+\|\frac{f_1^{j+1}+f_1^j}{2}\|^2_{-1}\right]+\frac{\Delta tC_{\nabla u^{n+1}}}{\nu_1+H_1}\sum_{j=1}^{n}\left[1+\kappa\|\nabla e_i^{j+1}\|^2\right]$$

$$+\Delta tC\sum_{j=1}^{n}(\|e_1^{j+1}\|^{1/2}\|\nabla e_1^{j+1}\|^{1/2}+\|e_2^{j+1}\|^{1/2}\|\nabla e_2^{j+1}\|^{1/2})\|\nabla e_i^{j+1}\|^2 \quad (3.3.30)$$

Proof 15 *Choosing $v_1=\tilde{u}_1^{n+1}$ in (3.2.15) gives*

$$\left(\frac{\tilde{u}_1^{n+1}-\tilde{u}_1^n}{\Delta t},\tilde{u}_1^{n+1}\right)+(\nu_1+H_1)\left(\nabla\tilde{u}_1^{n+1},\nabla\tilde{u}_1^{n+1}\right)$$
$$-\kappa\int_I\tilde{u}_2^n|[\tilde{u}^n]|^{1/2}|[\tilde{u}^{n-1}]|^{1/2}\tilde{u}_1^{n+1}ds-(\tilde{p}_1^{n+1},\nabla\cdot\tilde{u}_1^{n+1})$$
$$+\kappa\int_I|[\tilde{u}^n]|\tilde{u}_1^{n+1}\tilde{u}_1^{n+1}ds+c_1\left(\tilde{u}_1^{n+1};\tilde{u}_1^{n+1},\tilde{u}_1^{n+1}\right)=\left(\frac{f_1^{n+1}+f_1^n}{2},\tilde{u}_1^{n+1}\right)$$
$$+\frac{\Delta t(\nu_1+H_1)}{2}\left(\nabla(\frac{\hat{u}_1^{n+1}-\hat{u}_1^n}{\Delta t}),\nabla\tilde{u}_1^{n+1}\right)-\frac{1}{2}c_1(\hat{u}_1^n;\hat{u}_1^n,\tilde{u}_1^{n+1})$$
$$+\frac{\kappa}{2}\Delta t\int_I|[\hat{u}^n]|(\frac{\hat{u}_1^{n+1}-\hat{u}_1^n}{\Delta t})\tilde{u}_1^{n+1}ds-\frac{\kappa}{2}\Delta t\int_I\hat{u}_1^{n+1}(\frac{|[\hat{u}^{n+1}]|-|[\hat{u}^n]|}{\Delta t})\tilde{u}_1^{n+1}ds$$
$$+H_1\left(\nabla(\frac{\hat{u}_1^{n+1}+\hat{u}_1^n}{2}),\nabla\tilde{u}_1^{n+1}\right)+\frac{1}{2}c_1(\hat{u}_1^{n+1};\hat{u}_1^{n+1},\tilde{u}_1^{n+1})$$
$$-\kappa\int_I\hat{u}_2^n|[\hat{u}^n]|^{1/2}|[\hat{u}^{n-1}]|^{1/2}\tilde{u}_1^{n+1}ds+\frac{\kappa}{2}\int_I|[\hat{u}^{n+1}]|\hat{u}_2^{n+1}\tilde{u}_1^{n+1}ds$$
$$+\frac{\kappa}{2}\int_I|[\hat{u}^n]|\hat{u}_2^n\tilde{u}_1^{n+1}ds-\left(\frac{\hat{p}_1^{n+1}-\hat{p}_1^n}{2},\nabla\cdot\tilde{u}_1^{n+1}\right),\ \forall v_1\in X_{1,h}.\quad(3.3.31)$$

We will be applying the Cauchy-Schwarz inequality and Young's inequality to subsume all the $\hat{u}_1$-terms, leading to the telescoping series in the left hand side of (3.3.31) *- in exactly the same way the stability of the defect step was proven in [91].*

The nonlinear terms in the right hand side are treated as follows.

$$\frac{1}{2}c_1(\hat{u}_1^{n+1};\hat{u}_1^{n+1},\tilde{u}_1^{n+1}) - \frac{1}{2}c_1(\hat{u}_1^{n};\hat{u}_1^{n},\tilde{u}_1^{n+1})$$
$$= \frac{1}{2}c_1(\hat{u}_1^{n+1};\hat{u}_1^{n+1},\tilde{u}_1^{n+1}) - \frac{1}{2}c_1(\hat{u}_1^{n};\hat{u}_1^{n},\tilde{u}_1^{n+1}) + \frac{1}{2}c_1(\hat{u}_1^{n+1};\hat{u}_1^{n},\tilde{u}_1^{n+1}) - \frac{1}{2}c_1(\hat{u}_1^{n+1};\hat{u}_1^{n},\tilde{u}_1^{n+1})$$
$$= \frac{\Delta t}{2}c_1(\hat{u}_1^{n+1};\frac{\hat{u}_1^{n+1}-\hat{u}_1^{n}}{\Delta t},\tilde{u}_1^{n+1}) + \frac{\Delta t}{2}c_1(\frac{\hat{u}_1^{n+1}-\hat{u}_1^{n}}{\Delta t};\hat{u}_1^{n},\tilde{u}_1^{n+1}) = A + B$$

$$A \leq \frac{\Delta t}{2}\|\nabla\hat{u}_1^{n+1}\|\left\|\nabla\left(\frac{\hat{u}_1^{n+1}-\hat{u}_1^{n}}{\Delta t}\right)\right\|\|\nabla\tilde{u}_1^{n+1}\|$$
$$\leq \epsilon(\nu_1+H_1)\|\nabla\tilde{u}_1^{n+1}\|^2 + \frac{\Delta t^2}{16\epsilon(\nu_1+H_1)}\|\nabla\hat{u}_1^{n+1}\|^2\left\|\nabla\left(\frac{\hat{u}_1^{n+1}-\hat{u}_1^{n}}{\Delta t}\right)\right\|^2$$
$$\leq \epsilon(\nu_1+H_1)\|\nabla\tilde{u}_1^{n+1}\|^2 + \frac{2\Delta t}{16\epsilon(\nu_1+H_1)}\|\nabla\hat{u}_1^{n+1}\|^2\Delta t\left\|\nabla\left(\frac{e_1^{n+1}-e_1^{n}}{\Delta t}\right)\right\|^2$$
$$+\frac{2\Delta t}{16\epsilon(\nu_1+H_1)}\|\nabla\hat{u}_1^{n+1}\|^2\Delta t C^2_{\nabla\hat{u}_{1t}}$$

Similarly,

$$B \leq \epsilon(\nu_1+H_1)\|\nabla\tilde{u}_1^{n+1}\|^2 + \frac{2\Delta t}{16\epsilon(\nu_1+H_1)}\|\nabla\hat{u}_1^{n}\|^2\Delta t\left\|\nabla\left(\frac{e_1^{n+1}-e_1^{n}}{\Delta t}\right)\right\|^2$$
$$+\frac{2\Delta t}{16\epsilon(\nu_1+H_1)}\|\nabla\hat{u}_1^{n+1}\|^2\Delta t C^2_{\nabla\hat{u}_{1t}}.$$

Note that $\Delta t\|\nabla\hat{u}_1^{n}\|^2 \leq \Delta t\sum_{i=1}^{n}\|\nabla\hat{u}_1^{i}\|^2$ *and the stability bound for the defect step*

approximation can be utilized. The two interface terms on the left hand side of (3.3.31) are treated in the same way as in the stability proof in [91] .

Replacing $\hat{u}_i$ *with* $u_i - e_i$ *leads to*

$$\frac{\kappa}{2}\int_I |[\hat{u}^{n+1}]|(\hat{u}_2^{n+1} - \hat{u}_1^{n+1})\tilde{u}_1^{n+1}ds$$
$$= \frac{\kappa}{2}\int_I |[\hat{u}^{n+1}]|(u_2^{n+1} - u_1^{n+1})\tilde{u}_1^{n+1}ds - \frac{\kappa}{2}\int_I |[\hat{u}^{n+1}]|(e_2^{n+1} - e_1^{n+1})\tilde{u}_1^{n+1}ds$$

Repeating this replacement and applying the Cauchy-Schwarz and Young's inequalities, we obtain

$$\frac{\kappa}{2}\int_I |[\hat{u}^{n+1}]|(\hat{u}_2^{n+1} - \hat{u}_1^{n+1})\tilde{u}_1^{n+1}ds$$
$$\leq \frac{\kappa C_{\nabla u^{n+1}}}{2(\nu_1 + H_1)} + \frac{3\epsilon(\nu_1 + H_1)}{2}\|\nabla\tilde{u}_1^{n+1}\|^2 + \frac{C}{(\nu_1 + H_1)}(\|\nabla e_1^{n+1}\|^2 + \|\nabla e_2^{n+1}\|^2)$$
$$\frac{\kappa C_{\nabla u^{n+1}}}{2(\nu_1 + H_1)}(\|\nabla e_1^{n+1}\|^2 + \|\nabla e_2^{n+1}\|^2) + \frac{\epsilon(\nu_1 + H_1)}{2}\|\nabla\tilde{u}_1^{n+1}\|^2 + C(\|e_1^{n+1}\|^{1/2}\|\nabla e_1^{n+1}\|^{1/2}$$
$$+ \|e_2^{n+1}\|^{1/2}\|\nabla e_2^{n+1}\|^{1/2})(\|\nabla e_1^{n+1}\|^2 + \|\nabla e_2^{n+1}\|^2)$$

Next, we bound the interface term $W = \kappa\int_I \hat{u}_1^{n+1}|[\hat{u}^n]|\tilde{u}_1^{n+1}ds$.

$$W = \kappa\int_I u_1^{n+1}|[\hat{u}^n]|\tilde{u}_1^{n+1}ds - \kappa\int_I e_1^{n+1}|[\hat{u}^n]|\tilde{u}_1^{n+1}ds$$

Since $|a-b| \leq |a| + |b|$, $\|\nabla[\hat{u}^n]\| \leq \|\nabla\hat{u}_1^n\| + \|\nabla\hat{u}_2^n\|$. *Thus,*

$$W \leq \frac{C_{\nabla u^{n+1}}}{(\nu_1 + H_1)}(\|\nabla \hat{u}_1^n\|^2 + \|\nabla \hat{u}_2^n\|^2) + \epsilon(\nu_1 + H_1)\|\nabla \tilde{u}_1^{n+1}\|^2 \tag{3.3.32}$$

$$+C\|e_1^{n+1}\|^{1/2}\|\nabla e_1^{n+1}\|^{1/2}\|\nabla e_1^n\|\|\nabla \tilde{u}_1^{n+1}\|$$

$$+C\|e_1^{n+1}\|^{1/2}\|\nabla e_1^{n+1}\|^{1/2}\|\nabla e_2^n\|\|\nabla \tilde{u}_1^{n+1}\|$$

$$+C\|e_1^{n+1}\|^{1/2}\|\nabla e_1^{n+1}\|^{1/2}\|\nabla [u]^n\|\|\nabla \tilde{u}_1^{n+1}\|$$

The last three summands in the right hand side of (3.3.32) *are bounded by*

$$C\|e_1^{n+1}\|^{1/2}\|\nabla e_1^{n+1}\|^{1/2}\|\nabla [u]^n\|\|\nabla \tilde{u}_1^{n+1}\| \leq \frac{C}{(\nu_1 + H_1)}\|\nabla e_1^{n+1}\|^2 + \epsilon(\nu_1 + H_1)\|\nabla \tilde{u}_1^{n+1}\|^2,$$

and

$$C\|e_1^{n+1}\|^{1/2}\|\nabla e_1^{n+1}\|^{1/2}\|\nabla e_1^n\|\|\nabla \tilde{u}_1^{n+1}\| + C\|e_1^{n+1}\|^{1/2}\|\nabla e_1^{n+1}\|^{1/2}\|\nabla e_2^n\|\|\nabla \tilde{u}_1^{n+1}\|$$

$$\leq 2\epsilon(\nu_1 + H_1)\|\nabla \tilde{u}_1^{n+1}\|^2 + \frac{C}{(\nu_1 + H_1)}\|e_1^{n+1}\|\|\nabla e_1^{n+1}\|(\|\nabla e_1^n\|^2 + \|\nabla e_2^n\|^2). \tag{3.3.33}$$

In order to bound the last summand in the right hand side of (3.3.33)*, choose one of the two options below, depending on the relationship between the mesh diameter and*

the time step. Both of these upper bounds are of the required order of smallness.

$$\begin{cases} \frac{C}{(\nu_1+H_1)}\frac{1}{h}(h^2+\Delta t^2)(\|\nabla e_1^n\|^2+\|\nabla e_2^n\|^2) & if \Delta t < h \\ \frac{C}{(\nu_1+H_1)}[\Delta t(\|\nabla e_1^n\|^4+\|\nabla e_2^n\|^4)+\Delta t\|\nabla e_1^{n+1}\|^2] & if h < \Delta t \end{cases}$$

The terms $\frac{\kappa}{2}\int_I \hat{u}_1^n|[\hat{u}^n]|\tilde{u}_1^{n+1}ds$ *and* $\kappa\int_I \hat{u}_2^n|[\hat{u}^n]|\tilde{u}_1^{n+1}ds$ *are bounded in the same way as the term* W*.*

Since $|[\hat{u}^n]|^{1/2}|[\hat{u}^{n-1}]|^{1/2} \leq \frac{|[\hat{u}^n]|+|[\hat{u}^{n-1}]|}{2}$*, we get*

$$\kappa\int_I |\hat{u}_2^n||[\hat{u}^n]|^{1/2}|[\hat{u}^{n-1}]|^{1/2}|\tilde{u}_1^{n+1}|ds$$
$$= \frac{\kappa}{2}\int_I |\hat{u}_2^n||[\hat{u}^n]||\tilde{u}_1^{n+1}|ds + \frac{\kappa}{2}\int_I |\hat{u}_2^n||[\hat{u}^{n-1}]||\tilde{u}_1^{n+1}|ds = I + II \quad (3.3.34)$$

Both the I *and* II *terms are bounded similar to the bound on* W*. Terms in domain 2 are treated in exactly the same way and then the inequalities for domains 1 and 2 are added together. Finally, choosing* $\epsilon = \frac{1}{38}$ *allow us to subsume the* $\nabla\tilde{u}_i$*-terms in the LHS. Multiplying through by* $2\Delta t$ *and summing over the time levels gives us the desired result.* ■

We now have all the intermediate results that are needed for proving the accuracy of

the correction step solution $\tilde{\mathbf{u}}$.

Theorem 25 *(Accuracy of Correction Step) Let the assumptions of Theorems* 22 *and* 23 *be satisfied. Then* $\exists C > 0$ *independent of* $h, \Delta t$ *such that for any* $n \in \{0, 1, 2, \cdots, M-1 = \frac{T}{\Delta t} - 1\}$*, the solution* $\tilde{u}_i^{n+1}$ *of (3.2.15) satisfies*

$$\|\mathbf{u}^{n+1} - \tilde{\mathbf{u}}^{n+1}\|^2 + (\nu + H_1)\Delta t \sum_{j=1}^{n+1} \|\nabla(u_1^j - \tilde{u}_1^j)\|^2 + (\nu + H_2)\Delta t \sum_{j=1}^{n+1} \|\nabla(u_2^j - \tilde{u}_2^j)\|^2$$
$$\leq C\left(h^4 + h^2\Delta t^2 + H_1^4 + H_1^2\Delta t^2 + H_2^4 + H_2^2\Delta t^2 + (\Delta t)^4\right) \quad (3.3.35)$$

Proof 16 *First, sum* (3.3.5) *at time levels* t_n *and* t_{n+1} *and divide by 2, to obtain in* Ω_1*:*

$$\begin{aligned}
&\left(\frac{u_1^{n+1}-u_1^n}{\Delta t},v_1\right)+(\nu_1+H_1)(\nabla(\frac{u_1^{n+1}+u_1^n}{2}),\nabla v_1)\\
&\qquad+\frac{1}{2}c_1(u_1^{n+1};u_1^{n+1},v_1)+\frac{1}{2}c_1(u_1^n;u_1^n,v_1)\\
&-\left(\frac{p_1^{n+1}+p_1^n}{2},\nabla\cdot v_1\right)+\frac{\kappa}{2}\int_I|[u^{n+1}]|(u_1^{n+1}-u_2^{n+1})v_1ds\\
&\qquad+\frac{\kappa}{2}\int_I|[u^n]|(u_1^n-u_2^n)v_1ds\\
&=\left(\frac{f_1^{n+1}+f_1^n}{2},v_1\right)+H_1\left(\nabla\left(\frac{u_1^{n+1}+u_1^n}{2}\right),\nabla v_1\right)\\
&\qquad-\left(\frac{u_{1,t}^{n+1}+u_{1,t}^n}{2},v_1\right)+\left(\frac{u_1^{n+1}-u_1^n}{\Delta t},v_1\right)
\end{aligned}\tag{3.3.36}$$

For the $O(\Delta t^2)$-term introduce the notation $\frac{u_i^{n+1}-u_i^n}{\Delta t}-\frac{u_{i,t}^{n+1}+u_{i,t}^n}{2}\equiv\gamma_i^{n+1}$. Subtract the correction step equation (3.2.15) from (3.3.36). Denoting $ce_i^{n+1}=u_i(t_{n+1})-\tilde{u}_i^{n+1}, i=1,2$, we obtain

$$\left(\frac{ce_1^{n+1}-ce_1^n}{\Delta t},v_1\right)+(\nu_1+H_1)(\nabla ce_1^{n+1},\nabla v_1)$$
$$+c_1(u_1^{n+1};u_1^{n+1},v_1)-\frac{1}{2}c_1(u_1^{n+1};u_1^{n+1},v_1)$$
$$-c_1(\tilde{u}_1^{n+1};\tilde{u}_1^{n+1},v_1)+\frac{1}{2}c_1(u_1^n;u_1^n,v_1)+\frac{1}{2}c_1(\hat{u}_1^{n+1};\hat{u}_1^{n+1},v_1)-\frac{1}{2}c_1(\hat{u}_1^n;\hat{u}_1^n,v_1)$$
$$-\left(p_1^{n+1}-\tilde{p}_1^{n+1},\nabla\cdot v_1\right)+\frac{\kappa}{2}\int_I(u_1^{n+1}-u_2^{n+1})|[u^{n+1}]|v_1ds-\kappa\int_I\tilde{u}_1^{n+1}|[\tilde{u}^n]|v_1ds$$
$$+\kappa\int_I\tilde{u}_2^n|[\tilde{u}^n]|^{1/2}|[\tilde{u}^{n-1}]|^{1/2}v_1ds+\frac{\kappa}{2}\int_I(u_1^n-u_2^n)|[u^n]|v_1ds$$
$$=\frac{\Delta t(\nu_1+H_1)}{2}\left(\nabla(\frac{e_1^{n+1}-e_1^n}{\Delta t}),\nabla v_1\right)+\frac{H_1\Delta t}{2}\left(\nabla(\frac{u_1^{n+1}-u_1^n}{\Delta t}),\nabla v_1\right)$$
$$+H_1(\nabla e_1^{n+1},\nabla v_1)+(\gamma_1^{n+1},v_1)+\frac{\Delta t}{2}\left(\frac{p_1^{n+1}-p_1^n}{\Delta t}-\frac{\hat{p}_1^{n+1}-\hat{p}_1^n}{\Delta t},\nabla\cdot v_1\right)$$
$$+\kappa\int_I\hat{u}_2^n|[\hat{u}^n]|^{1/2}|[\hat{u}^{n-1}]|^{1/2}v_1ds-\kappa\int_I\hat{u}_1^{n+1}|[\hat{u}^n]|v_1ds$$
$$+\frac{\kappa}{2}\int_I\hat{u}_1^{n+1}|[\hat{u}^{n+1}]|v_1ds+\frac{\kappa}{2}\int_I\hat{u}_1^n|[\hat{u}^n]|v_1ds$$
$$-\frac{\kappa}{2}\int_I\hat{u}_2^{n+1}|[\hat{u}^{n+1}]|v_1ds-\frac{\kappa}{2}\int_I\hat{u}_2^n|[\hat{u}^n]|v_1ds \quad (3.3.37)$$

Similarly to the error decomposition in the case of the defect approximation, decompose $ce_1^{n+1}=u_1^{n+1}-\tilde{u}_1^{n+1}=\phi_1^{n+1}-\eta_1^{n+1},\phi_1\in X_{1,h}$. *We now choose* $v_1=\phi_1^{n+1}\in X_{1,h}$ *in (3.3.37).*

Notice that after applying the Cauchy-Schwarz and Young's inequalities, the first five terms in the right hand side will provide the expected second order of smallness, $O(\Delta t(h+H_1+\Delta t))$. *This follows from the results of Theorems* 22 *and* 23.

We now briefly introduce the approach to treating the twelve interface terms of (3.3.37). After the proper pairing, the proof follows similarly to the treatment of the interface terms in Theorem 23.

Combine $-\frac{\kappa}{2}\int_I u_1^{n+1}|[u^{n+1}]|\phi_1^{n+1}ds$ *and* $-\frac{\kappa}{2}\int_I u_1^{n}|[u^{n}]|\phi_1^{n+1}ds$ *with half of* $\kappa\int_I \tilde{u}_1^{n+1}|[\tilde{u}^{n}]|\phi_1^{n+1}ds$ *term for each.*

Similarly, pair $\frac{\kappa}{2}\int_I u_2^{n+1}|[u^{n+1}]|\phi_1^{n+1}ds$ *and* $\frac{\kappa}{2}\int_I u_2^{n}|[u^{n}]|\phi_1^{n+1}ds$ *with half of* $-\kappa\int_I \tilde{u}_2^{n}|[\tilde{u}^{n}]|^{1/2}|[\tilde{u}^{n-1}]|^{1/2}\phi_1^{n+1}ds$ *term for each.*

Also, add and subtract $I \equiv \kappa\int_I[u^{n+1}]|[u^{n+1}]|\phi_1^{n+1}ds$ *from the rest of the interface terms. Pair up* I *with* $-\kappa\int_I \hat{u}_1^{n+1}|[\hat{u}^{n}]|\phi_1^{n+1}ds$ *and* $\kappa\int_I \hat{u}_2^{n}|[\hat{u}^{n}]|^{1/2}|[\hat{u}^{n-1}]|^{1/2}\phi_1^{n+1}ds$. *Combine* $-I$ *with the remainder of the interface terms. Then follow the proof of Theorem* 23 *to obtain the corresponding bounds.*

The nonlinear terms are treated as follows.

$$
\begin{aligned}
&c_1(u_1^{n+1};u_1^{n+1},\phi_1^{n+1})-c_1(\tilde{u}_1^{n+1};\tilde{u}_1^{n+1},\phi_1^{n+1})-\frac{1}{2}c_1(u_1^{n+1};u_1^{n+1},\phi_1^{n+1})\\
&+\frac{1}{2}c_1(\hat{u}_1^{n+1};\hat{u}_1^{n+1},\phi_1^{n+1})+\frac{1}{2}c_1(u_1^{n};u_1^{n},\phi_1^{n+1})-\frac{1}{2}c_1(\hat{u}_1^{n};\hat{u}_1^{n},\phi_1^{n+1})\\
&=c_1(u_1^{n+1};ce_1^{n+1},\phi_1^{n+1})+c_1(ce_1^{n+1};\tilde{u}_1^{n+1},\phi_1^{n+1})-\frac{1}{2}c_1(u_1^{n+1};e_1^{n+1},\phi_1^{n+1})\\
&-\frac{1}{2}c_1(e_1^{n+1};\hat{u}_1^{n+1},\phi_1^{n+1})+\frac{1}{2}c_1(u_1^{n};e_1^{n},\phi_1^{n+1})+\frac{1}{2}c_1(e_1^{n};\hat{u}_1^{n},\phi_1^{n+1})
\end{aligned}
$$

Adding and subtracting more nonlinear terms and writing $ce_1^{n+1}=\eta_1^{n+1}-\phi_1^{n+1}$ *we get*

$$
\begin{aligned}
&-c_1(u_1^{n+1};\phi_1^{n+1},\phi_1^{n+1})+c_1(u_1^{n+1};\eta_1^{n+1},\phi_1^{n+1})-c_1(\phi_1^{n+1};\tilde{u}_1^{n+1},\phi_1^{n+1})\\
&+c_1(\eta_1^{n+1};\tilde{u}_1^{n+1},\phi_1^{n+1})+\frac{\Delta t}{2}c_1(\frac{u_1^{n+1}-u_1^{n}}{\Delta t};e_1^{n},\phi_1^{n+1})+\frac{\Delta t}{2}c_1(u_1^{n+1};\frac{e_1^{n+1}-e_1^{n}}{\Delta t},\phi_1^{n+1})\\
&+\frac{\Delta t}{2}c_1(e_1^{n+1};\frac{u_1^{n+1}-u_1^{n}}{\Delta t},\phi_1^{n+1})-\frac{\Delta t}{2}c_1(e_1^{n+1};\frac{e_1^{n+1}-e_1^{n}}{\Delta t},\phi_1^{n+1})\\
&+\frac{\Delta t}{2}c_1(\frac{e_1^{n+1}-e_1^{n}}{\Delta t};\hat{u}_1^{n},\phi_1^{n+1}).
\end{aligned}
$$

The first of these terms is identically zero; the third term is treated by using the sharper bound (3.2.11) and then it is subsumed using the Gronwall's lemma. The remainder

of the nonlinear terms provide the necessary second order of smallness. Terms in domain 2 are treated in exactly the same way. Finally, summing over $i = 1, 2$ and using the Gronwall's lemma completes the proof. ■

3.4 Computational Testing

We use a manufactured solution test to illustrate the theoretical findings of this chapter. An exact solution in the domain $\Omega = \Omega_1 \cup \Omega_2$ with $\Omega_1 = [0, 1] \times [0, 1]$ and $\Omega_2 = [0, 1] \times [0, -1]$ is given by

$$
\begin{aligned}
u_{1,1} &= a\nu_1 e^{-t} x^2 (1-x)^2 (1+y) + a e^{-t/2} x(1-x)\nu_1/\sqrt{\kappa a} \\
u_{1,2} &= a\nu_1 e^{-t} xy(2+y)(1-x)(2x-1) + a e^{-t/2} y(2x-1)\nu_1/\sqrt{\kappa a} \\
u_{2,1} &= a\nu_1 e^{-t} x^2 (1-x)^2 (1+\frac{\nu_1}{\nu_2} y) \\
u_{2,2} &= a\nu_1 e^{-t} xy(1-x)(2x-1)(2+\frac{\nu_1}{\nu_2} y),
\end{aligned}
$$

where $u_{i,j} : \Omega_i \to R, \forall i, j = 1, 2$. Parameters are chosen as follows: $a = 1$, $\nu_1 = 0.5$, $\nu_2 = 0.1$, $\kappa = 1$ and the final time $T = 1$. The solution has a vortex region in the lower subdomain.

Pressures in both domains are set to zero (for simplicity only, not a requirement), and the right hand side forcing terms, initial and boundary values are calculated

accordingly. For simplicity, we have used the true solution for two initial values. Instead, one could use one step of the Geometric Averaging Method as a starting method to find the second initial value. In order to compute the convergence rates easily, we have chosen the mesh size(h), time step(Δt), and both artificial viscosities (H_i) equal to $1/N$, where N is the number of mesh points on per unit line segment. Taylor-Hood elements, piecewise quadratic polynomials for the velocity and piecewise linear polynomials for the pressure, have been used in these computations.

Table 3.1
AV approximation $\hat{u}$.

N	$\|\| u - \hat{u} \|\|_{L^2(0,T;L^2(\Omega))}$	rate	$\|\| u - \hat{u} \|\|_{L^2(0,T;H^1(\Omega))}$	rate
2	1.4798e-002	-	7.3869e-002	-
4	9.4941e-003	0.64	6.8654e-002	0.10
8	5.5097e-003	0.78	4.9680e-002	0.46
16	2.9407e-003	0.90	2.9957e-002	0.72
32	1.5262e-003	0.94	1.5786e-002	0.92
64	7.9193e-004	0.94	7.7512e-003	1.02
128	4.0867e-004	0.95	3.7515e-003	1.04

Table 3.2
CS approximation $\tilde{u}$.

N	$\|\| u - \tilde{u} \|\|_{L^2(0,T;L^2(\Omega))}$	rate	$\|\| u - \tilde{u} \|\|_{L^2(0,T;H^1(\Omega))}$	rate
2	1.0087e-002	-	6.0656e-002	-
4	5.1671e-003	0.96	4.2536e-002	0.51
8	2.3203e-003	1.15	2.3754e-002	0.84
16	8.7794e-004	1.40	1.0149e-002	1.22
32	2.8166e-004	1.64	3.3514e-003	1.60
64	8.1197e-005	1.79	9.2868e-004	1.85
128	2.2172e-005	1.87	2.3908e-004	1.96

As seen in Table (3.1) and Table (3.2), the convergence rates of the artificial viscosity (AV) approximation (3.2.14) in both the $||.||_{L^2(0,T;L^2(\Omega))}$ and $||.||_{L^2(0,T;H^1(\Omega))}$ norms are 1, whereas those of the correction step (CS) approximation (3.2.15) in both norms are 2. These results are consistent with the theory developed in this report. We note that the correct convergence rates require not just the improvement of the time accuracy, but also the reduction of artificial viscosity effects on the solution. In terms of qualitative assessment, consider Figure (3.1) and Figure (3.2).

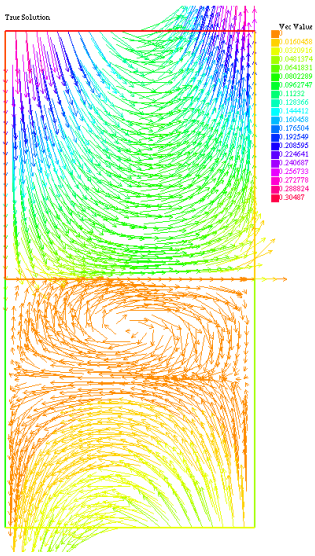

Figure 3.1: True Solution

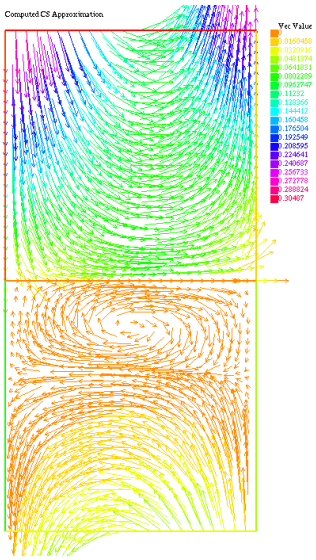

Figure 3.2: Computed Solution

It can be clearly seen that the computed solution successfully captures all the structures of the true solution, including the vortex in the second domain. Beyond the theory, we note that the correction step improves the accuracy of the computed solution even for large values of the time step, mesh and viscosity values outside of the asymptotic regime. This is important for atmosphere-ocean applications, since discretization parameters for these simulations are not expected to lie in the asymptotic regime.

3.5 Summary and future work

A method was proposed to reduce time-consistency errors and artificial viscosity effects in computational simulations for a model of two coupled fluids. Our model was chosen to roughly represent the numerical viscosity (or diffusion) and flux coupling techniques used in many atmosphere-ocean interaction (AOI) simulations. The point of the simplified model has been to illustrate the general algorithmic approach, but also to provide a rigorous numerical analysis and testing to illustrate the theory, which would have been too cumbersome for the full physics and numerics of an application code. We believe that our analysis helps to begin filling in gaps in the literature; few examples of numerical analysis exist that seek to address the AOI coupling problem (see [91, 92, 95, 104, 116]).

The formal, global consistency in time was improved using deferred correction. The deferred correction approach allowed the lower-order numerics to be employed for a predictor-type calculation, which was then modified to create a corrector step with a formal increase in the order of accuracy in time. This improvement applied to the global time stepping method, but in particular the coupling consistency was lifted to second order, which would typically be of first order in practice. Defect correction was applied to mitigate artificial viscosity effects, which we demonstrated could be implemented as a slight modification to the deferred correction step. We subsequently

proved the unconditional stability and optimal convergence of the method, as well as the formal reduction of numerical viscosity effects.

A numerical example was provided to illustrate the theory. A manufactured solution was derived for the coupled fluid model, so that errors could be computed explicitly as time step and artificial viscosity parameters were varied. In this way, the predictions of the theory were demonstrated clearly. That is, the second-order convergence rate was verified as the time step was decreased, as well as the improved accuracy using defect correction to reduce the artificial viscosity effects. Beyond the theory, a significant improvement was observed for the largest values of time step and artificial viscosity parameters. This indicates the possibility of a benefit in application, where solutions are marginally resolved due to turbulent behavior and a wide range of scales.

In this chapter we have provided an initial step toward numerical improvements for AOI simulations, but some important issues remain to be considered in future work. One is the extension of the methodology to account for the existence of additional physics, more complex geometry and different numerical methods encountered in application codes. We have explained in Sections 3.1.1-3.1.2 that the combined defect-deferred correction (DDC) approach may, in principle, be applied to a broad class of numerical methods. In this regard, the most important extension will be to consider smaller time steps in the "atmosphere" fluid regime and incorporate a more general class of flux coupling methods, such as in [95, 96]. This extension will illuminate

another benefit of the DDC approach: improvement of time consistency within each fluid regime individually, not just for the coupling (as has been emphasized in this chapter).

Another issue for future study is that new algorithmic approaches for AOI are not practical unless they can be integrated into existing code structures. We believe the implementation would be reasonable, since one may leverage the existing code structure used for the base (predictor) step to a considerable degree for the corrector calculation. Roughly speaking, this is because the corrector step is equivalent to a second predictor step with additional source terms and an algebraic change in the flux calculations.

Finally, code efficiency must be addressed, but this cannot be determined until testing is performed using an application-level code. We have hope that the defect-deferred correction approach would lead to an improvement in efficiency because of the significant improvement in accuracy observed in our test using parameter choices outside of the regime of asymptotic convergence. The cost of the DDC method is around 3 to 4 times that of the base method; to achieve the same accuracy with the base method alone (by decreasing the time step size, for example) may cost much more than a factor of 3 to 4. Furthermore, reducing artificial viscosity effects in current, coupled AOI simulations is not as simple as just reducing parameter values. The defect correction approach may provide an efficient way to reduce these effects.

Chapter 4

An Efficient Defect Correcting Extrapolation Technique

4.1 Introduction

As of today, solving differential equations analytically is impossible for most of the real-life problems. For this reason, practitioners use numerical techniques to approximate their solutions. This idea follows with the choice of a discretization parameter (possibly more than one), and continues with computing approximations as a function of this parameter. Consistency of the approximation requires its convergence to the true solution in the limiting case as the discretization parameter approaches 0. Even

though the accuracy of computed approximation relies mostly on the choice of the discretization parameter being close to zero, such values of these parameters either result in a prohibitively high computational cost, or introduce extra errors due to machine round-off. Therefore, users are limited in their choice of these discretization parameters.

Around the beginning of the 20th century, mathematicians including Richardson noticed that errors of many discretized approximations lead to asymptotic expansions for discretization parameter. He then suggested a technique, which he called "the deferred approach to the limit", that uses two different approximations of a true solution in order to gain more accuracy by eliminating the dominating power term of the discretization parameter in the error expansion. In his early work on what we now call the Richardson extrapolation technique, he applied this method to vibration of a stretched string of beads, Laplace's equation in a square, vibration of a clamped plate and stresses in a masonry dam [117],[118].

In another paper(1923), Richardson noted that at discontinuities error expansion series may not converge, but commented "there are, so to speak, in the mathematical country, precipices and pit-shafts down which it would be possible to fall, but that need not deter us from walking about."[118].

In 1927, he examined the method in details and showed that it has many applications [119]. Since his frontier works, this technique has been widely used

for various purposes and applications; increasing accuracy, obtaining grid independent solutions, uncertainty quantification, computational fluid dynamics, and so on [118],[120],[121],[122],[123],[124].

In addition to what has been done by employing Richardson extrapolation, as proposed in this report, it can be used to correct the defect error caused by artificial viscosity, conductivity, etc. added to an equation in order to regularize the system. While doing this, it does not require a whole correction step, which mostly solves the problem at least one more time doubling computational cost. Instead, the new approach uses an approximation to artificially-diffused equation on a twice coarser mesh with a twice large time step, which reduces the computational cost as it gives the same or a better convergence rates than the existing two-step defect correction methods.

The error introduced by an artificial quantity is only of order one alone for most of the artificial quantity methods including [25],[100],[125],[126] which means that the error function of artificial viscosity (AV) approximations looks like

$$E(h, \Delta t, H) = CH + O(h^m + \Delta t^n).$$

Extrapolating once eliminates the error contribution of the artificial quantity H, and

the new error looks like

$$E_{new}(h, \Delta t, H) = O(h^m + \Delta t^n).$$

As a consequence of extrapolation, we will be able to remove the error effect of artificial quantity at all provided that the solution is smooth and discretization parameters are small enough; a new approach for "defect correction". Moreover, if Euler time integrator is employed in the artificial quantity approximation, extrapolation increases time accuracy as well.

$$E(h, \Delta t, H) = CH + C\Delta t + O(h^m + \Delta t^2),$$

$$E_{new}(h, \Delta t, H) = O(h^m + \Delta t^2).$$

In addition, the proposed defect correction method with extrapolation (DCE) can be applied repeatedly with several other solutions on coarser meshes and time steps to increase the accuracy even more with a very low extra computational time. While this idea could be employed with various defect correction methods for various PDEs, in this report we are going to focus on the Navier-Stokes Equations (NSE).

The motion of incompressible fluid flow in the flow domain $\Omega = (0, L)^d$ is governed by the Navier-Stokes equations: find the velocity-pressure pair $u : \Omega \times (0, T] \to R^d, (d = 2, 3)$ and $p : \Omega \times (0, T] \to R$ satisfying

$$\begin{aligned} u_t + u \cdot \nabla u - \nu \Delta u + \nabla p &= f, \text{ for } x \in \Omega, 0 < t \leq T \\ \nabla \cdot u &= 0, \ x \in \Omega, \text{ for } 0 \leq t \leq T, \\ u(x, 0) &= u_0(x), \text{ for } x \in \Omega. \end{aligned} \tag{4.1.1}$$

Kolmogorov theory (K41) [66] states that turbulent flow is a continuum of scales, with the smallest scales (in 3D flow) being of order $O(Re^{-3/4})$, where Reynolds number is inverse proportional to the viscosity coefficient ν. As a result, in order to capture all the small scales in a turbulent flow, the number of mesh points in space for each time step has to be $O(Re^{9/4})$. It is common to have $Re \sim O(10^8)$ in real-life problems. Hence, the direct numerical simulation (DNS) of 3D turbulent flow is not computationally economic or even feasible. It is desired to use pre-existing codes when it comes to turbulent flows in complex geometries. The DCE technique is used (but is not limited) to correct the defect and boost convergence rate of a legacy code given as AV Approximation of NSE in [25].

$$(\frac{u^{h,n+1}-u^{h,n}}{k}, v^h) + (\nu + H)(\nabla u^{h,n+1}, \nabla v^h)$$
$$+b^*(u^{h,n+1}, u^{h,n+1}, v^h) - (p^{h,n+1}, \nabla \cdot v^h) = (f(t_{n+1}), v^h), \forall v^h \in X^h,$$
$$(\nabla \cdot u^{h,n+1}, q^h) = 0, \forall q^h \in Q^h.$$

This report presents an analytical testing verifying convergence rates, two computational analysis and comparison of the proposed DCE method against various defect correction methods applied to NSE; namely, defect correction with BDF2-3 (DC-BDF2, DC-BDF3), Trapezoidal Rule (DC-Trap) and DDC given in [111]. Lastly, it provides 2 and 3D qualitative testing of well-known benchmark problem fluid past backward-facing step.

4.2 Notation and Preliminaries

Throughout this paper, the norm $||.||$ denotes the usual $L^2(\Omega)$ norm of scalars, vectors and tensors, induced by the usual L^2 inner-product, denoted by $(\cdot, \cdot)$. The space in which velocity sought(at time t) is

$$X = H_0^1(\Omega)^d = \{v \in L^2(\Omega)^d : \nabla v \in L^2(\Omega)^{dxd} \text{ and } v = 0 \text{ on } \partial\Omega\}.$$

with the norm $||v||_X = ||\nabla v||$. The space dual to X is

equipped with the norm

$$||f||_{-1} = \sup_{v \in X} \frac{(f, v)}{||\nabla v||}.$$

The space that pressure (at time t) belongs to is

$$Q = L_0^2(\Omega) = \{q \in L^2(\Omega) : \int_\Omega q(x)dx = 0\}.$$

Introduce the space of weakly divergence-free functions

$$X \supset V = \{v \in X : (\nabla \cdot v, q) = 0, \forall q \in Q\}.$$

For measurable $v : [0, T] \to X$, we define

$$||v||_{L^p(0,T;X)} = (\int_0^T ||v||_X^P dt)^{\frac{1}{p}}, 1 \leq p < \infty,$$

and

$$||v||_{L^\infty(0,T;X)} = ess \sup_{0 \leq t \leq T} ||v(t)||_X.$$

Define the trilinear form on $X \times X \times X$

$$b(u, v, w) = \int_{\Omega} u \cdot \nabla v \cdot w dx.$$

Throughout the paper, we shall assume that the velocity-pressure finite element spaces $X^h \subset X$ and $Q^h \subset Q$ are conforming, have typical approximation properties of finite element spaces commonly in use, and satisfy the discrete inf-sup, or LBB^h, condition

$$\inf_{q^h \in Q^h} \sup_{v^h \in X^h} \frac{(q^h, \nabla \cdot v^h)}{\|\nabla v^h\| \|q^h\|} \geq \beta^h > 0, \tag{4.2.1}$$

where β^h is bounded away from zero uniformly in h. Examples of such spaces can be found in [32]. We shall consider $X^h \subset X$, $Q^h \subset Q$ to be spaces of continuous piecewise polynomials of degree m and $m-1$, respectively, with $m \geq 2$ as we introduce at least second order accuracy.

Theorem 26 (Richardson Extrapolation) *Suppose ϕ^* is the sought true solution with a method $\phi(h)$ which depends on h, so that*

$$\phi(h) = \phi^* + Ch^k + O(h^{k+1}).$$

Define

$$R(h,\alpha) := \frac{\alpha^k \phi(h) - \phi(\alpha h)}{\alpha^k - 1},\ \textit{for some real } \alpha \neq 0, 1.$$

Then

$$R(h,\alpha) = \phi^* + O(h^{k+1})$$

Proof 17 *The well-know proof of this theorem is given as follows:*

$$\begin{aligned} R(h,\alpha) - \phi^* &= \frac{\alpha^k \phi(h) - \phi(\alpha h)}{\alpha^k - 1} - \phi^* = \frac{\alpha^k(\phi(h) - \phi^*) - (\phi(\alpha h) - \phi^*)}{\alpha^k - 1} \\ &= \frac{\alpha^k(Ch^k + O(h^{k+1})) - (C\alpha^k h^k + O(h^{k+1}))}{\alpha^k - 1} = O(h^{k+1}) \end{aligned}$$

4.3 Artificial Viscosity Algorithm of NSE and Its Error Estimates

The motion of incompressible fluid flow in the flow domain $\Omega = (0, L)^d$ is governed by the Navier-Stokes equations: find the velocity-pressure pair $u : \Omega \times (0, T] \to R^d, (d = 2, 3)$ and $p : \Omega \times (0, T] \to R$ satisfying (4.1.1).

Algorithm 4.3.1 (AV approximation for NSE) *Let* $\Delta t > 0$, $N = \frac{T}{\Delta t}$, $f \in L^2(\Omega)$. *Given* $u^{h,n}$, *find* $u^{h,n+1} \in X^h$, $n = 0, 1, 2, \cdots, N-1$, *satisfying*

$$(\frac{u^{h,n+1} - u^{h,n}}{k}, v^h) + (\nu + H)(\nabla u^{h,n+1}, \nabla v^h)$$
$$+b^*(u^{h,n+1}, u^{h,n+1}, v^h) - (p^{h,n+1}, \nabla \cdot v^h) = (f(t_{n+1}), v^h), \forall v^h \in X^h,$$
$$(\nabla \cdot u^{h,n+1}, q^h) = 0, \forall q^h \in Q^h.$$

Definition 3.1 Let

$$C_u := ||u(x,t)||_{L^\infty(0,T;L^\infty(\Omega))},$$

$$C_{\nabla u} := ||\nabla u(x,t)||_{L^\infty(0,T;L^\infty(\Omega))},$$

$$\tilde{C}_u := ||u(x,t)||_{L^\infty(0,T;L^2(\Omega))},$$

$$\tilde{C}_{\nabla u} := ||\nabla u(x,t)||_{L^\infty(0,T;L^2(\Omega))},$$

and introduce $\tilde{C}$, satisfying

$$\inf_{v\in V^h} ||\nabla(u-v)|| \le C_1 \inf_{v\in X^h} ||\nabla(u-v)|| \le C_2 h^m ||u||_{H^{m+1}} \le \tilde{C} h^m$$

Also, using the constant $C(\Omega)$ from Lemma 2.3, we define $\bar{C} := 1728 C^4(\Omega)$.

Theorem 27 (Error Estimate of AV Approximation to NSE) *Let* $f \in L^2(0,T;H^{-1})$*, let* $u^{h,i}$ *satisfy the algorithm (4.3.1)*

for all $i = 0, 1, 2, \cdots, N-1$*,*

$$\Delta t \le \frac{\nu + H}{4C_u^2 + 2(\nu+H)C_{\nabla u} + 2\bar{C}\tilde{C}^4(\nu+H)^{-2}h^{4m}},$$

$$u \in L^2(0,T;H^{m+1}(\Omega)) \cap L^\infty(0,T;L^\infty(\Omega)), \nabla u \in L^\infty(0,T,L^\infty(\Omega)),$$

$$u_t \in L^2(0,T;H^{m+1}(\Omega)), u_{tt} \in L^2(0,T;L^2(\Omega)), p \in L^2(0,T;H^m(\Omega)).$$

Then there exist a constant $C = C(\Omega, T, u, p, f, \nu + H)$*, such that*

$$\max_{1\le i\le N}||u(t_i)-u^{h,i}||+\Big(\Delta t\sum_{i=1}^{n+1}(H+\nu)||\nabla(u(t_i)-u^{h,i})||^2\Big)^{1/2}$$
$$\le C(h^m+H+\Delta t)$$

Proof 18 *Can be found in [25]*

In order to observe what the error estimate looks like after extrapolation, we need to see the pattern of the error function. To this end, let us first prove extended error estimate of AV approximation.

Theorem 28 (Extended Error Estimate of AV Approximation to NSE)

Let the assumptions of Theorem (27) be satisfied, and

$$u_{ttt}\in L^2(0,T;L^2(\Omega)),$$

Then there exist a constant $C=C(\Omega,T,u,p,f,\nu+H)$*, such that*

$$\max_{1\le i\le N}||u(t_i)-u^{h,i}||+\Big(\Delta t\sum_{i=1}^{n+1}(H+\nu)||\nabla(u(t_i)-u^{h,i})||^2\Big)^{1/2}\le C(H+\Delta t)+O(\Delta t^2+h^m)$$

Proof 19 *By Taylor expansion,* $\frac{u(t_{n+1})-u(t_n)}{\Delta t} = u_t(t_{n+1}) - \Delta t\rho^{n+1} + \Delta t^2\sigma^{n+1}$, *where* $\rho^{n+1} = u_{tt}(t_{n+1})$ *and* $\sigma^{n+1} = u_{ttt}(t_{n+\theta})$, *for some* $\theta \in [0,1]$.

Follow the same steps starting with the equation (4.4) in [25] with an additional term $\Delta t^2(\sigma^{n+1}, v)$. *Replace* v *with* $\phi^{h,n+1}$ *as is done in the reference report. By the definition of* $\|\cdot\|_{-1}$ *and Young's inequality*

$$\begin{aligned}\Delta t^2(\sigma^{n+1}, \phi^{h,n+1}) &\leq \Delta t^2\|\sigma^{n+1}\|_{-1}\|\nabla\phi^{h,n+1}\| \\ &\leq \frac{1}{4\epsilon(H+\nu)}\Delta t^4\|\sigma^{n+1}\|_{-1}^2 + \epsilon(H+\nu)\|\nabla\phi_1^{h,n+1}\|^2. \quad (4.3.1)\end{aligned}$$

Choosing an appropriate ϵ, *the following inequality can be found.*

$$
\begin{aligned}
\frac{\|\phi_1^{h,n+1}\|^2 - \|\phi_1^{h,n}\|^2}{2\Delta t} + \frac{H+\nu}{2}\|\nabla\phi_1^{h,n+1}\|^2 \\
\leq \frac{C}{H+\nu}\|\frac{\eta_1^{n+1}-\eta_1^n}{\Delta t}\|_{-1}^2 \\
+C(H+\nu)\|\nabla\eta_1^{n+1}\|^2 \\
+\frac{C}{H+\nu}\inf_{q^h\in Q^h}\|p(t_{n+1})-q^{h,n+1}\|^2 \\
+\frac{C}{H+\nu}H^2\|\nabla u(t_{n+1})\|^2 + \frac{C}{H+\nu}\Delta t^2\|\rho^{n+1}\|_{-1}^2 \\
+\frac{C}{H+\nu}\Delta t^4\|\sigma^{n+1}\|_{-1}^2 + \frac{C}{H+\nu}(\|\nabla\eta_1^{n+1}\|^2 + \|\nabla\eta_1^{n+1}\|^4) \\
+(\frac{1}{2}C_{\nabla u} + \frac{C_u^2}{H+\nu} + \frac{\bar{C}}{(H+\nu)^3}\|\nabla\eta_1^{n+1}\|^4)\|\phi_1^{h,n+1}\|^2.
\end{aligned}
$$

In addition to the assumptions of 27, it follows from the new regularity assumptions of the theorem that

$$
\Delta t\sum_{i=0}^{n}\|\rho^{i+1}\|_{-1}^2 \leq C\Delta t\sum_{i=0}^{n}\|\rho^{i+1}\|^2 \leq C,
$$

$$\Delta t \sum_{i=0}^{n} \|\sigma^{i+1}\|_{-1}^2 \leq C\Delta t \sum_{i=0}^{n} \|\sigma^{i+1}\|^2 \leq C.$$

Summing (4.3.2) over all time levels and multiply by $2\Delta t$ gives equation (4.18) in [25] with the following extra term on the right hand side,

$$\frac{1}{H+\nu}\Delta t \sum_{i=0}^{n} C\Delta t^4.$$

Keeping this extra term on the right hand side and treating exactly the same way that [25] treats to the term with Δt^2 gives the desired result.

The same idea can be employed to notice the fact that, when sufficiently enough time derivatives are provided, the time error in AV approximation of NSE has a tail of errors $C_1\Delta t$, $C_2\Delta t^2$, $C_3\Delta t^3$, and so on; in other words, it has an asymptotic error expansion. This property allows us to gain accuracy in time while correcting the defect due to the artificial viscosity, and even lets us to achieve higher time accuracies with repeated extrapolation.

4.4 Defect Correcting Extrapolation Technique

The theoretical reasoning of this defect correction approach is very similar to Richardson extrapolation. While it deals with approximations of only one size parameter with a tail of increasing orders such as Δt, Δt^2, Δt^3 and so on, we extend its usage to more than one size parameters, namely, artificial quantity H and the time step size Δt. Having only of order 1 error contribution due to the artificial quantity H allows us to use this approach as a defect corrector, which removes H from the error function after a simple extrapolation in contrast to other defect correction methods which gives $O(H^2)$ accuracy with a correction step.

Next, we are going to discuss how the technique works with algorithm 4.3.1. Although we consider only NSE, it can be generelized for other artificial quantity methods with the same or similar error pattern.

Algorithm 4.4.1 (2nd order Defect Correcting Extrapolation (DCE2))
Let $u^h(\Delta t, H, T)$ and $u^h(\alpha\Delta t, \alpha H, T)$ be two different outputs of the AV approximations given in algorithm 4.3.1 at the final time T with a sufficient space accuracy. Let not α be too close to 0 or 1. Find

$$\tilde{u}_2^h(\Delta t, H, T) := \frac{\alpha u^h(\Delta t, H, T) - u^h(\alpha\Delta t, \alpha H, T)}{\alpha - 1}. \tag{4.4.1}$$

Algorithm 4.4.2 (kth Order Defect Correcting Extrapolation (DCEk))

For $k \geq 3$, let $\tilde{u}_{k-1}^h(\Delta t, H, T)$ and $\tilde{u}_{k-1}^h(\alpha\Delta t, \alpha H, T)$ be two outputs of algorithm (DCE(k-1)) at the final time T with a sufficient space accuracy. Find

$$\tilde{u}_k^h(\Delta t, H, T) := \frac{\alpha^{k-1}\tilde{u}_{k-1}^h(\Delta t, H, T) - \tilde{u}_{k-1}^h(\alpha\Delta t, \alpha H, T)}{\alpha^{k-1} - 1}. \tag{4.4.2}$$

Extrapolation techniques rely on error coefficients to be constants. For this reason, smoothness criteria for error estimates are very crucial. The choice of α is up to the user; however, we have to make sure that it does not get too close to 1 so that machine precision does not ruin algorithm.

We expect a second order of accuracy upon DCE2 as it does the main correction for the defect caused by artificial viscosity. Extra extrapolations beyond this point increases the order of accuracy by 1. Therefore, we expect a kth order of accuracy in general when DCEk applied.

4.5 Testing the Model

In this section, we are going to present testing results for our model. First, we give results for an analytical testing with a well-known solution of Navier Stokes equation, namely, Green-Taylor vortex decay problem. A computational testing with both quantitative and qualitative results come next.

4.5.1 Analytical Test

We consider first the Green-Taylor vortex decay problem [129], [130], which is an exact solution of the NSE with no forcing and periodic boundary conditions. In $\Omega = (0,1) \times (0,1)$, solutions take the form:

$$\begin{aligned} u_1(x,y,t) &= -\cos(n\pi x)\sin(n\pi y)e^{-2n^2\pi^2\nu t}, \\ u_2(x,y,t) &= \sin(n\pi x)\cos(n\pi y)e^{-2n^2\pi^2\nu t}, \\ p(x,y,t) &= -\frac{1}{4}\big(\cos(2n\pi x) + \sin(2n\pi y)\big)e^{-4n^2\pi^2\nu t}, \end{aligned}$$

where n can be chosen as any positive integer. This exact NSE solution is made of an $n \times n$ array of oppositely signed vortices that decay as $t \to \infty$. It has been used as a numerical test in [131], [132], and [133], and many other papers. It also has been used as an analytical test in [134].

For simplicity, we rescale the domain, and choose $n = 1$ so that the solution yields the following form:

$$\begin{aligned} u_1(x,y,t) &= -\cos(x)\sin(y)e^{-2\nu t} \\ u_2(x,y,t) &= \sin(x)\cos(y)e^{-2\nu t} \\ p(x,y,t) &= -\frac{1}{4}\big(\cos(2x)+\sin(2y)\big)e^{-4\nu t}. \end{aligned}$$

The solution above is easily extended to an exact solution of the NSE with an artificial viscosity h given by

$$
\begin{aligned}
u_1(x,y,t) &= -\cos(x)\sin(y)e^{-2(\nu+h)t} \\
u_2(x,y,t) &= \sin(x)\cos(y)e^{-2(\nu+h)t} \\
p(x,y,t) &= -\frac{1}{4}\big(\cos(2x)+\sin(2y)\big)e^{-4(\nu+h)t}.
\end{aligned}
$$

Similar solutions for the artificial viscosities $2h$ and $4h$ can be obtained easily.

Since sinusoidal terms are the same for all of the solutions, ignoring them and Taylor expanding exponential terms give

$$e^{-2(\nu+h)t} = e^{-2\nu t}\big(1-2th+2t^2h^2+O(h^3)\big), \tag{4.5.1}$$

$$e^{-2(\nu+2h)t} = e^{-2\nu t}\big(1-4th+8t^2h^2+O(h^3)\big), \tag{4.5.2}$$

$$e^{-2(\nu+4h)t} = e^{-2\nu t}\big(1-8th+32t^2h^2+O(h^3)\big). \tag{4.5.3}$$

Comparing these results with the true solution $e^{-2\nu t}$, we can easily observe first order accuracy with each AV approximation provided h is sufficiently small.

After the first time extrapolation (DCE2) of 4.5.1 and 4.5.2, and also 4.5.2 and 4.5.3, solutions take the following form:

$$2e^{-2(\nu+h)t} - e^{-2(\nu+2h)t} = e^{-2\nu t}\big(1 - 4t^2h^2 + O(h^3)\big), \tag{4.5.4}$$

$$2e^{-2(\nu+2h)t} - e^{-2(\nu+4h)t} = e^{-2\nu t}\big(1 - 16t^2h^2 + O(h^3)\big). \tag{4.5.5}$$

These results clearly show that both analytical solutions are second order accurate in terms of h.

Continuing this process (DCE3) with 4.5.4 and 4.5.5 similarly yields third order accuracy. One can continue applying the DCEk algorithm to gain even more accuracy. We have to note that even though each extrapolation increases error constant, the common factor $e^{-2\nu t}$ decreases exponentially fast for our accuracies' favor.

4.5.2 Computational Tests

4.5.2.1 Quantitative Testing

In this subsection, we are going to present various convergence and computational time results of DCE and its comparison with existing methods; DC-BDF2, DC-BDF3, DC-Trap and DDC methods. Through this section, α has chosen to be 2, and all the sizes($\Delta t, H$ and h) are chosen to be equal and refined together. Solutions(with existing defect correction methods and DCE) at final time in coarse meshes transformed onto the finest mesh by Freefem++[127] interpolation matrix in order to compute error norms. Final time has been chosen to be $T = 1$ for all of the computations. Forcing functions and initial and boundary conditions are calculated to comply with given true solutions. N_i refers to the number of mesh points on a unit line segment, thus $h = \Delta t = H = 1/N_i$. $N_i - N_j$ values in the table refers to the computed solutions with once extrapolation DCE2 with the corresponding N values. Similarly, $N_i - N_j - N_k$ means twice extrapolation DCE3, and so on.

Before we present computational results, we need to draw your attention to a point that even if the computations are not done with the most efficient ways, existing correction methods and DCE are both threated the same. In this regard, computational times should be read as rates in sequential computation instead of actual

computational time.

Start with NSE with a given true solution in $\Omega = [0,1]^2$:

$$u_1(x,y,t) = e^{-t}(x+y^3),$$

$$u_2(x,y,t) = -e^{-t}(x^3+y),$$

$$p(x,y,t) = 0.$$

In order to numerically verify that expected convergence rates are achieved, we perform a convergence analysis with P3-P2 finite elements; piecewise cubic polynomials for velocity and quadratic polynomials for pressure. Tables (4.1) - (4.2) show computational results for $\nu = 1$. As observed from tables, DCE2 makes the correction as proposed, and we gain an additional order of accuracy with each extrapolation.

Table 4.1
Once extrapolated DCE2, $\nu = 1$, P3-P2.

N	$\|\| u(T) - \tilde{u}^h(T) \|\|_{L^2(\Omega)}$	rate	$\|\| u(T) - \tilde{u}^h(T) \|\|_{H^1(\Omega)}$	rate
2-4	0.00096183	-	0.0102855	-
4-8	0.000273098	1.82	0.00223319	2.20
8-16	8.01382e-005	1.77	0.000614004	1.86
16-32	2.18876e-005	1.87	0.000166776	1.88
32-64	5.72887e-006	1.93	4.36288e-005	1.93
64-128	1.4661e-006	1.97	1.11646e-005	1.97

Table 4.2
Twice extrapolated DCE3, $\nu = 1$, P3-P2.

N	$\|\| u(T) - \tilde{u}^h(T) \|\|_{L^2(\Omega)}$	rate	$\|\| u(T) - \tilde{u}^h(T) \|\|_{H^1(\Omega)}$	rate
2-4-8	0.000123665	-	0.00263579	-
4-8-16	1.71684e-005	2.85	0.000294023	3.16
8-16-32	2.48723e-006	2.79	2.95468e-005	3.31
16-32-64	3.429e-007	2.86	3.29008e-006	3.17
32-64-128	4.51888e-008	2.92	3.84695e-007	3.10

The rest of the computational part is dedicated to comparison of various methods.

Tables (4.3) - (4.11) show computational results with Taylor-Hood finite elements —quadratics(P2) for velocity and piecewise linears(P1) for pressure. As seen in tables (4.4) and (4.7), DC-BDF2 and DC-BDF3 give very similar results as error due to defect dominates all other error contributions(space and time). In order to expect a better accuracy from a defect correction with BDF integrator, one has to add one more correction step(which increases computational time by half (1.5x)). In spite of the fact that employing BDF3 instead of BDF2 does not produce any better results, fortunately, this argument does not apply to DCE methods.

Keeping above argument in mind, the comparison of DCE2 and BDF2 shows that the latter gives twice better accuracy, but requires almost twice as much time needed for DCE2. As suggested by tables (4.3), (4.5) and (4.6), lost accuracy can be regained with further extrapolations (DCE3 and DCE4) with an additional 1% extra computational time for each.

Table 4.3
Once extrapolated DCE2, $\nu = 0.1$, P2-P1.

N	$\|\| e(T) \|\|_{L^2(\Omega)}$	rate	$\|\| e(T) \|\|_{H^1(\Omega)}$	rate	Comp. Time
2-4	0.0086303	-	0.0812381	-	0.3
4-8	0.00557602	0.63	0.0454532	0.83	2
8-16	0.00302498	0.88	0.0235575	0.94	14
16-32	0.00130627	1.21	0.0102259	1.20	124
32-64	0.000456872	1.51	0.00362236	1.49	959
64-128	0.000137902	1.72	0.00110496	1.71	9116

Table 4.4
Defect Correction with BDF2, $\nu = 0.1$, P2-P1.

N	$\|\| e(T) \|\|_{L^2(\Omega)}$	rate	$\|\| e(T) \|\|_{H^1(\Omega)}$	rate	Comp. Time
2	0.00850592	-	0.0688755	-	0.3
4	0.00640781	0.40	0.0492258	0.48	0.5
8	0.00399222	0.68	0.0305899	0.68	4
16	0.00196225	1.02	0.0152057	1.00	26
32	0.000753834	1.38	0.00592989	1.35	220
64	0.000240861	1.64	0.00191929	1.62	1859
128	6.86871e-005	1.81	0.000552079	1.79	15347

Table 4.5
Twice extrapolated DCE3, $\nu = 0.1$, P2-P1.

N	$\|\| e(T) \|\|_{L^2(\Omega)}$	rate	$\|\| e(T) \|\|_{H^1(\Omega)}$	rate	Comp. Time
2-4-8	0.00485526	-	0.0456883	-	2
4-8-16	0.00219288	1.14	0.0181232	1.33	14
8-16-32	0.000737836	1.57	0.00603343	1.58	123
16-32-64	0.000175409	2.07	0.00147149	2.04	971
32-64-128	3.20009e-005	2.45	0.000277792	2.41	9225

Table 4.6
Three times extrapolated DCE4, $\nu = 0.1$, P2-P1.

N	$\|\| e(T) \|\|_{L^2(\Omega)}$	rate	$\|\| e(T) \|\|_{H^1(\Omega)}$	rate	Comp. Time
2-4-8-16	0.00185997	-	0.0178279	-	14
4-8-16-32	0.000534314	1.79	0.00489538	1.86	123
8-16-32-64	9.59466e-005	2.48	0.000938427	2.38	974
16-32-64-128	1.16833e-005	3.03	0.000141862	2.73	9238

Table 4.7
Defect Correction with BDF3, $\nu = 0.1$, P2-P1.

N	$\|\| e(T) \|\|_{L^2(\Omega)}$	rate	$\|\| e(T) \|\|_{H^1(\Omega)}$	rate	Comp. Time
2	0.0101987	-	0.0810543	-	0.2
4	0.00639727	0.67	0.0491753	0.72	0.8
8	0.00396871	0.68	0.0304718	0.69	4
16	0.00198013	1.00	0.0153461	0.99	26
32	0.000759157	1.38	0.00597128	1.36	227
64	0.00024228	1.65	0.00193031	1.63	1854
128	6.90473e-005	1.81	0.000554875	1.80	18507

Above comparisons have been done between DCE and DC-BDF because tables (4.4), (4.8) and (4.9) suggest that DC-BDF2 gives very similar error results with that of DC-Trap and DDC in a slightly better computational time.

Table 4.8
Defect Correction with Trapezoidal Rule, $\nu = 0.1$, P2-P1.

N	$\| e(T) \|_{L^2(\Omega)}$	rate	$\| e(T) \|_{H^1(\Omega)}$	rate	Comp. Time
2	0.0377949	-	0.290277	-	0.2
4	0.0134339	1.49	0.146063	0.99	0.8
8	0.00402036	1.74	0.0461772	1.66	6
16	0.00188649	1.09	0.0167081	1.47	48
32	0.000721738	1.38	0.00593077	1.49	410
64	0.000230334	1.65	0.0018682	1.67	4285
128	6.56533e-005	1.81	0.000532486	1.81	26518

Table 4.9
Defect-Deferred Correction, $\nu = 0.1$, P2-P1.

N	$\|\| e(T) \|\|_{L^2(\Omega)}$	rate	$\|\| e(T) \|\|_{H^1(\Omega)}$	rate	Comp. Time
2	0.00872515	-	0.0705203	-	0.2
4	0.00647898	0.42	0.0500251	0.50	0.8
8	0.00409903	0.66	0.0315381	0.66	6
16	0.00200472	1.03	0.015602	1.02	46
32	0.000768792	1.38	0.0060734	1.36	371
64	0.000245749	1.65	0.00196635	1.62	3420
128	7.01289e-005	1.81	0.000565952	1.80	22334

Convergence rates in defect correction methods, in general, suffer a lot with small viscosity coefficient. Results for $\nu = 0.0001$ clearly show that DCE4 and DC-BDF2 give comparable errors as seen in the tables (4.10) and (4.11). On the other hand, DCE4 needs only half of the computational time that is required for DC-BDF2 to produce similar results.

Table 4.10
Defect Correction with BDF2, $\nu = 0.0001$, P2-P1.

N	$\|\| e(T) \|\|_{L^2(\Omega)}$	rate	$\|\| e(T) \|\|_{H^1(\Omega)}$	rate	Comp. Time
2	0.0122554	-	0.0962342	-	0.1
4	0.0132328	-0.11	0.101209	-0.07	0.6
8	0.0134072	-0.02	0.10585	-0.06	4
16	0.0108925	0.29	0.0975906	0.11	26
32	0.00656881	0.72	0.0754153	0.37	205
64	0.0031415	1.06	0.0522411	0.53	1703
128	0.00131784	1.25	0.0355434	0.56	14297

Table 4.11
Three times extrapolated DCE4, $\nu = 0.0001$, P2-P1.

N	$\|\| e(T) \|\|_{L^2(\Omega)}$	rate	$\|\| e(T) \|\|_{H^1(\Omega)}$	rate	Comp. Time
2-4-8-16	0.0123562	-	0.109878	-	15
4-8-16-32	0.0073926	0.74	0.0872938	0.33	115
8-16-32-64	0.00323392	1.19	0.0608015	0.52	962
16-32-64-128	0.00125093	1.37	0.0413493	0.56	8333

4.5.2.2 Qualitative Testing

In this subsection, we are going to present qualitative results with both 2D and 3D fluid past backward-facing step problem; see e.g. [135]. Through this subsection, α has chosen to be 2. Final times and diffusion coefficients are $T = 15$ and $\nu = 0.001$ for both cases. Parabolic inflows with maximum inlet equals 2, no-slip boundary conditions on the walls and steps and "do nothing" boundary conditions for outflow have been enforced. Right hand side forcing functions are set to be zero. Computations performed with deal.II — a general-purpose object-oriented finite element library [128]. For simplicity, computations were performed on the same mesh, even though this is not necessary.

Start with 2D case: qualitative results with 2×2 backward-facing step on the domain $\Omega = [0, 16] \times [0, 4]$ are given for DCE1 (AV approximation), DCE2, DCE3, DCE4 and DDC. Initial values have been chosen to be zero. The finest mesh size is fixed $h = 1/8$ for all of the computations. The figure (4.1) clearly demonstrate that each extrapolation fosters overall accuracy of 2D model problem.

As seen in the figures (4.1) and (4.2), DCE4 and DDC give reasonably same qualitative properties that are consistent with [135] both in terms of reattachment length and capturing top vortex while DNS fails to converge.

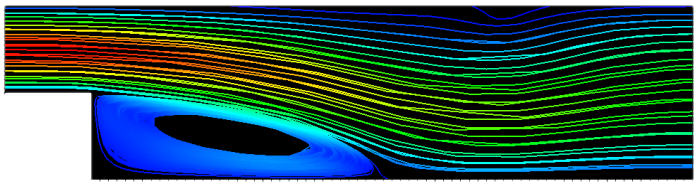

(a) DCE1, $\Delta t = H = 1/32$

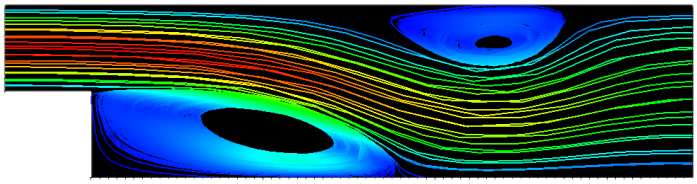

(b) DCE2, $\Delta t = H = 1/32, 1/16$

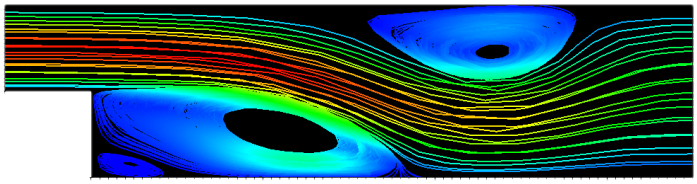

(c) DCE3, $\Delta t = H = 1/32, 1/16, 1/8$

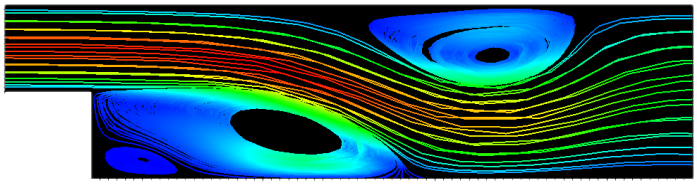

(d) DCE4, $\Delta t = H = 1/32, 1/16, 1/8, 1/4$

Figure 4.1: 2D flow past backward-facing step with DCEk streamlines, $T = 15$, $\nu = 0.001$

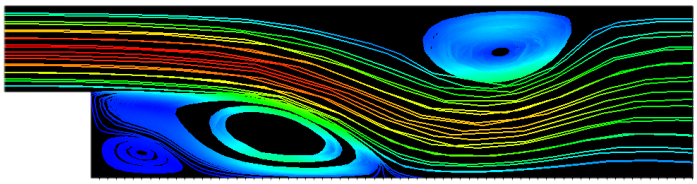

(a) DDC, $\Delta t = H = 1/32$

Figure 4.2: 2D flow past backward-facing step with DDC streamlines, $T = 15$, $\nu = 0.001$

3D case: qualitative results with $2 \times 2 \times 2$ backward-facing step on the domain $\Omega = [0, 16] \times [0, 4] \times [0, 2]$ are given for DCE1, DCE2, DCE3, DCE4 and DDC.

In order to increase computational speed, initial values have been chosen to be the solution of DCE1 at T=10 started with zero initial values, and $H = \Delta t = 1$. The mesh size is fixed $h = 1/2$ for all of the computations.

Figure (4.3) suggests that each extrapolation contribute overall accuracy of the 3D model problem as well.

As seen in the figures (4.3) and (4.4), DCE4 gives a slightly better result than DDC while DNS fails to converge. In addition, qualitative results look consistent with the literature in terms of reattachment length. On the other hand, one can extend the length of the domain and solve with finer mesh in order to observe the top vortex. As a result, even though the mesh sizes have been chosen very coarse, qualitative results demonstrate that DCE methods provide reliable simulations.

Briefly, DCE methods perform very well on NSE: as it increases accuracy dramatically with each additional extrapolation, computational time remains the same. Comparing with other existing defect correction methods, DCE performs reasonably better both in terms of computational cost(time/memory) and accuracy.

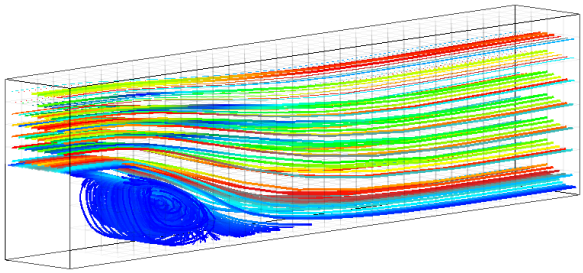

(a) DCE1, $\Delta t = H = 1/32$

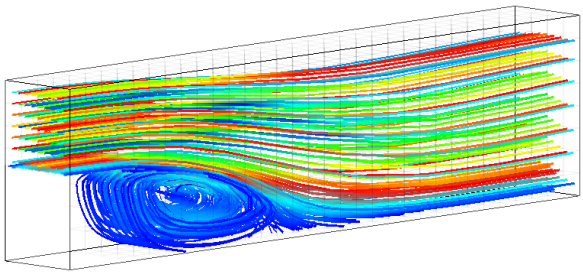

(b) DCE2, $\Delta t = H = 1/32, 1/16$

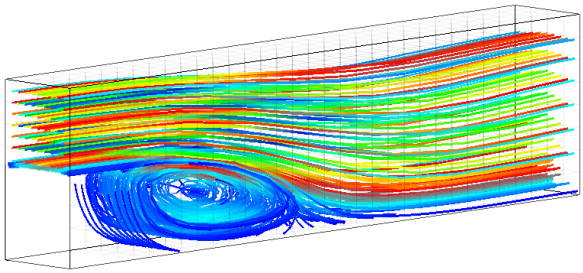

(c) DCE3, $\Delta t = H = 1/32, 1/16, 1/8$

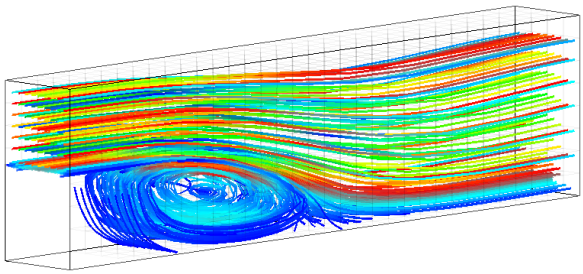

(d) DCE4, $\Delta t = H = 1/32, 1/16, 1/8, 1/4$

Figure 4.3: 3D flow past backward-facing step streamlines, $T = 15$, $\nu = 0.001$

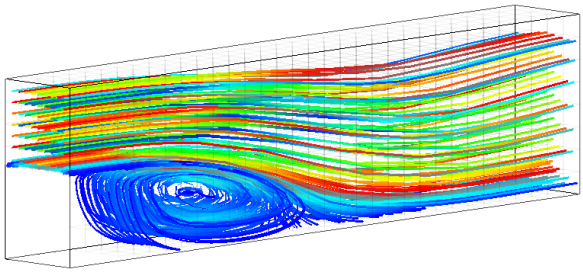

(a) DDC, $\Delta t = H = 1/32$

Figure 4.4: 3D flow past backward-facing step with DDC streamlines, $T = 15$, $\nu = 0.001$

Conclusion

Methods for solving nearly singular, time-dependent problems are presented. Those presented in the first three chapters combine both deferred correction method for the time derivative and the defect correction method for the spatial operator. Methods are applied to the Navier-Stokes equations, and the stability and the error estimate results for velocity are given. As observed in both theoretical and numerical results, all methods are high accurate in both time and space. In the fourth chapter, a new technique for defect correction is employed and shown to be performing as proposed earlier.

References

[1] N.A. Adams and S. Stolz, Deconvolution methods for subgrid-scale approximation in large-eddy simulation, in: *Modern Simulation Strategies for Turbulent Flow*, 2001, B. Geurts (editor), pp. 21-41, R. T. Edwards.

[2] S. Stolz, N. A. Adams and L. Kleiser, The Approximate Deconvolution Model for Compressible Flows: Isotropic Turbulence and Shock-Boundary-Layer Interaction , in: *Fluid Mechanics and Its Applications. Advances in LES of Complex Flows*, vol. 65, 2006, pp. 33-47, Springer Netherlands.

[3] C. Cardoso Manica and S. K. Merdan, Finite element error analysis of a zeroth order approximate deconvolution model based on a mixed formulation, JMAA, Vol. 331, No. 1, pp. 669-685, 2007.

[4] W. Layton and R. Lewandowski, Residual stress of approximate deconvolution models of turbulence, Journal of Turbulence, Vol. 7, Issue 46, p. 1-21, 2006.

[5] A. Labovsky, C. Trenchea, *Large Eddy Simulation for Turbulent Magnetohydrodynamic Flows*, Journal of Mathematical Analysis and Applications, 377 (2011), pp.516-533.

[6] A. Labovsky, C. Trenchea, *A family of Approximate Deconvolution Models for MagnetoHydroDynamic Turbulence*, Numerical Functional Analysis and Optimization, vol.31(12), pp.1362-1385, 2010.

[7] A. Labovsky, W.J. Layton, C.C. Manica, M. Neda, L.G. Rebholz, *The stabilized extrapolated trapezoidal finite-element method for the Navier-Stokes equations*, Computer Methods in Applied Mechanics and Engineering, vol. 198, Issues 9-12, 2009, pp. 958-974.

[8] A. Dunca and Y. Epshteyn, On the Stolz-Adams deconvolution model for the large eddy simulation of turbulent flows, SIAM J. Math. Anal., Vol. 37(6), pp. 1890-1902, 2006.

[9] K. Bohmer, P. W. Hemker, H. J. Stetter, The defect correction approach, in: K. Bohmer, H. J. Stetter (Eds.),*Defect Correction Methods. Theory and Applications*, Springer Verlag, 1984, pp. 1–32.

[10] P. W. Hemker, Mixed defect correction iteration for the accurate solution of the convection diffusion equation, pp. 485-501 in: *Multigrid Methods*, L.N.M. vol. 960, (W. Hackbusch and U. Trottenberg, eds.) Springer Verlag, Berlin 1982.

[11] P. W. Hemker, The use of defect correction for the solution of a singularly perturbed o.d.e., preprint, Mathematisch Centrum. Numerieke Wiskunde ; NW 139/82

[12] O. Axelsson and W. Layton, Defect correction methods for convection dominated, convection-diffusion equations, RAIRO J. Numer. Anal. 24 (1990) pp. 423-455.

[13] O. Axelsson and W. Layton, Optimal interior estimates for the defect-correction, finite element approach to 2-D convection-diffusion problems, ICMA report 88-116, Univ. of Pittsburgh, 1988.

[14] A. Bouaricha, Tensor-Krylov methods for Large Nonlinear Equations, Computational Optimization and Appl., 5 (1996), pp. 207-232.

[15] X.-C. Cai, Scalable nonlinear iterative methods for partial differential equations, LLNL report, Livermore, CA, 2000.

[16] W. Layton, H. K. Lee, J. Peterson, A defect-correction method for the incompressible Navier–Stokes equations, Applied Mathematics and Computation, Vol. 129, Issue 1, 2002, pp. 1-19.

[17] V. Ervin and W. Layton, High resolution minimal storage algorithms for convection dominated, convection diffusion equations, pp. 1173-1201 in: *Trans. of the Fourth Army Conf. on Appl. Math. and Comp.*, U.S. Army Res. Office, 1987.

[18] V. Ervin and W. Layton, An analysis of a defect correction method for a model convection diffusion equation, SIAM J. Numer. Anal., 26 (1989), 169-179.

[19] V. Ervin, W. Layton, J. Maubach, Adaptive defect correction methods for viscous incompressible flow problems, SIAM J. Numer. Anal., 37 (2000), pp. 1165-1185.

[20] H. Elman, Y.-T. Shih, Iterative methods for stabilized discrete convection-diffusion problems, IMA J. Numer. Anal., 20 (2000), pp. 333-358.

[21] W. Heinrichs, Defect correction for convection dominated flow, SIAM J. Sci. Comput., 17 (1996), 1082-1091

[22] P. Hemker, An accurate method without directional bias for the numerical solution of a 2-D elliptic singular perturbation problem, pp. 192-206 in: *Theory And Applications Of Singular Perturbations*, Lecture Notes in Math. 942, W. Eckhaus and E.M. de Jaeger, eds., Sprienger-Verlag, Berlin, 1982

[23] W. Layton, *Introduction to the Numerical Analysis of Incompressible Viscous Flows*, SIAM publications (Computational Science and Engineering Series), 2008, ISBN: 978-0-898716-57-3.

[24] M. Gunzburger, *Finite element methods for viscous incompressible flows: A guide to theory, practice, and algorithms*, Academic Press, Boston, 1989.

[25] A. Labovsky, *A Defect Correction Method for the Time-Dependent Navier-Stokes Equations*, Numerical Methods for Partial Differential Equations, vol.25(1), pp.1-25, 2008.

[26] W. Layton, L. Rebholz, C. Trenchea, Modular Nonlinear Filter Stabilization of Methods for Higher Reynolds Numbers Flow, University of Pittsburgh, technical report, 2010.

[27] J. Heywood, R. Rannacher, Finite-element approximations of the nonstationary Navier-Stokes problem. Part 4: Error analysis for second-order time discretization, SIAM J. Numer. Anal., Vol. 27, No. 2, pp.353-384 (1990)

[28] B. Koren, Multigrid and Defect-Correction for the Steady Navier-Stokes Equations, *Applications to Aerodynamics*, C. W. I. Tract 74, Centrum voor Wiskunde en Informatica, Amsterdam, 1991.

[29] M.-H. Lallemand, B. Koren, Iterative defect correction and multigrid accelerated explicit time stepping schemes for the steady Euler equations, SIAM Journal on Scientific Computing, vol. 14, issue 4, 1993.

[30] V. J. Ervin, H. K. Lee, Defect correction method for viscoelastic fluid flows at high Weissenberg number, Numerical Methods for Partial Differential Equations, Volume 22, Issue 1, pp. 145 - 164, 2006.

[31] P. W. Hemker, G. I. Shishkin, L. P. Shishkina, High-order time-accurate schemes for singularly perturbed parabolic convection-diffusion problems with

Robin boundary conditions, Computational Methods in Applied Mathematics, Vol. 2 (2002), No. 1, pp. 3-25.

[32] V. Girault, P.A. Raviart, Finite element approximation of the Navier-Stokes equations, *Lecture notes in mathematics*, no. 749, Springer-Verlag, 1979.

[33] J. H. Mathews, K. D. Fink, Numerical methods using MATLAB, Pearson Prentice Hall, 2004.

[34] M. L. Minion, Semi-Implicit Projection Methods for Incompressible Flow based on Spectral Deferred Corrections, Appl. Numer. Math., 48(3-4), 369-387, 2004

[35] M. L. Minion, Semi-Implicit Projection Methods for Ordinary Differential Equations, Comm. Math. Sci., 1(3), 471–500, 2003.

[36] A. Bourlioux, A. T. Layton, M. L. Minion, High-Order Multi-Implicit Spectral Deferred Correction Methods for Problems of Reactive Flows, Journal of Computational Physics, Vol. 189, No. 2, pp. 651-675, 2003.

[37] W. Kress, B. Gustafsson, Deferred Correction Methods for Initial Boundary Value Problems, Journal of Scientific Computing, Springer Netherlands, Vol. 17, No. 1-4, 2002.

[38] M. Aggul, J. Connors, D. Erkmen and A. Labovsky, A Defect-Deferred Correction Method for Fluid-Fluid Interaction, submitted, 2017.

[39] A. Dutt, L. Greengard, V. Rokhlin, Spectral deferred correction methods for ordinary differential equations, BIT 40 (2), pp. 241-266, 2000.

[40] Y. Saad, Iterative Methods for Sparse Linear Systems. Second edition, published by SIAM, 2003.

[41] Sagaut, P., Large eddy simulation for incompressible flows,*Scientific Computation*, Springer Verlag, 2006.

[42] John, V., Large eddy simulation of turbulent incompressible flows,*Lecture Notes in Computational Science and Engineering*, Springer Verlag, 2004.

[43] Berselli, L.C. and Iliescu, T. and Layton, W.J., Mathematics of large eddy simulation of turbulent flows,*Scientific Computation*, Springer Verlag, 2006.

[44] J. Borggaard and T. Iliescu, Approximate deconvolution boundary conditions for large eddy simulation, *APPLIED MATHEMATICS LETTERS*, vol. 19(8), 2006, pp. 735-740.

[45] P. Moin and M. Wang, Wall modeling for large-eddy simulation of turbulent boundary layers, IUTAM Symposium on One Hundred Years of Boundary Layer Research, *Solid Mechanics and Its Applications*, 2006, Volume 129, Session 5, 269-278.

[46] S.Y. Kadioglu, R. Klein and M.L. Minion, A fourth-order auxiliary variable projection method for zero-Mach number gas dynamics, *J. Comp. Physics*, 2008, Volume 227, 2012-2043.

[47] J.F. Gibson, J. Halcrow and P. Cvitanovic, Equilibrium and traveling-wave solutions of plane Couette flow, *J. Fluid Mech.*, Vol. 638, pp. 243 - 266, 2009; arXiv:0808.3375v2.

[48] K. Bohmer, P. W. Hemker, H. J. Stetter, The defect correction approach, in: K. Bohmer, H. J. Stetter (Eds.),*Defect Correction Methods. Theory and Applications*, Springer Verlag, 1984, pp. 1–32.

[49] P. W. Hemker, Mixed defect correction iteration for the accurate solution of the convection diffusion equation, pp. 485-501 in: *Multigrid Methods*, L.N.M. vol. 960, (W. Hackbusch and U. Trottenberg, eds.) Springer Verlag, Berlin 1982.

[50] P. W. Hemker, The use of defect correction for the solution of a singularly perturbed o.d.e., preprint, Mathematisch Centrum. Numerieke Wiskunde ; NW 139/82

[51] O. Axelsson and W. Layton, Defect correction methods for convection dominated, convection-diffusion equations, RAIRO J. Numer. Anal. 24 (1990) pp. 423-455.

[52] O. Axelsson and W. Layton, Optimal interior estimates for the defect-correction, finite element approach to 2-D convection-diffusion problems, ICMA report 88-116, Univ. of Pittsburgh, 1988.

[53] W. Layton, H. K. Lee, J. Peterson, A defect-correction method for the incompressible Navier–Stokes equations, Applied Mathematics and Computation, Vol. 129, Issue 1, 2002, pp. 1-19.

[54] V. Ervin and W. Layton, High resolution minimal storage algorithms for convection dominated, convection diffusion equations, pp. 1173-1201 in: *Trans. of the Fourth Army Conf. on Appl. Math. and Comp.*, U.S. Army Res. Office, 1987.

[55] V. Ervin and W. Layton, An analysis of a defect correction method for a model convection diffusion equation, SIAM J. Numer. Anal., 26 (1989), 169-179.

[56] V. Ervin, W. Layton, J. Maubach, Adaptive defect correction methods for viscous incompressible flow problems, SIAM J. Numer. Anal., 37 (2000), pp. 1165-1185.

[57] H. Elman, Y.-T. Shih, Iterative methods for stabilized discrete convection-diffusion problems, IMA J. Numer. Anal., 20 (2000), pp. 333-358.

[58] W. Heinrichs, Defect correction for convection dominated flow, SIAM J. Sci. Comput., 17 (1996), 1082-1091

[59] P. Hemker, An accurate method without directional bias for the numerical solution of a 2-D elliptic singular perturbation problem, pp. 192-206 in: *Theory And Applications Of Singular Perturbations*, Lecture Notes in Math. 942, W. Eckhaus and E.M. de Jaeger, eds., Sprienger-Verlag, Berlin, 1982

[60] W. Layton, *Introduction to the Numerical Analysis of Incompressible Viscous Flows*, SIAM publications (Computational Science and Engineering Series), 2008, ISBN: 978-0-898716-57-3.

[61] M. Gunzburger, *Finite element methods for viscous incompressible flows: A guide to theory, practice, and algorithms*, Academic Press, Boston, 1989.

[62] B. Koren, Multigrid and Defect-Correction for the Steady Navier-Stokes Equations, *Applications to Aerodynamics*, C. W. I. Tract 74, Centrum voor Wiskunde en Informatica, Amsterdam, 1991.

[63] M.-H. Lallemand, B. Koren, Iterative defect correction and multigrid accelerated explicit time stepping schemes for the steady Euler equations, SIAM Journal on Scientific Computing, vol. 14, issue 4, 1993.

[64] V. J. Ervin, H. K. Lee, Defect correction method for viscoelastic fluid flows at high Weissenberg number, Numerical Methods for Partial Differential Equations, Volume 22, Issue 1, pp. 145 - 164, 2006.

[65] W. Kress, B. Gustafsson, Deferred Correction Methods for Initial Boundary Value Problems, Journal of Scientific Computing, Springer Netherlands, Vol. 17, No. 1-4, 2002.

[66] A. N. Kolmogorov, The local structure of turbulence in incompressible viscous fluid for very large Reynolds numbers, *Doklady Akademii Nauk SSSR*, vol 30, p.913, 1941.

[67] J.F. Gibson, J. Halcrow and P. Cvitanovic, Equilibrium and traveling-wave solutions of plane Couette flow, *J. Fluid Mech.*, Vol. 638, pp. 243 - 266, 2009; arXiv:0808.3375v2.

[68] H. J. Stetter, The defect correction principle and discretization methods, *Numerische Mathematik*, vol. 29(4), pp. 425-443, 1978.

[69] R. Frank, W. Ueberhuber, Iterated Defect Correction for the Efficient Solution of Stiff Systems of Ordinary Differential Equations, BIT 17, 1977, pp. 146-159.

[70] J. Heywood, R. Rannacher, Finite-element approximations of the nonstationary Navier-Stokes problem. Part 4: Error analysis for second-order time discretization, SIAM J. Numer. Anal., 2 (1990)

[71] M. Gunzburger, A. Labovsky, *High Accuracy Method for Turbulent Flow Problems*, M3AS: Mathematical Models and Methods in Applied Sciences, vol. 22 (6), 2012.

[72] G. P. Galdi, An Introduction to the Mathematical Theory of the Navier-Stokes Equations, Springer Tracts in Natural Philosophy, Volume I, Springer-Verlag, New York, 1994.

[73] O. Axelsson and W. Layton, Optimal interior estimates for the defect-correction, finite element approach to 2-D convection-diffusion problems, ICMA report 88-116, Univ. of Pittsburgh, 1988.

[74] R.A. Adams and J.J.F. Fournier, *Sobolev Spaces*, vol. 140 of Pure and Applied Mathematics, Academic Press, 2003.

[75] U. M. Ascher, S. J. Ruuth and B. T. R. Wetton, Implicit-explicit methods for time-dependent partial differential equations, SIAM J. Num. Anal. 32(3), 1995.

[76] J.-W. Bao, J. M. Wilczak, J.-K. Choi and L. H. Kantha, *Numerical simulations of air-sea interaction under high wind conditions using a coupled model: A study fo hurricane development*, Monthly Weather Review, Vol. 128 (2000), pp. 2190-2210.

[77] G. Bellon, A. H. Sobel and J. Vialard, *Ocean-atmospere coupling in the monsoon intraseasonal oscillation: A simple model study*, Journal of Climate, Vol. 21, 2008, pp. 5254-5270.

[78] D. Bresch and J. Koko, *Operator-splitting and Lagrange multiplier domain decomposition methods for numerical simulation of two coupled Navier-Stokes fluids*, Int. J. Appl. Math. Comput. Sci., Vol. 16(4), 2006, pp. 419–429.

[79] C. Bernardi, T. Chacon-Rebello M. Gomez, R. Lewandowski, F. Murat, A model of two coupled turbulent fluids, Part II: Numerical approximations by spectral discretization, SIAM Jour. Num. Analysis, Vol. 40, No. 6, pp. 2368-2394, 2002.

[80] H. Blum, S. Lisky and R. Rannacher, A Domain Splitting Algorithm for Parabolic Problems, Computing 49, 11-23, 1992.

[81] K. Böhmer, P. W. Hemker, H. J. Stetter, The defect correction approach, in: K. Böhmer, H. J. Stetter (Eds.),*Defect Correction Methods. Theory and Applications*, Springer Verlag, 1984, pp. 1–32.

[82] S.C. Brenner and L.R. Scott, *The Mathematical Theory of Finite Element Methods*, Springer-Verlag, 2002.

[83] D. Bresch and J. Koko, Operator-Splitting and Lagrange Multiplier Domain Decomposition Methods for Numerical Simulation of Two Coupled Navier-Stokes Fluids, Int. J. Appl. Math. Comput. Sci., Vol. 16, No. 4, 2006, pp. 419-429.

[84] C. L. Brossier, V. Ducrocq and H. Giordani, *Effects of the air-sea coupling time frequency on the ocean response during Mediterranean intense events*, Ocean Dynamics, Vol. 59 (2009), pp. 539-549.

[85] F. O. Bryan, B. G. Kauffman, W. G. Large and P. R. Gent, *The NCAR CESM flux coupler*, Tech. Rept. NCAR/TN-424+STR, NCAR, 1996.

[86] E. Burman, Miguel A. Fernández, Stabilization of explicit coupling in fluid-structure interaction involving fluid incompressibility, Comput. Methods Appl. Mech. Engrg. 198 (2009), pp. 766-784.

[87] E. Burman, P. Hansbo, Interior penalty stabilized Lagrange multiplier for the finite element solution of elliptic interface problems, to appear in IMA Journal of Numerical Analysis, available online April 7, 2009.

[88] R. B. Neale, *et. al.*, *Description of the NCAR community atmosphere model (CAM 5.0)*, NCAR Tech. Note NCAR/TN-486+ STR (2010).

[89] P. Causin, J.-F. Gerbeau and F. Nobile, Added-mass effect in the design of partitioned algorithms for fluid-structure problems, Comput. Meth. Appl. Mech. Engrg., Vol. 194, No. 42-44, 2005, pp. 4506-4527.

[90] J. Connors, J. Howell and W. Layton, *Partitioned timestepping for a parabolic two domain problem*, SIAM Jour. Num. Anal., Vol. 47, No. 5, 2009.

[91] J. Connors, J. Howell and W. Layton, *Decoupled time stepping methods for fluid-fluid interaction*, SIAM Jour. Num. Analysis, Vol. 50, No. 3, 2012, pp. 1297-1319.

[92] J. Connors and B. Ganis, *Stability of algorithms for a two domain natural convection problem and observed model uncertainty*, Computational Geosciences, Vol. 15, No. 3 (2011), pp. 509-527.

[93] C. N. Dawson and Q. Du, A Finite Element Domain Decomposition Method

for Parabolic Equations, Fourth International Symposium on Domain Decomposition Methods for PDEs, edited by R. Glowinski et al, pp. 255-263, SIAM, Philadelphia, 1991.

[94] S. D. Nicholls and S. G. Decker, *Impact of coupling an ocean model to WRF nor'easter simulations*, Monthly Weather Review 143.12 (2015), pp. 4997-5016.

[95] F. Lemarié, E. Blayo and L. Debreu, *Analysis of ocean-atmosphere coupling algorithms: consistency and stability*, Procedia Computer Science, Vol. 51 (2015), pp. 2066-2075.

[96] F. Lemarié, P. Marchesiello, L. Debreu and E. Blayo, *Sensitivity of ocean-atmosphere coupled models to the coupling method: example of tropical cyclone Erica*, Doctoral dissertation, INRIA Grenoble; INRIA, 2014.

[97] F. Hecht, A. LeHyaric and O. Pironneau. Freefem++ version 2.24-1, 2008. `http://www.freefem.org/ff++`.

[98] Randall, D.A., R.A. Wood, S. Bony, R. Colman, T. Fichefet, J. Fyfe, V. Kattsov, A. Pitman, J. Shukla, J. Srinivasan, R.J. Stouffer, A. Sumi and K.E. Taylor, 2007: Climate Models and Their Evaluation. In: Climate Change 2007: The Physical Science Basis. Contribution of Working Group I to the Fourth Assessment Report of the Intergovernmental Panel on Climate Change [Solomon, S., D. Qin, M. Manning, Z. Chen, M. Marquis, K.B. Averyt, M.Tignor and H.L. Miller (eds.)].

Cambridge University Press, Cambridge, United Kingdom and New York, NY, USA.

[99] M. Jochum, G. Danabasoglu, M. Holland, Y.-O. Kwon and W. G. Large, *Ocean viscosity and climate*, Journal of Geophysical Research, Vol. 113, C06017, 2008, pp. 1-24.

[100] A. Labovsky, A Defect Correction Method for the Evolutionary Convection Diffusion Problem with Increased Time Accuracy, Computational Methods in Applied Mathematics, Vol. 9, No. 2, 2009, pp. 154-164.

[101] Large, W.G., McWilliams, J.C. and Doney, S.C., *Oceanic vertical mixing: A review and a model with a nonlocal boundary layer*, Reviews of Geophysics, Vol. 32 (1994), pp. 363-403.

[102] R. Lewandowski, *Analyse Mathématique et Océanographic*, collection RMA, Masson, 1997.

[103] J.-L. Lions, R. Temam and S. Wang, *Models of the coupled atmosphere and ocean (CAO I)*, Computational Mechanics Advances, Vol. 1 (1993), pp. 5-54.

[104] J.-L. Lions, R. Temam and S. Wang, *Numerical analysis of the coupled atmosphere ocean models (CAO II)*, Computational Mechanics Advances, Vol. 1 (1993), pp. 55-119.

[105] M. L. Minion, *Semi-Implicit Spectral Deferred Correction Methods for Ordinary Differential Equations*, Comm. Math. Sci. 1 (2003), 471–500.

[106] M. L. Minion, Semi-Implicit Projection Methods for Ordinary Differential Equations, Comm. Math. Sci., 1(3), 471–500, 2003.

[107] P. A. Mooney, D. O. Gill, F. J. Mulligan and C. L. Bruyère, *Hurrican simulation using different representations of atmosphere-ocean interaction: the case of Irene*, Atmospheric Science Letters, Vol. 17, No. 7, 2016, pp. 415-421.

[108] J. Nelson, R. He, J. C. Warner and J. Bane, *Air-sea interactions during strong winter extratropical storms*, Ocean Dynamics, Vol. 64, No. 9, 2014, pp. 1233-1246.

[109] N. Perlin, E. D. Skyllingstad, R. M. Samelson, P. L. Barbour, *Numerical simulation of air-sea coupling during coastal upwelling*, Journal of Physical Oceanography, Vol. 37 (2007), pp. 2081-2093.

[110] R. Smith, et. al., *The parallel ocean program (POP) reference manual*, Tech. Rep. LAUR-01853 141 (2010): 1-140.

[111] M. Aggul, A. Labovsky, *A High Accuracy Minimally Invasive Regularization Technique for Navier-Stokes Equations at High Reynolds Number*, Numerical Methods for Partial Differential Equations, vol. 33(3), pp. 814-839, 2017.

[112] D. Erkmen, A. Labovsky, *Defect-Deferred Correction Method for the Two-Domain Convection-Dominated Convection-Diffusion Problem*, Journal of Mathematical Analysis and Applications, vol. 450(1), pp. 180-196, 2017.

[113] B. Wang and X. Xie, *Coupled modes of the warm pool climate system. Part 1: The role of air-sea interaction in maintaining Madden-Julian Oscillation*, Journal of Climate, Vol. 11, 1998, pp. 2116-2135.

[114] W. L. Washington and C. L. Parkinson, *An Introduction to Three-Dimensional Climate Modeling: Second Edition*, University Science Books, Sausalito, California, 2005.

[115] R. M. Yablonsky, I. Ginis., *Limitation of one-dimensional ocean models for coupled hurricane–ocean model forecasts*, Monthly Weather Review 137.12 (2009): 4410-4419.

[116] Y. Zhang, Y. Hou and L. Shan, *Stability and convergence analysis of a decoupled algorithm for a fluid-fluid interaction problem*, SIAM Journal on Numerical Analysis, Vol. 54, No. 5 (2016), pp. 2833-2867.

[117] Richardson, L. F., *The Approximate Arithmetical Solution by Finite Differences of Physical Problems Involving Differential Equations with an Application to the Stress in a Masonry Dam*, Philosophical Transactions of the Royal Society of London. Series A, vol. 210, no. 467, pp. 307-357, 1910.

[118] D. C. Joyce, *Survey of Extrapolation Processes in Numerical Analysis* , SIAM Review 1971 13:4, 435-490.

[119] Richardson, L. F. and Gaunt, J. Arthur, *The Deferred Approach to the Limit.* , Philosophical Transactions of the Royal Society of London. Series A, vol. 226, no. 643, pp. 299-361, 1927.

[120] Burg, C., *Application of Richardson extrapolation to the numerical solution of partial differential equations*, Numerical Methods for Partial Differential Equations, Vol. 25, No. 4, pp. 810-832, 2009.

[121] Celik I, Karatekin O., *Numerical Experiments on Application of Richardson Extrapolation With Nonuniform Grids*, J. Fluids Eng., Vol. 119(3), pp. 584-590, 1997.

[122] Xing T, Stern F., *Factors of Safety for Richardson Extrapolation.*, ASME. J. Fluids Eng., 2010;132(6):061403-061403-13.

[123] W. Shyy and M. Garbey and A. Appukuttan and J. Wu , *EVALUATION OF RICHARDSON EXTRAPOLATION IN COMPUTATIONAL FLUID DYNAMICS*, Numerical Heat Transfer, Part B: Fundamentals, vol.41, no. 2, pp.139-164, 2002.

[124] Chang, Chuang-Chang and Chung, San-Lin and Stapleton, Richard C., *Richardson extrapolation techniques for the pricing of American-style options*, Journal of Futures Markets, vol.27, no.8, pp.791-817, 2007.

[125] D. Erkmen, A. Labovsky, *Defect-deferred correction method for the two-domain convection-dominated convection–diffusion problem*, Journal of Mathematical Analysis and Applications, Vol. 450, No. 1, 2017, pp. 180-196.

[126] M. Aggul, D. Erkmen, J. Connors, A. Labovsky, *A Defect-Deferred Correction Method for Fluid-Fluid Interaction, SIAM Jour. Num. Anal., 2017, under review.*

[127] Hecht, F., *New development in FreeFem++*, Journal of Numerical Mathematics, vol 20, no 3-4, p.251–265, 2012.

[128] W. Bangerth and R. Hartmann and G. Kanschat, *deal.II – a General Purpose Object Oriented Finite Element Library*, ACM Trans. Math. Softw., vol 33, no 4, p.24/1–24/27, 2007.

[129] A.E. Green and G.I. Taylor, *Mechanism of the production of small eddies from larger ones*, Proc. Royal Soc. A, 158:499–521, 1937.

[130] G.I. Taylor, *On decay of vortices in a viscous fluid*, Phil. Mag., 46:671–674, 1923.

[131] A. Chorin, *Numerical solution for the Navier-Stokes equations*, Math. Comp.,22:745–762, 1968.

[132] V. John and W. J. Layton, *Analysis of numerical errors in Large Eddy Simulation*, SIAM J. Numer. Anal., 40(3):995–1020, 2002.

[133] D. Tafti, *Comparison of some upwind-biased high-order formulations with a second order central-difference scheme for time integration of the incompressible Navier-Stokes equations.*, Comput. & Fluids, 25:647–665, 1996.

[134] W. J. Layton, L. G. Rebholz, *On relaxation times in the Navier-Stokes-Voigt model*, International Journal of Computational Fluid Dynamics, Vol. 27, 2013 - Is. 3

[135] G. Biswas, M. Breuer, F. Durst, *Backward-Facing Step Flows for Various Expansion Ratios at Low and Moderate Reynolds Numbers*, Journal of Fluids Engineering, Vol. 126, Is. 3, 2004, pp. 362-374.

[136] N. Jiang, S. Kaya and W. Layton, Analysis of Model Variance for Ensemble Based Turbulence Modeling, *Computational Methods in Applied Mathematics*, 15(2), pp. 173-188, 2014.

[137] N. Jiang and W. Layton, Algorithms and models for turbulence not at statistical equilibrium, *Computers & Mathematics with Applications*, Vol. 71, n. 11, pp. 2352 - 2372, 2016.

[138] M. Gunzburger and N. Jiang and M. Schneier, An Ensemble-Proper Orthogonal Decomposition Method for the Nonstationary Navier–Stokes Equations, *SIAM Journal on Numerical Analysis*, 2017, Vol. 55, n. 1, pp. 286-304, 2017.